[redacted]
**Trias Westland B.V.**
**Nieuweweg 1**
**2685 AP  Poeldijk**

Leiderdorp, 29 maart 2021

**Oplegger "Geological report TW OK II"**

Bijgevoegd document "Geological report TW OK II", is in 2018 opgesteld door PanTerra Geoconsultants, ten behoeve van de SDE+ subsidie aanvraag van doublet TW2. Het document omschrijft de geothermische potentie van de toen nog te boren putten NLW-GT-03 en -04. Ten tijde van rapportage was put NLW-GT-01 reeds geboord en getest, put NLW-GT-02 werd geboord.

Het geothermische reservoir is de Delft Zandsteen Member. Deze zandsteenlaag maakt deel uit van de Schieland Groep en is het voornaamste geothermische reservoir in de regio. Op basis van seismische interpretatie van de ondergrond en naburige putten werd de diepte van het reservoir ingeschat op circa 2300 tot 2400 m en de bruto dikte circa 55 tot 75 m met een N/G van circa 90%. Gebaseerd op petrofysica en puttesten nabij, waaronder NLW-GT-01, werd de permeabiliteit ingeschat op 650 mD, met een lage inschatting van 450 mD en hoge inschatting van 1000 mD.

Het vermogen van het doublet is afhankelijk van geologische parameters, putconfiguratie en operationele instellingen. Op basis van het putontwerp is uitgegaan van een maximum debiet van 525 $m^3$/uur. De benodigde injectiedruk bevindt zich ruim onder de SodM limiet van 0.135 bar/m. Het resulterende P50 vermogen is 32 MW, met een P90 van 25 MW en P10 van 41 MW. De berekende COP (Coefficient Of Performance) range is 13 – 14 – 15 (P90 – P50 -P10).

# Geological report TW OK II

March 2018

PanTerra Project G1363b

# Geological report TW OK II

**Author**

[redacted]

**Prepared for**
Trias Westland BV
Postbus 1
2685 ZG Poeldijk

# Contents

# 1 Summary

## 1.1 Planned doublets and applied parameters

This report summarizes the geothermal potential of planned doublet NLW-GT-03 and -04 in the Naaldwijk 2II and De Lier IV geothermal exploration concessions in the municipality of Westland in the province Zuid-Holland. Production and injection will occur within the Naaldwijk 3 concession. All referred concessions are owned by Trias Westland B.V., the operator of the planned doublet.

The target reservoirs are fluvial sands in the Delft Sandstone Member (part of the Schieland Group). These reservoirs have already been successfully tested by nearby geothermal well NLW-GT-01, NLW-GT-02 is currently being drilled. Bothe wells are operated by Trias Westland B.V.. The new doublet will consist of two wells, injector NLW-GT-03 and producer NLW-GT-04 (Figure 2-1) and the produced heat will be used for greenhouse heating and possibly in the future, district heating. This report will be used to underpin the SDE+ application for the new doublet.

The doublet performance has been calculated with DoubletCalc 1.4.3, a screeshot of the input parameters is shown in Figure 1-1. The pump pressure difference is set to 110 bar (see section 9.3). The pump pressure difference is current restricted by the maximum flowrate possible through the tubing which is 525 $m^3$/h. Lower pressures will result in lower flow rates and decrease in geothermal power (Figure 1-4) but would increase the COP. The permeability of the reservoir is the most significant uncertainty as it has major impact on the doublet performance. However due to the NLW-GT-01 well situated close to the planned doublet this uncertainty is relatively small for the planned doublet. This is reflected by the permeability range and the related P10, P50 and P90 geothermal power estimates (Figure 1-1 and Figure 1-2).

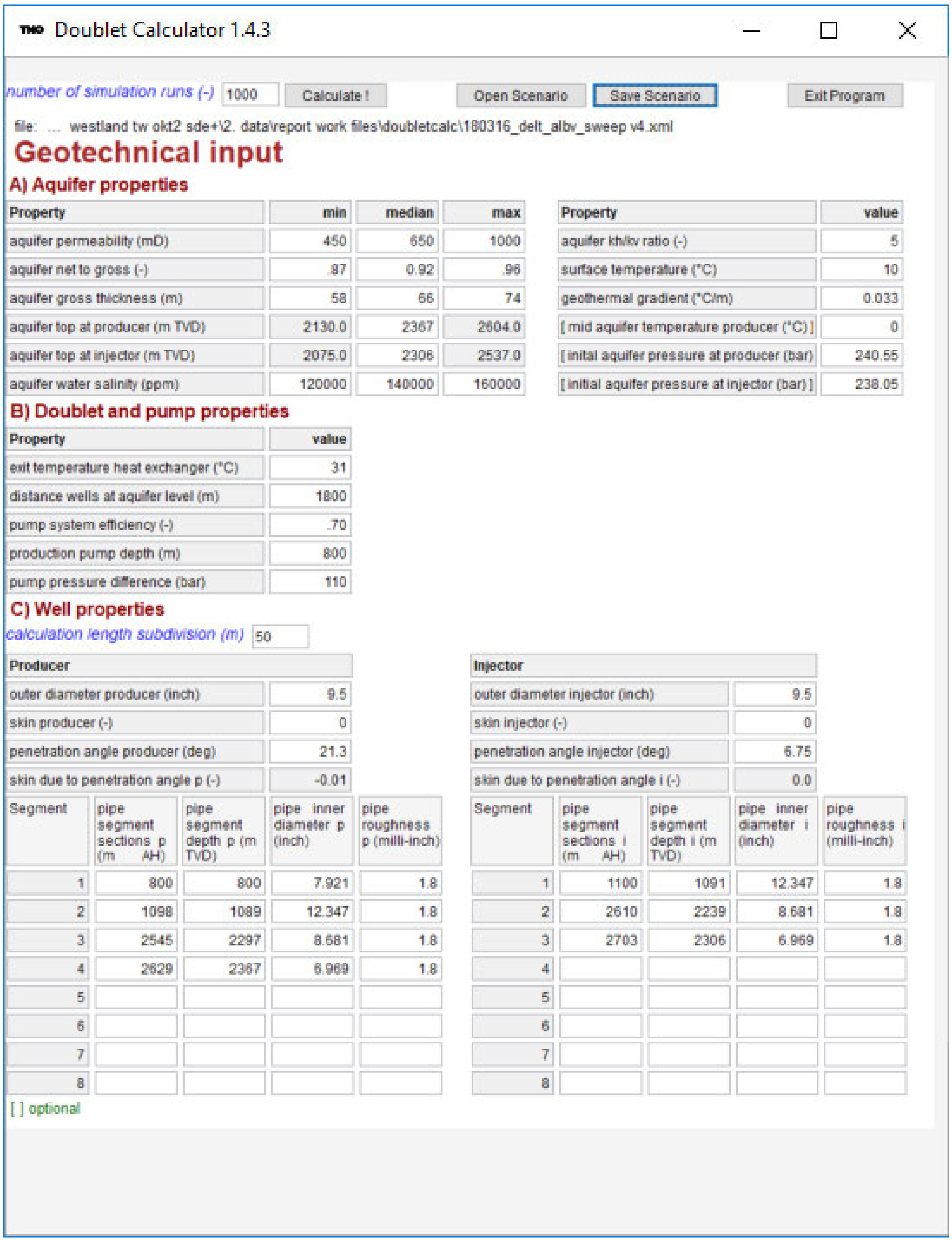

Doublet Calculator 1.4.3

number of simulation runs (-) 1000 | Calculate ! | Open Scenario | Save Scenario | Exit Program

file: ... westland tw okt2 sde+\2. data\report work files\doubletcalc\180316_delt_albv_sweep v4.xml

Geotechnical input

A) Aquifer properties

| Property | min | median | max |
|---|---|---|---|
| aquifer permeability (mD) | 450 | 650 | 1000 |
| aquifer net to gross (-) | .87 | 0.92 | .96 |
| aquifer gross thickness (m) | 58 | 66 | 74 |
| aquifer top at producer (m TVD) | 2130.0 | 2367 | 2604.0 |
| aquifer top at injector (m TVD) | 2075.0 | 2306 | 2537.0 |
| aquifer water salinity (ppm) | 120000 | 140000 | 160000 |

| Property | value |
|---|---|
| aquifer kh/kv ratio (-) | 5 |
| surface temperature (°C) | 10 |
| geothermal gradient (°C/m) | 0.033 |
| [ mid aquifer temperature producer (°C) ] | 0 |
| [ inital aquifer pressure at producer (bar) | 240.55 |
| [ initial aquifer pressure at injector (bar) ] | 238.05 |

B) Doublet and pump properties

| Property | value |
|---|---|
| exit temperature heat exchanger (°C) | 31 |
| distance wells at aquifer level (m) | 1800 |
| pump system efficiency (-) | .70 |
| production pump depth (m) | 800 |
| pump pressure difference (bar) | 110 |

C) Well properties

calculation length subdivision (m) 50

| Producer | |
|---|---|
| outer diameter producer (inch) | 9.5 |
| skin producer (-) | 0 |
| penetration angle producer (deg) | 21.3 |
| skin due to penetration angle p (-) | -0.01 |

| Segment | pipe segment sections p (m AH) | pipe segment depth p (m TVD) | pipe inner diameter p (inch) | pipe roughness p (milli-inch) |
|---|---|---|---|---|
| 1 | 800 | 800 | 7.921 | 1.8 |
| 2 | 1098 | 1089 | 12.347 | 1.8 |
| 3 | 2545 | 2297 | 8.681 | 1.8 |
| 4 | 2629 | 2367 | 6.969 | 1.8 |
| 5 | | | | |
| 6 | | | | |
| 7 | | | | |
| 8 | | | | |

| Injector | |
|---|---|
| outer diameter injector (inch) | 9.5 |
| skin injector (-) | 0 |
| penetration angle injector (deg) | 6.75 |
| skin due to penetration angle i (-) | 0.0 |

| Segment | pipe segment sections i (m AH) | pipe segment depth i (m TVD) | pipe inner diameter i (inch) | pipe roughness i (milli-inch) |
|---|---|---|---|---|
| 1 | 1100 | 1091 | 12.347 | 1.8 |
| 2 | 2610 | 2239 | 8.681 | 1.8 |
| 3 | 2703 | 2306 | 6.969 | 1.8 |
| 4 | | | | |
| 5 | | | | |
| 6 | | | | |
| 7 | | | | |
| 8 | | | | |

[ ] optional

**Figure 1-1: DoubletCalc 1.4.3 input screen for the the planned NLW-GT-03 and NLW-GT-04 doublet.**

## 1.2 Expected geothermal power

The P50 geothermal power estimate is 32.18 MW, the P90 power estimate is 24.52 MW. Relevant DoubletCalc screenshots are displayed in Figure 1-1 to Figure 1-4.

Doublet Calculator 1.4.3 Result Table

probabilistic plots | fingerprinting | export base case details

file: ... lokale warmte\00_gt\pro\etp tw ok ii\2. bo\doubletcalc\180322_delt_albv_sweep v4_final.xml

## Geotechnics (Input)

| Property | min | median | max |
|---|---|---|---|
| aquifer permeability (mD) | 450.0 | 650.0 | 1000.0 |
| aquifer net to gross (-) | 0.87 | 0.92 | 0.96 |
| aquifer gross thickness (m) | 58.0 | 66.0 | 74.0 |
| aquifer top at producer (m TVD) | 2130.0 | 2367.0 | 2604.0 |
| aquifer top at injector (m TVD) | 2075.0 | 2306.0 | 2537.0 |
| aquifer water salinity (ppm) | 120000.0 | 140000.0 | 160000.0 |

| Property | value |
|---|---|
| number of simulation runs (-) | 1000.0 |
| aquifer kh/kv ratio (-) | 5.0 |
| surface temperature (°C) | 10.0 |
| geothermal gradient (°C/m) | 0.033 |
| [ mid aquifer temperature producer (°C) ] | 0.0 |
| inital aquifer pressure at producer (bar) ] | 240.6 |
| [ initial aquifer pressure at injector (bar) ] | 238.1 |
| exit temperature heat exchanger (°C) | 31.0 |
| distance wells at aquifer level (m) | 1800.0 |
| pump system efficiency (-) | 0.7 |
| production pump depth (m) | 800.0 |
| pump pressure difference (bar) | 110.0 |
| outer diameter producer (inch) | 9.5 |
| skin producer (-) | 0.0 |
| skin due to penetration angle p (-) | -0.01 |
| pipe segment sections p (m AH) | 800.0,1098.0,2545.0,2629.0 |
| pipe segment depth p (m TVD) | 800.0,1089.0,2297.0,2367.0 |
| pipe inner diameter p (inch) | 7.92,12.35,8.68,6.97 |
| pipe roughness p (milli-inch) | 1.8,1.8,1.8,1.8 |
| outer diameter injector (inch) | 9.5 |
| skin injector (-) | 0.0 |
| skin due to penetration angle i (-) | 0.0 |
| pipe segment sections i (m AH) | 1100.0,2610.0,2703.0 |
| pipe segment depth i (m TVD) | 1091.0,2239.0,2306.0 |
| pipe inner diameter i (inch) | 12.35,8.68,6.97 |
| pipe roughness i (milli-inch) | 1.8,1.8,1.8 |

## Geotechnics (Output)

| Monte Carlo cases (stochastic inputs) | P90 | P50 | P10 |
|---|---|---|---|
| aquifer kH net (Dm) | 32.41 | 39.69 | 51.44 |
| mass flow (kg/s) | 124.42 | 155.18 | 189.6 |
| pump volume flow (m³/h) | 418.3 | 522.9 | 637.0 |
| required pump power (kW) | 1826.1 | 2282.3 | 2780.4 |
| geothermal power (MW) | 24.52 | 32.18 | 40.76 |
| COP (kW/kW) | 13.0 | 14.1 | 15.1 |
| aquifer pressure at producer (bar) | 240.55 | 240.55 | 240.55 |
| aquifer pressure at injector (bar) | 238.05 | 238.05 | 238.05 |
| pressure difference at producer (bar) | 24.46 | 28.36 | 33.08 |
| pressure difference at injector (bar) | 48.44 | 57.68 | 68.27 |
| aquifer temperature at producer * (°C) | 84.88 | 89.21 | 93.55 |
| temperature at heat exchanger (°C) | 84.07 | 88.51 | 92.83 |

| base case (median value inputs) | value |
|---|---|
| aquifer kH net (Dm) | 39.47 |
| mass flow (kg/s) | 154.44 |
| pump volume flow (m³/h) | 518.6 |
| required pump power (kW) | 2263.9 |
| geothermal power (MW) | 31.8 |
| COP (kW/kW) | 14.0 |
| aquifer pressure at producer (bar) | 240.55 |
| aquifer pressure at injector (bar) | 238.05 |
| pressure difference at producer (bar) | 28.99 |
| pressure difference at injector (bar) | 58.83 |
| aquifer temperature at producer * (°C) | 89.2 |
| temperature at heat exchanger (°C) | 88.42 |
| pressure at heat exchanger (bar) | 57.47 |

* @ mid aquifer depth

**Figure 1-2: Output screen from DoubletCalc for the planned NLW-GT-03 and NLW-GT-04 doublet.**

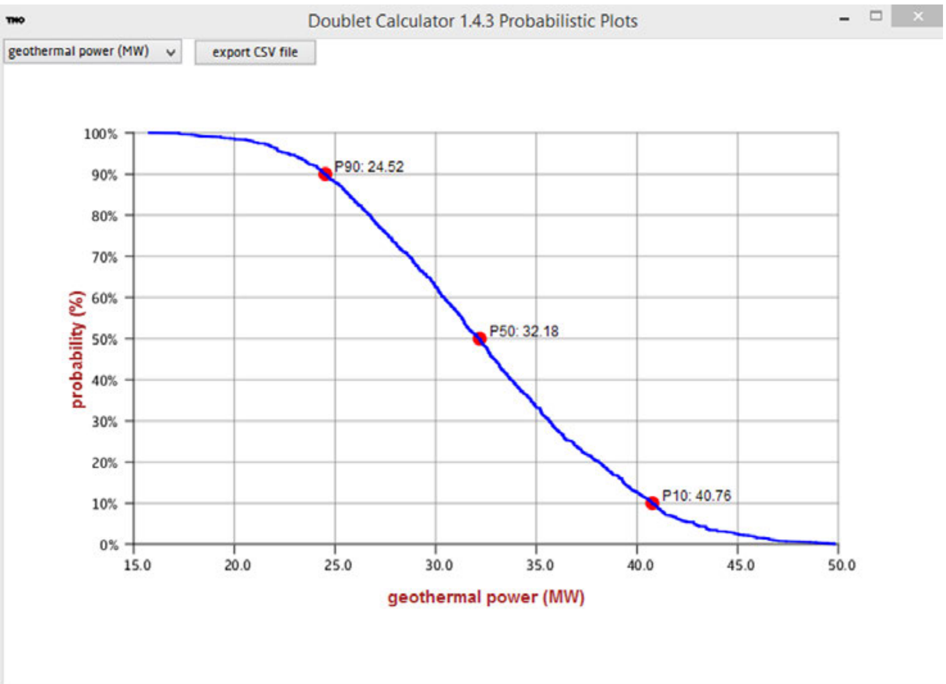


**Figure 1-3: Probability versus geothermal power for the planned NLW-GT-03 and NLW-GT-04 doublet.**

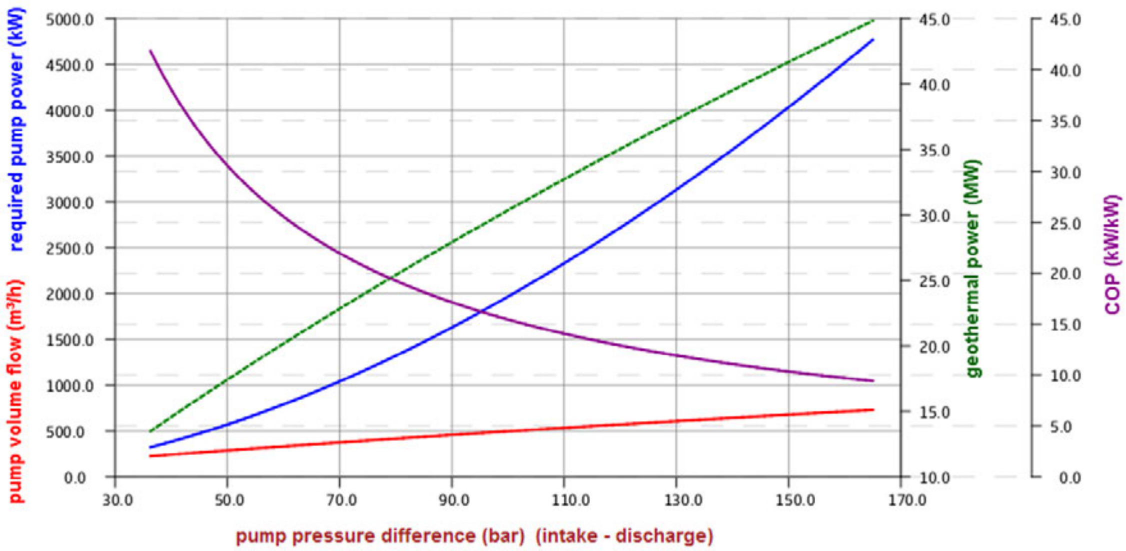


**Figure 1-4: Fingerprinting plot for the Delft sandstone reservoir the planned NLW-GT-03 and NLW-GT-04 doublet.**

# 2 Doublet location and wells

## 2.1 Doublet Location

The planned doublet is located in the municipality of Westland, in the geothermal exploration licences Naaldwijk 2II and de Lier IV, both owned by Trias Westland B.V. Injection and production will occur from Naaldwijk 3 (owned by Trias Westland B.V.) and possibly the requested licence De Lier V when the concession is granted to Trias Westland B.V.. A detailed geological study has been performed of a larger area which also included exploration licences Naaldwijk 3 and De Lier V (Figure 2-1). The reservoir properties and maps produced during that detailed geological study are presented in this report.

## 2.2 Wells

The new doublet will consist of two wells; injector NLW-GT-03 and producer NLW-GT-04. The locations of the two wells are displayed in Figure 2-1.

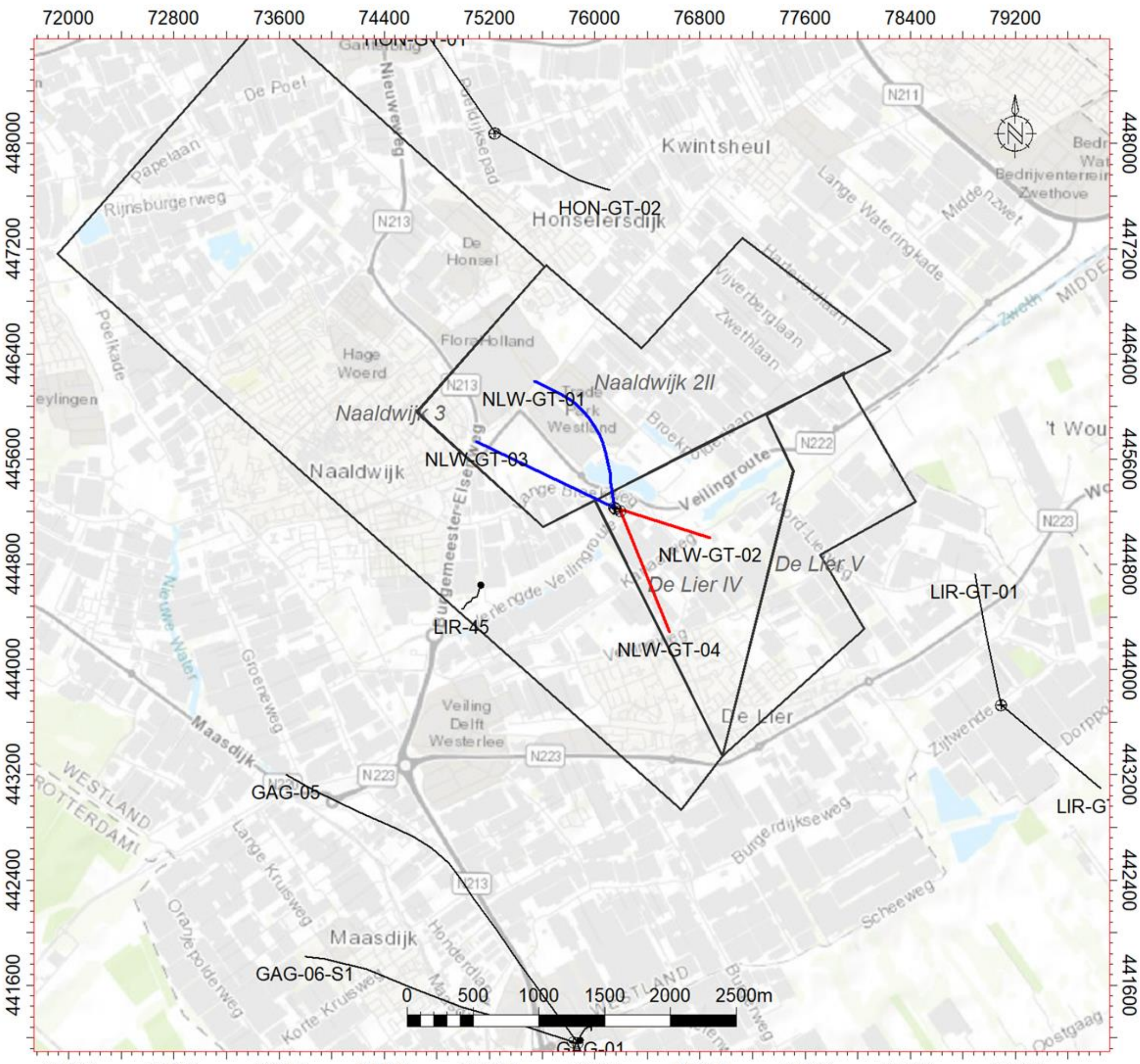


**Figure 2-1: Map view of the study area and planned doublet (NLW-GT-03 and NLW-GT-04). The exploration licences are outlined in black. The well trajectories of producers are shown in red, the trajectories of injectors are in blue. Nearby wells, including geothermal wells NLW-GT-01 and -02 (currently being drilled) have been added as well.**

# 3 Application SDE+ Garantieregeling

This report forms the basis of an SDE+ application.

## 3.1 Application SDE+

SDE+ application is performed for a full doublet, consisting of two new wells, NLW-GT-03 and -04.

# 4 Geological setting

## 4.1 Structural setting

The study area is located in the West Netherlands Basin which is an inverted rift basin (Figure 4-1). Sediments in this basin range in age from Jurassic to recent and are overlying Triassic and older sediments. The Upper Jurassic and Lower Cretaceous (Figure 4-2) start with the continental sediments of the Nieuwerkerk Formation. These sediments were deposited in subsiding half-grabens, while adjacent highs were subjected to erosion. In the Nieuwerkerk Formation, the Delft Sandstone (Figure 4-3) has in general good reservoir properties. The Delft Sandstone is interpreted to be deposited as stacked distributary-channel deposits in a lower coastal plain setting resulting in massive sandstone sequences. The thickness of the Delft Sandstone is influenced by the syn-rift deposition of the sediments and therefore the Delft Sandstone is of variable thickness, a thickness up to 130m is observed. The sandstone consists of fine- to coarse-grained sand, the lateral continuity is difficult to predict.

At the base of the marine Rijnland Group the Rijswijk Sandstone Member, the Berkel Sandstone Member and the Berkel Sand-Claystone Member can be found (Figure 4-2 and Figure 4-3 ). These members are expected to be good aquifers for geothermal exploitation. The Rijswijk Sandstone consists of coastal sands. The majority of the Rijswijk Sands were deposited as basal transgressive sands unconformably over an uneven surface of the Nieuwerkerk Formation. This caused a reworking of the underlying Nieuwerkerk Formation and an infill of the existing palaeotopography. The paleotopography was related to the existing active syn-sedimentary faults that caused variation in thicknesses of 0 to 70 m of the Rijswijk Sandstone Member. The Rijswijk Sands consist of fine-to coarse-grained, cross-bedded sandstone with some thin lagoonal shale intercalations, marine fossils and glauconite. The Berkel Sandstone Member comprising E-W oriented coastal barrier sand or beach complexes is deposited along the fringe of the West Netherlands Basin. It consists of very fine- to medium-grained sandstone. The Berkel Sand-Claystone Member was deposited in a similar setting but comprises more claystone intervals than the Berkel Sandstone. The Berkel and Rijswijk sandstones combined are referred to as the Vlieland formation.

In the Late Cretaceous, during the deposition of the Chalk Group, the West Netherlands Basin was inverted. This was accompanied by compressional movements and resulted in convergent oblique-slip faulting, general uplift, erosion and basin inversion, which reactivated pre-existing normal faults. The major tectonic feature in the region of the license is a NW-SE trending inverted 'pop-up' anticline. The structure is bounded by two faults.

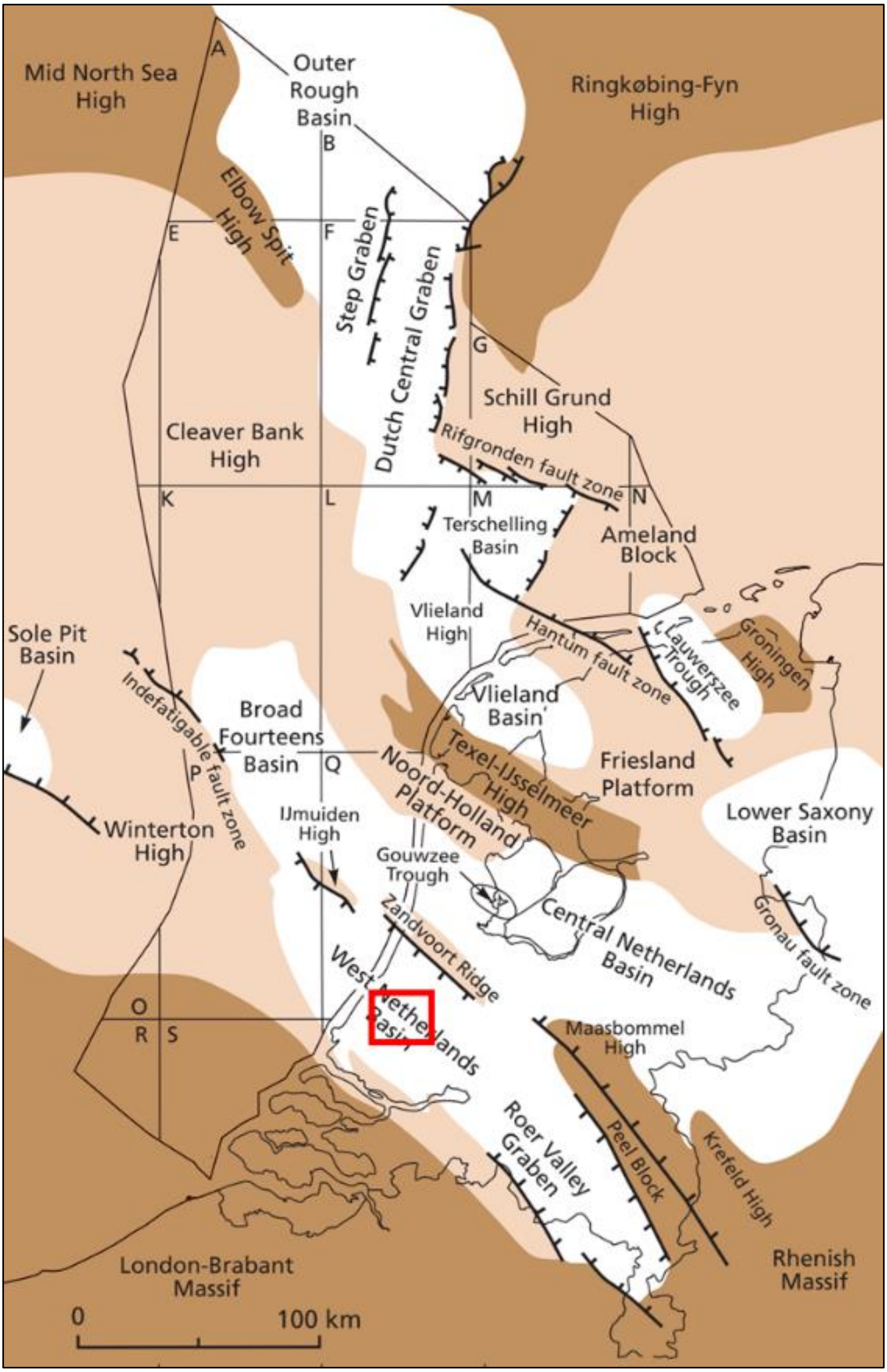


**Figure 4-1: Structural elements of Late Jurassic and Early Cretaceous in the Netherlands (from Herngreen & Wong, 2007). The area of interest is highlighted by the red square. Dark brown: structural high, partly subaerial landmass; light brown: platform, intermittently flooded; white: basin.**

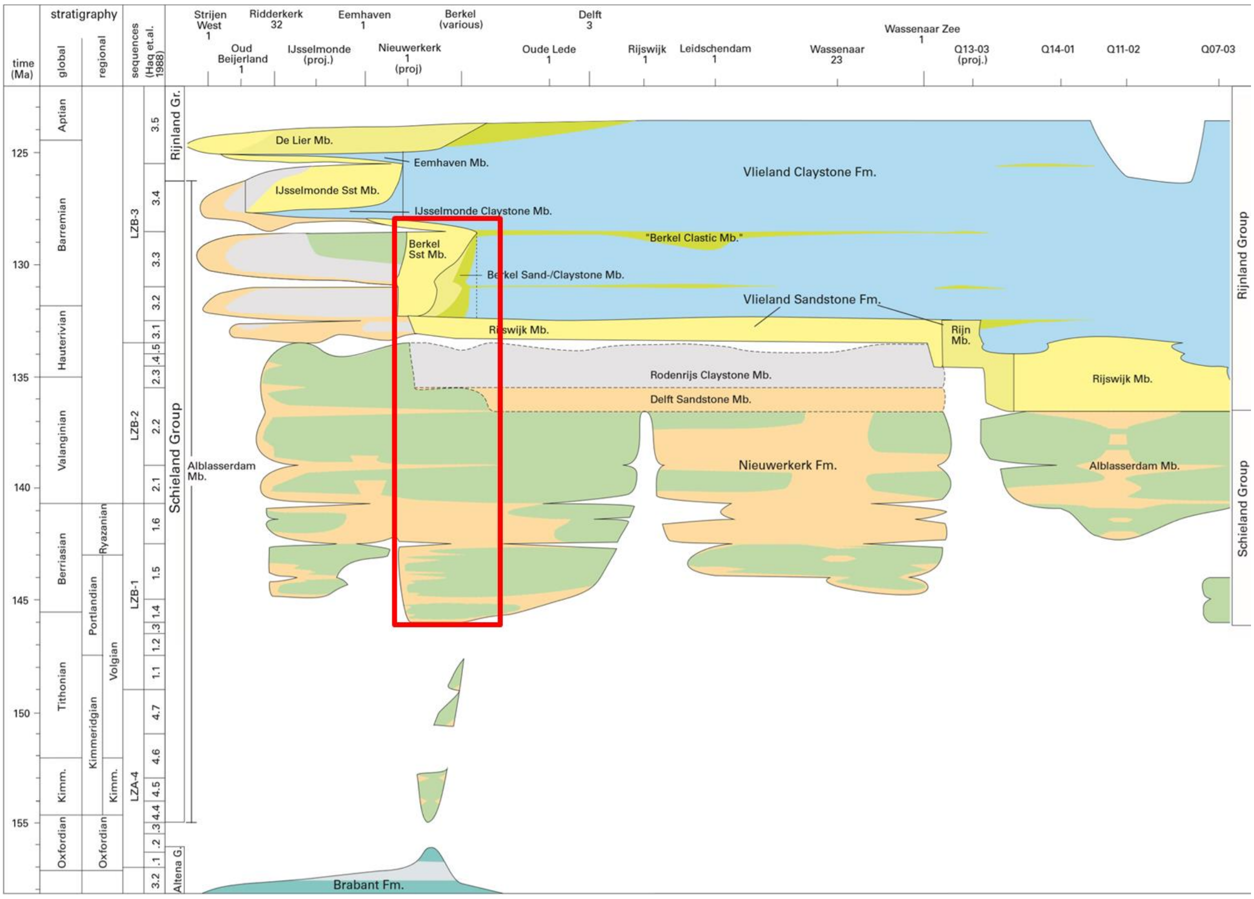


**Figure 4-2: Stratigraphy of the West Netherlands Basin. The red rectangle shows the schematic stratigraphy in the subsurface of the area of interest (from van Adrichem Boogaert & Kouwe, 1994).**

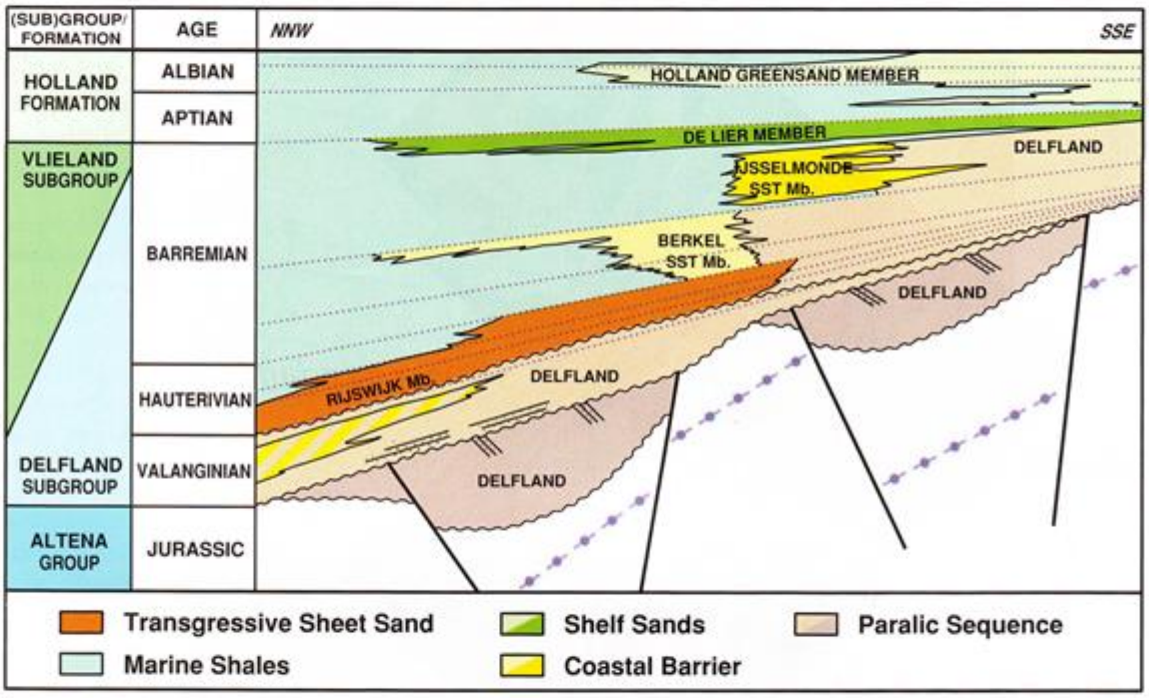


**Figure 4-3: Schematic Lower Cretaceous stratigraphy of the West Netherlands Basin. The diagram illustrates the stratigraphic position and geometry of several reservoir layers in this basin (from Racero-Banea & Drake, 1996).**

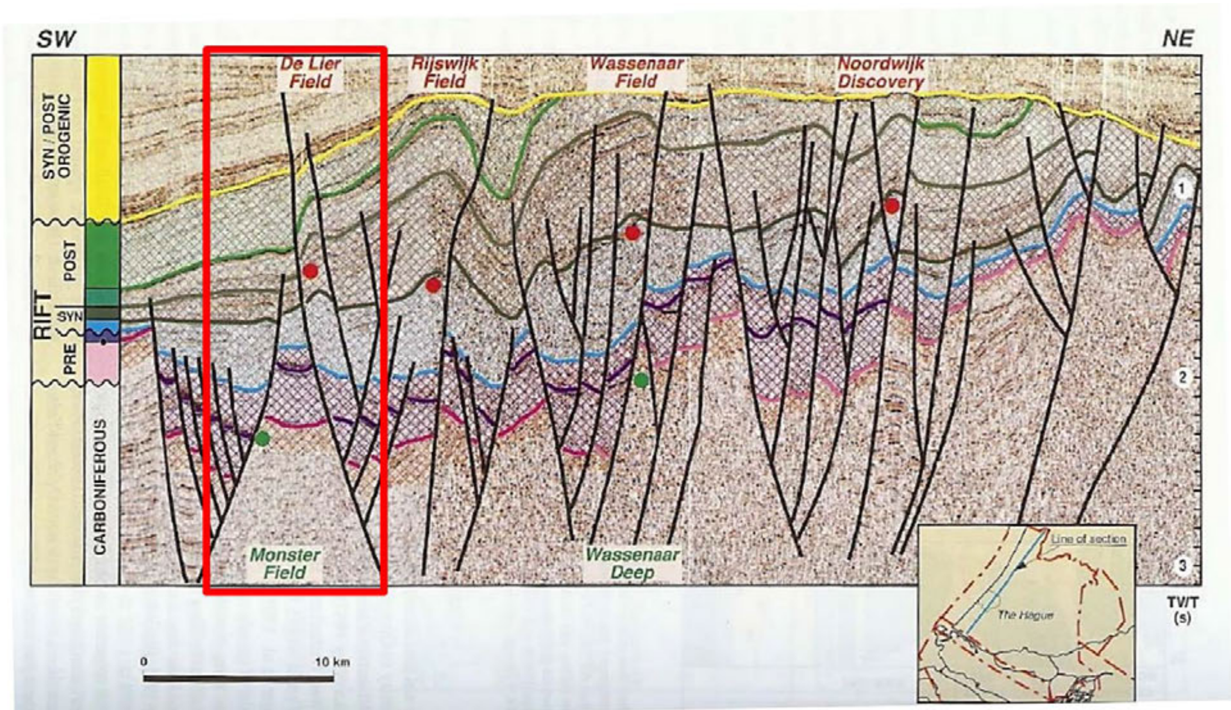


**Figure 4-4: Published seismic section showing the structures which dominate the study area. The figure was published by Racero-Baena and Drake (1996). The horst structure related to the De Lier Field extends towards the Southeast. The planned geothermal wells are situated on the southern part of the horst.**

## 4.2 Risk of encountering hydrocarbons

The study area is in a basin with a mature oil and gas source, the Posidonia Formation (De Jager et al. 1996) that has generated and still is generating large quantities of oil and gas. Many oil and gas fields are present in close proximity to the proposed doublet (Figure 4-5). Hydrocarbons can be present in two forms: 1) oil and gas accumulations or 2) gas dissolved in formation water and oil dispersed in formation water.

### 4.2.1 **Traps with accumulations of free oil and/or gas**

Several oil and gas fields are present near the planned doublet (Table 4-1). De Gaag and Maasdijk fields produce gas from the Triassic Buntsandstein, the De Lier field produces oil and gas from the Cretaceous De Lier Member and Holland Greensand Member. None of these fields have produced or produce from the target geothermal reservoirs.

**Table 4-1: Oil- and gas fields near the planned doublet.**

| Field | Content | Status | Reservoir |
|---|---|---|---|
| De Lier | Oil & Gas | Producing | De Lier Member/Holland Greensand Member |
| Gaag | Gas | Producing | Bunter |
| Maasdijk | Gas | Producing | Bunter |

### 4.2.2 **Hydrocarbons dissolved or dispersed in formation water**

In most surrounding geothermal wells, dispersed oil and/or dissolved gas is present in the produced formation water from the reservoirs (Vlieland Sandstone Formation and/or Nieuwerkerk Formation). The reservoirs acted and may still act as migration paths for hydrocarbons. Four out of the six doublets in the West Netherlands Basin (Table 4-2) co-produce gas in quantities between 1 and 1.5 $Nm^3$ for each produced $m^3$ of formation water. The first Ammerlaan doublet PNA-GT-01 and -02 also produced small quantities of oil. After the completion of the doublet, production was halted temporarily in 2011 but continued a few weeks after. Since then minor to no oil was (co)produced. It is likely that the planned doublet will produce small quantities of dissolved gas, similar to other geothermal doublets in the area. Free oil and gas is not expected because no structural or stragraphic trap is observed. The nearby well LIR-45 did encounter some oil during an RFT, but this was from the Rijswijk Member.

**Table 4-2: Hydrocarbon observations in nearby geothermal doublets. Data from Bakker (2010).**

| Geothermal doublet | Normalized volume of gas per volume of produced water |
|---|---|
| Den Haag | 1.5 $Nm^3/m^3$ |
| PNA-GT-01 and 02 | 0.5 $Nm^3/m^3$; small amounts of oil are present |
| PNA-GT-03 and -04 | 1 $Nm^3/m^3$ |
| VDB-01, -02, 03, 04 | traces |
| HON-GT-01 and -02 | 1 to 1.5 $Nm^3/m^3$ |

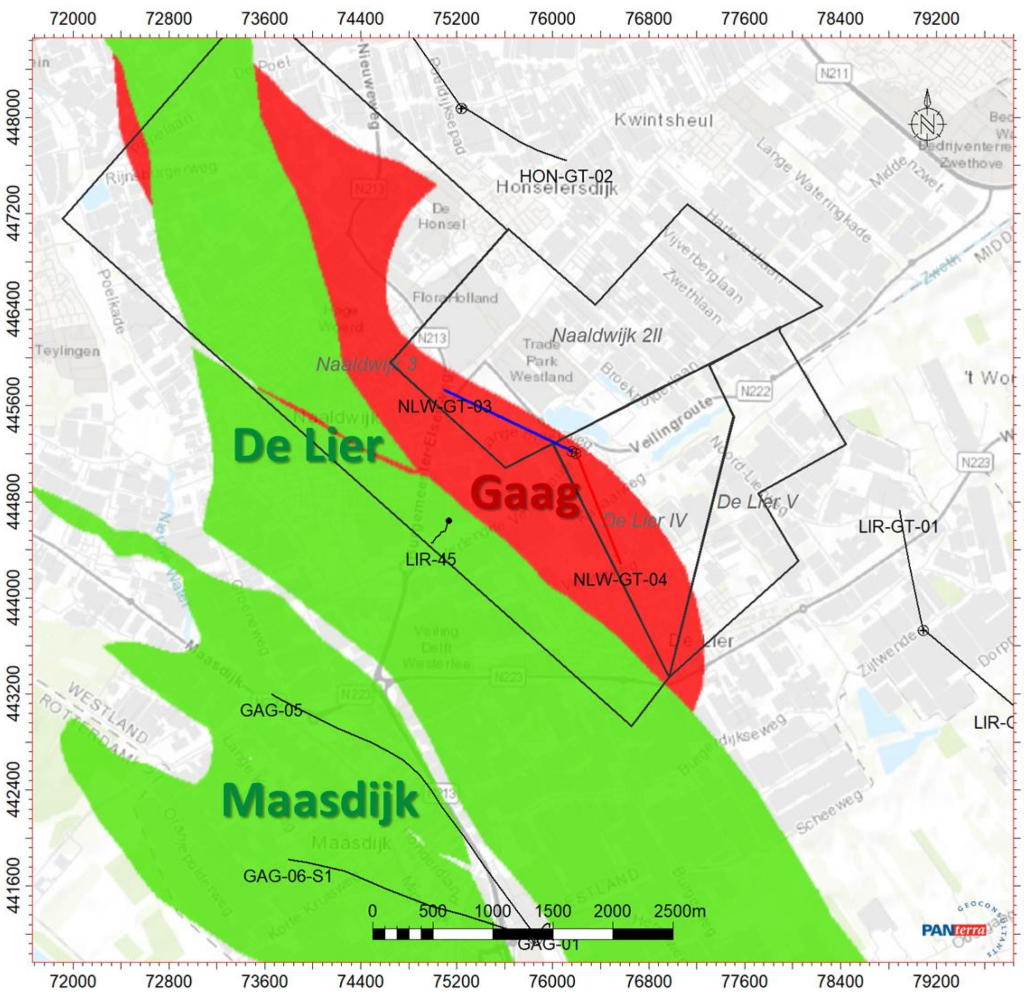


**Figure 4-5: Location of the planned doublet with respect to oil and gas fields (source www.nlog.nl).**

# 5 Available well and seismic data

## 5.1 Reference wells

Reference wells are listed in Table 5-1 and plotted in Figure 5-1. Wells were chosen based on proximity to the target area, data availability and quality and reservoir characteristics. The most important wells are NLW-GT-01 and LIR-45 they are located very close to the new doublet. There is significant well control in and around the study area; the well data quantity and seismic quality is sufficient for determination of reservoir characteristics and to tie wells to seismic.

**Table 5-1: Selected wells for the study and the purpose for which well data were used.**

| Well | Year drilled | Seismic (correlation or QC Velocity model) | petrophysics | correlation | notes |
|---|---|---|---|---|---|
| GAG-05 | 1998 | yes | yes* | yes | |
| HON-GT-01 | 2012 | yes | yes | yes | |
| HON-GT-02 | 2012 | yes | yes | yes | |
| LIR-45 | 1982 | yes | yes | yes | |
| LIR-GT-01 | 2014 | yes | yes | | No logs in public domain |
| LIR-GT-02 | 2014 | yes | yes | | No logs in public domain |
| MON-02 | 1982 | | yes* | | |
| MON-03 | 1990 | | yes* | | |
| NLW-GT-01 | 2018 | yes | yes | yes | |

*petrophysical interpretation performed by TNO in 2013 (www.NLOG.nl)

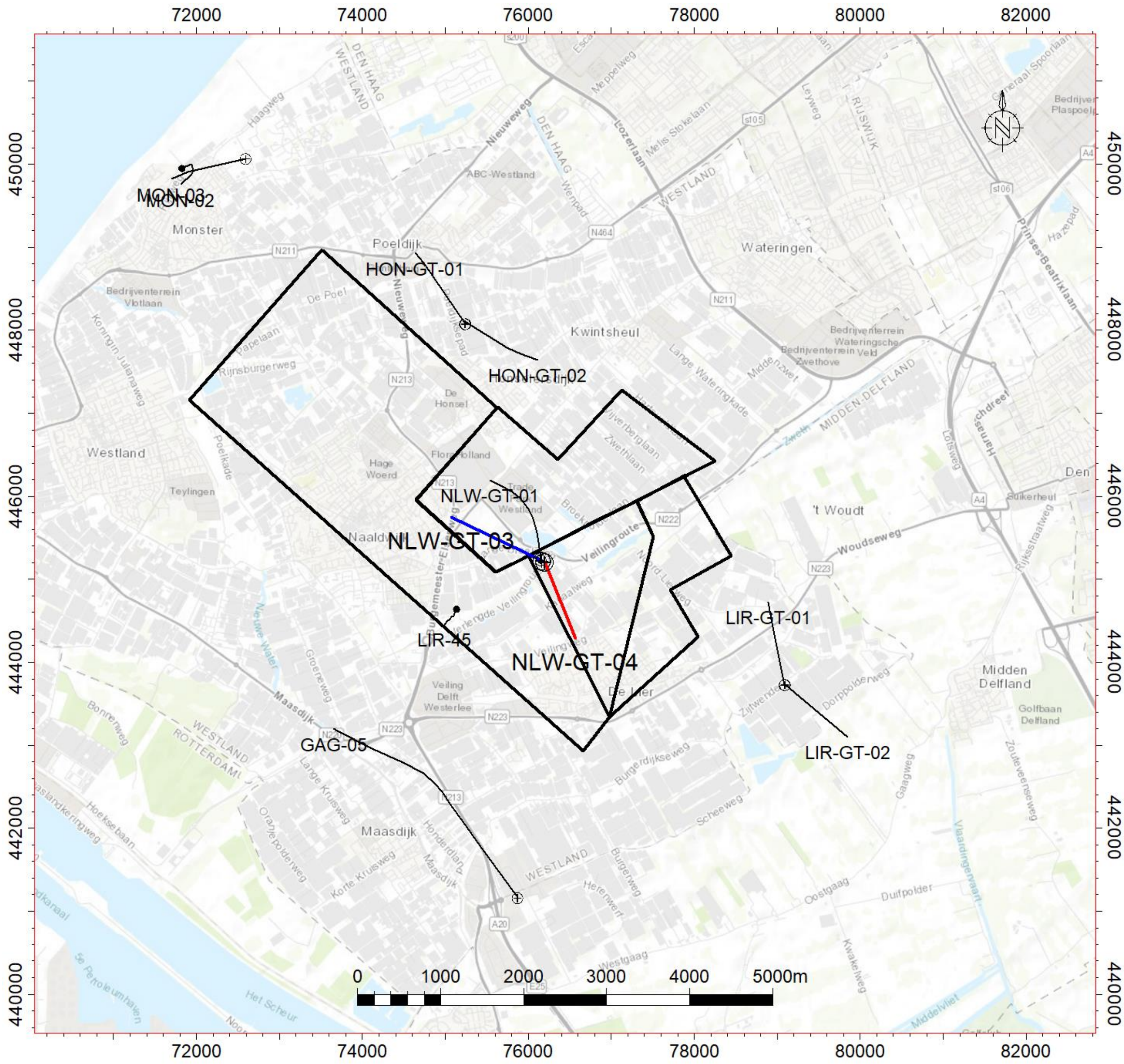


Figure 5-1: Map of the reference wells. The license boundaries are outlined in black.

## 5.2 Seismic data

Where present, seismic interpretation was performed on a small NAM reprocessed time cube (Figure 5-2), recently made available by the NAM. Outside of this cube, the interpretations were made based on the larger L3NAM1990c time survey that is available via NLOG.nl. The tie between the two cubes is quite good and no shifts were required. The reprocessed cube however, is of a better quality with better definition of faults and more continues reflections and reduced noise. The geometries of the surveys are given in Figure 5-3.

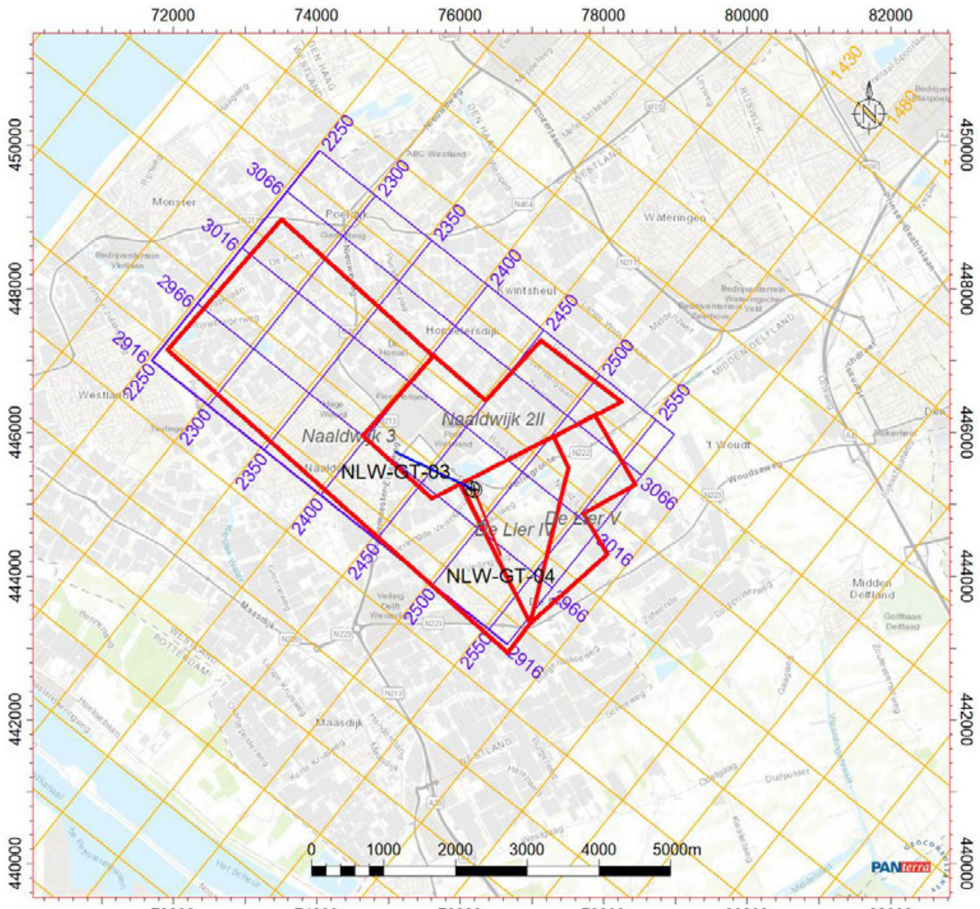


Figure 5-2: Location of the planned doublet and geothermal licences (in red) with respect to the NAM reprocessed 3D seismic time cube (in purple) and the larger L3NAM1990c survey (in orange).

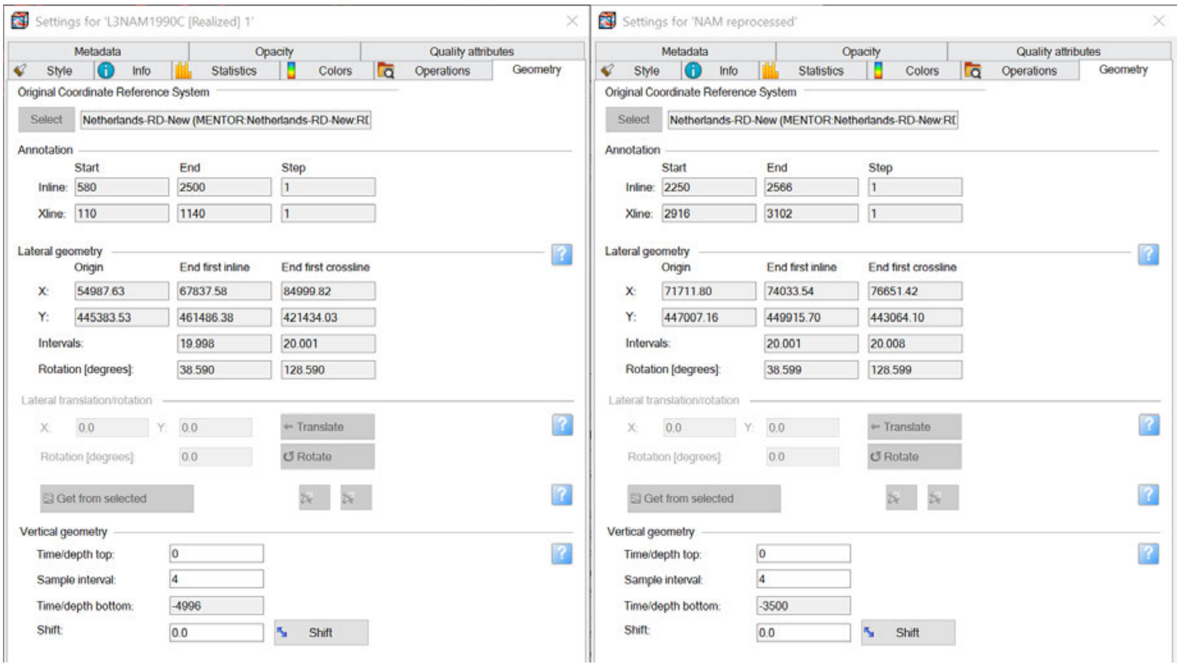


Figure 5-3: Geometry of the L3NAM 1990c survey (left) and the NAM reprocessing (right).

## 5.3 Coordinate system and system of units

The location of most data is in the new Netherlands National Triangulation System (*Rijksdriehoekstelsel*). Georeferenced data of different projection systems were converted to this system.

| | |
|---|---|
| Name: | Netherlands National System new: *Rijksdriehoekstelsel* new |
| Type: | Double Stereographic |
| Central Meridian: | 5.387638889 |
| Origin Latitude: | 52.156160556 |
| Scale Factor: | 0.999907900 |
| False Northing: | 463000.000000 |
| False Easting: | 155000.000000 |
| | |
| Units: | Meters |
| | |
| Datum: | Netherlands |
| Ellipsoid: | Bessel 1841 |
| Prime Meridian: | Greenwich |
| Transform Method: | Molodensky |
| Delta x (m): | 593 |
| Delta y (m): | 26 |
| Delta z (m): | 478 |

The units used in this report relate to the International System of Units (abbreviated SI from the French Système International). All distances are expressed in metres or in kilometres. Temperatures are expressed in degrees Celsius.

## 5.4 Additional data

GIS files (shapefiles and raster data) have been downloaded from the TNO portal in order to compare results and create maps:

- Well locations
- Seismic data
- Licenses
- Oil and gas fields

All shapefiles and raster files have been transformed from the UTM 31, ED50 to the *Rijksdriehoekstelsel* coordinate system with the Netherlands datum if necessary.

## 5.5 Database

Seismic data, formation tops, time-depth relations and deviation data were loaded in Petrel (version 2017) for seismic interpretation and time-depth conversion. The velocity model was derived in through regression of velocity data in excel. Well data (logs, formation tops, core data, etc.) were also loaded in Interactive Petrophysics (version 4.4) for curve QC. Maps were created using Petrel 2017.

# 6 Seismic interpretation and depth model

## 6.1 Method

Seismic interpretation was performed in Petrel 2017. Horizons were interpreted using auto-tracking where possible and otherwise picked every 10th in- and crossline.

## 6.2 Well to seismic ties

Checkshots from well LIR-45 were used to tie the well to the seismic (Figure 6-1). In general, there is good confidence in the seismic picks based on the well tie; the seismic character of the horizons (e.g. hard kick, soft kick, see Table 6-1) is in good agreement with the sonic logs of the wells. An example of a well tie is displayed in Figure 6-1. The seismic loops belonging to the base Vlieland (or top Rodenrijs Member) and the base of the delft sandstone could not be established with great certainty. The picks are therefore referred to as Near Base Vlieland and Near Base Delft. The Near Base Vlieland pick is tracked on the continuous event nearest the appropriate well top which was a through. The Base Delft has been picked on the through which forms the first angular unconformity below the Near Base Vlieland pick. This is in accordance with the geological model presented in section 7.1.

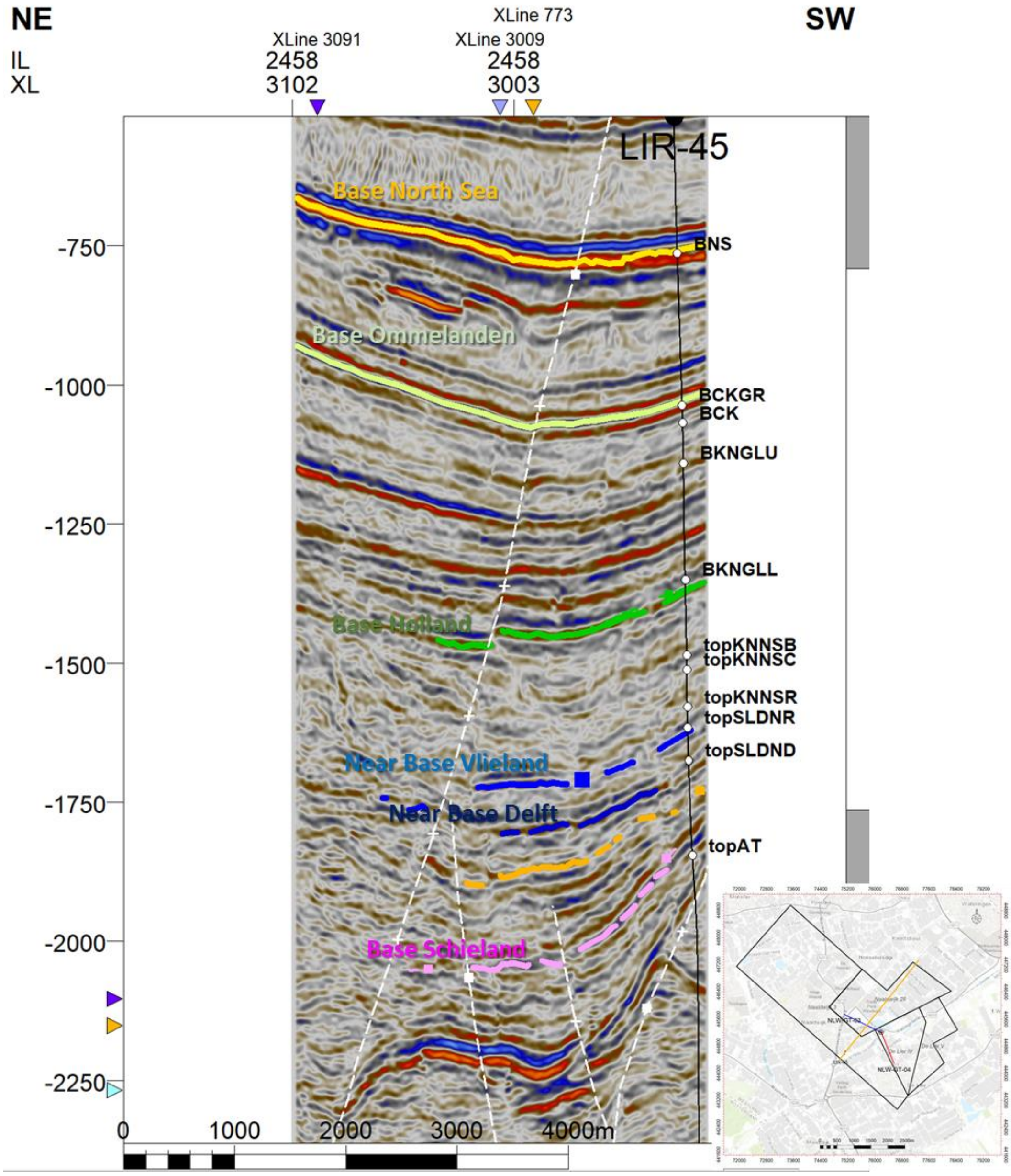


**Figure 6-1: Well tie for well LIR-45. There is a good match between picked reflectors and well tops.**

Table 6-1: Interpreted horizons used for this study.

| Horizon | Lithostrati-graphic code | Seismic character | Quality | Interpretation method |
|---|---|---|---|---|
| **Base North Sea** | BNS | Strong hard kick | Excellent | Auto-tracked |
| **Base Ommelanden** | BCKGR | Strong soft kick | Excellent | Auto-tracked |
| **Base Holland** | BKNGL | Hard kick, lowest hardkick above 'transparent' Vlieland section | Moderate to good | Auto-tracked /Manual pick |
| **Near base Vlieland** | BSLDNR | Hard kick, sometimes difficult to map | Moderate | Manual pick |
| **Near base Delft** | SLDNA | Very weak hard kick, often difficult to map | Very poor | Manual pick |

## 6.3 Gridding algorithm

All horizons were gridded using the convergent interpolation methodology after which grids were minimally smoothed. Cell size is 50m x 50m.

## 6.4 Time-depth conversion

A depth dependent linear velocity function is used to convert the time interpretations to depth. The $V_0$, k function applied describes the interval velocity as a function of depth, Z, and has the following form:

$$V_{int} = V_0 + k * Z \qquad (1)$$

Vertical lithological changes are not modelled with this function and the $V_0$ and k parameters describe the combined effects of burial and lateral lithological changes. The input data consists of interval time and interval depth pairs derived from checkshot calibrated integrated sonic logs. In order to improve the robustness of the model the input dataset from NLOG (used for VELMOD 1 through 4) has been used. The wells with velocity data within a ~24 km square around the target location have been included (see Figure 5-1).

In total, four velocity layers have been defined; The North Sea Supergroup, Chalk Group (down to Base Ommelanden), a combined Texel, Holland Formation and Vlieland subgroup and Schieland Group. The $V_0$ and k parameters for the best fit model for each layer are summarized in Table 6-2. Table 6-3 summaries the error of the velocity model between the picks in the well and the depth of the calculated seismic horizon of Base Vlieland. This is the base of the velocity layer nearest the top of the Delft Sandstone Member. Please note that the numbers in this table represent the uncorrected results i.e. no well correction has been applied at any level. As seen in the table of the Base Vlieland, the $V_0$, k model results in an average depth error of 0.99% with a maximum of 3.27 % for GAG-05. The calculated error for the other horizons are given in Appendix 10.8, The generated depth maps are shown in Appendix 10.4.

Table 6-2: V0- and k parameters of the velocity layers of the updated velocity model.

| Velocity layer | $V_0$ (m/s) | k ($s^{-1}$) |
|---|---|---|
| North Sea | 1,780 | -0.435 |
| Chalk | 1,550 | -1.485 |
| Holland+Vlieland | 2,200 | -0.69 |
| Schieland | 2,900 | -0.28 |

**Table 6-3: Residuals per well at the Base Vlieland before applying well adjustment.**

| Base Vlieland<br>Well | Base in well (mTVDss) | Residual (m) | Residual (%) |
|---|---|---|---|
| GAG-05 | -2402.89 | -78.46 | 3.27% |
| HON-GT-01 | -2277.63 | -3.93 | 0.17% |
| HON-GT-02 | -2308.84 | -23.05 | 1.00% |
| LIR-45 | -2069.51 | 0.68 | 0.03% |
| LIR-GT-01 | -2190.08 | -29.74 | 1.36% |
| LIR-GT-02 | -2256.13 | 3.57 | 0.16% |
| NLW-GT-01 | -2229.63 | 20.33 | 0.91% |
| **Average** | | **-15.8** | **0.99%** |

## 6.5 Top and base reservoir map

The mapped top and base reservoir maps are displayed in Figure 6-2 and Figure 6-3. The new Naaldwijk geothermal wells are located in the same fault block as the recently completed NLW-GT-01 well and NLW-GT-02 which is currently being drilled. A series of NW-SE trending normal and thrust faults are present in the study area. The target locations of the planned doublet are situated in the centre of the fault block and the pair is oriented parallel to the local fault trend, minimizing the risk of the presence of faults in between the injector and producer.

As the Top of the reservoir could not be picked, a top reservoir map was created by shifting the depth converted Top Rodenrijs map down to the top reservoir well tops with an isochore map.

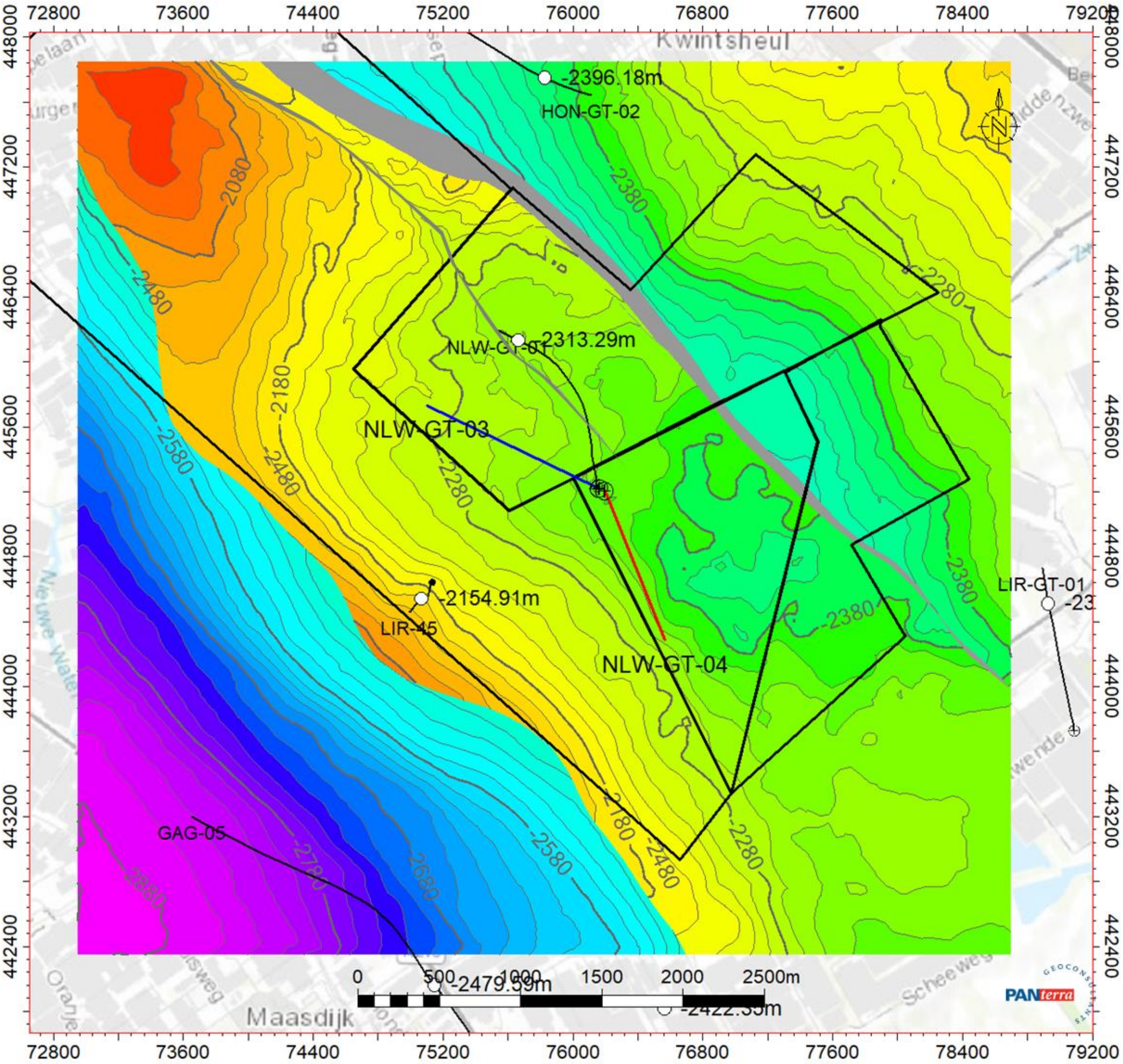


**Figure 6-2: Depth map of top Delft reservoir with the well trajectories of the planned doublet (NLW-GT-03 and -04) and other nearby wells.**

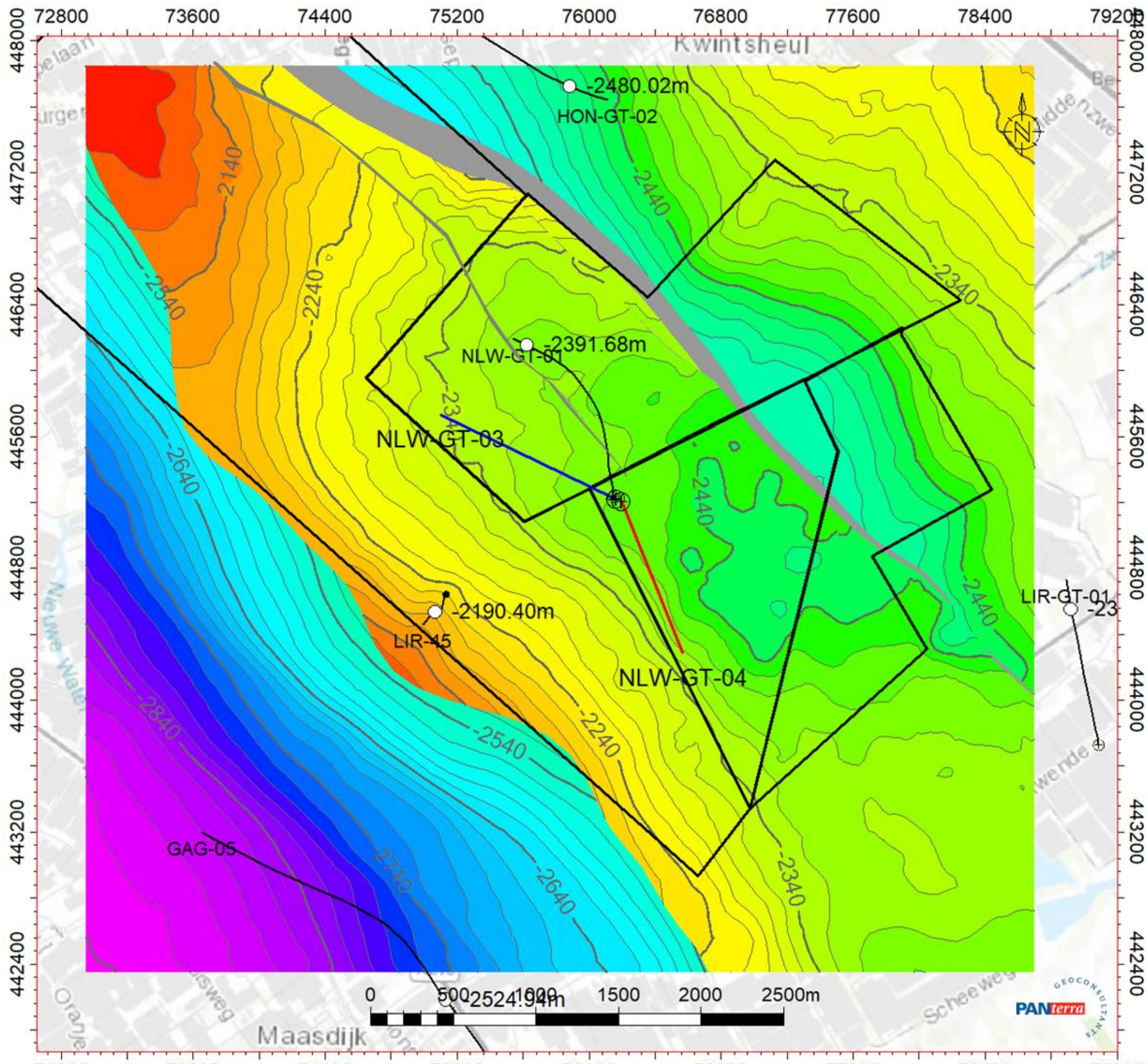


**Figure 6-3: Depth map of base reservoir with the well trajectories of the planned doublet (NLW-GT-03 and -04) and other nearby wells.**

### 6.5.1 Reservoir thickness maps

The reservoir thickness map was created by subtracting the depth converted and well top corrected interpretation of the base reservoir map from the top reservoir map.

The pick of the Top Rodenrijs (on which top reservoir is based), and to a higher degree the interpretation of the Base Delft is somewhat uncertain. For both horizons, the actual loop could not be identified with certainty. However, the picked loops are definitely close to the actual event. The correction of the picked horizons with respect to the well tops, combined with the fact that there is reasonable well control, ensure that the errors are restricted. The thickness map shown in Figure 6-4 shows a clear trend in which the thickness of the reservoir increases towards the Northeast within the target fault block. This can also be observed in seismic cross-section (see Figure 9-2 and Figure 9-3).

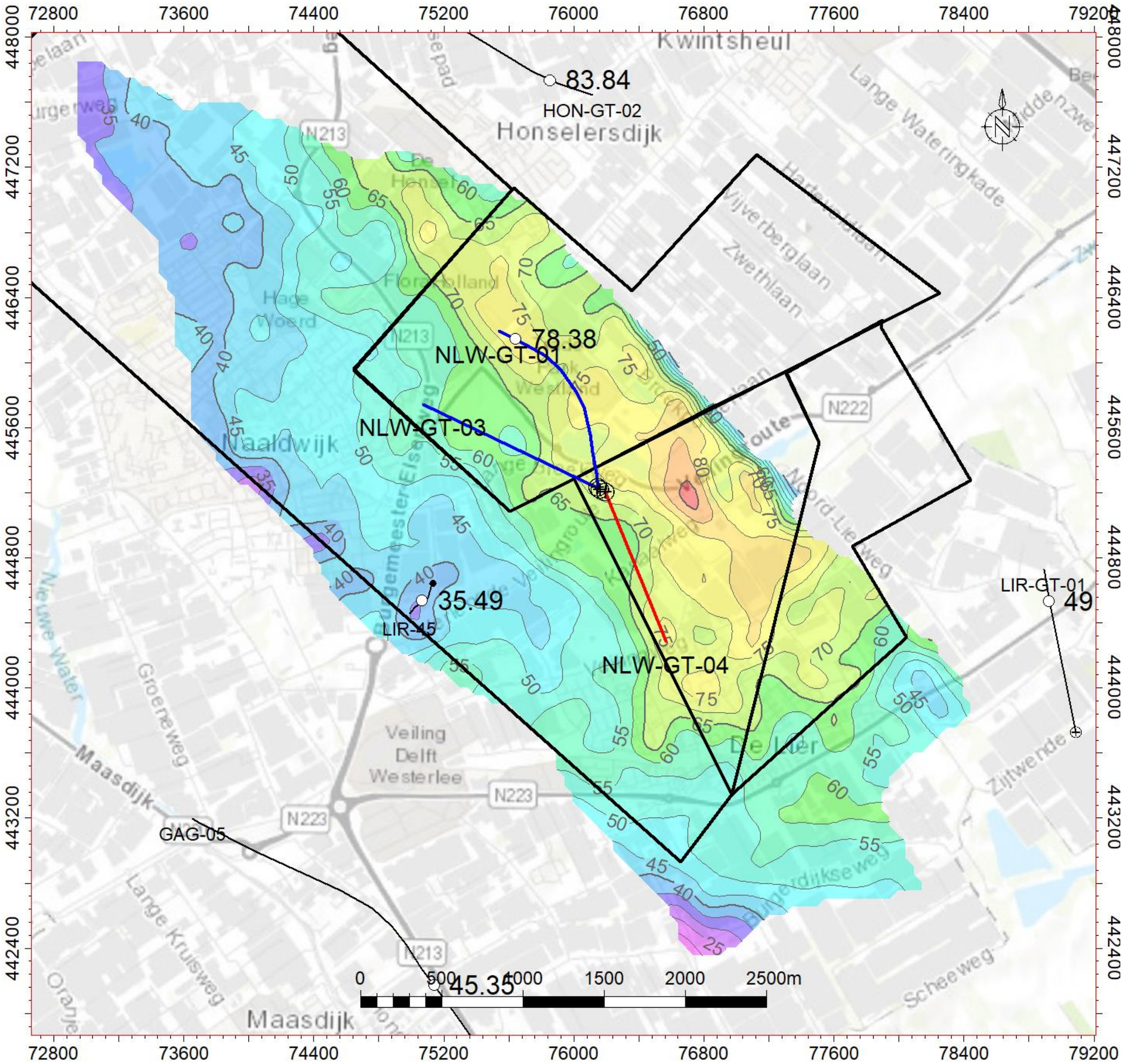


**Figure 6-4: Thickness map of the reservoir based on seismic data. The isochore points of the wells used in the analysis are highlighted by the white circles.**

### 6.5.2 Coordinates of the planned wells

Coordinates for the planned wells are listed in Table 6-4 and Table 6-5.

**Table 6-4: RD coordinates of the top and base reservoir, surface location and TD location of the planned well NLW-GT-03.**

| | NLW-GT-03 | | |
|---|---|---|---|
| **Pick** | **X (RD)** | **Y (RD)** | **TVDSS (m)** |
| Surface location | 76159.0 | 445224.0 | 0.0 |
| Top Reservoir | 75211.6 | 445677.9 | -2305.9 |
| Base Reservoir | 75162.9 | 445701.2 | -2366.3 |
| TD | 75073.5 | 445744.1 | -2419.8 |

**Table 6-5: RD coordinates of the top and base reservoir, surface location and TD location of planned well NLW-GT-04.**

| | NLW-GT-04 | | |
|---|---|---|---|
| **Pick** | **X (RD)** | **Y (RD)** | **TVDSS (m)** |
| Surface location | 76193.0 | 445209.0 | 0.0 |
| Top Reservoir | 76531.4 | 444371.5 | -2366.9 |
| Base Reservoir | 76540.6 | 444348.6 | -2403.9 |
| TD | 76566.0 | 444285.7 | -2505.1 |

## 6.6 Uncertainty in the depth maps

The low residuals (see Appendix 10.8) give confidence in the accuracy of the depth maps. Moreover, there is a good match between the well tops of wells LIR-45 and NLW-GT-01 with the seismic reflectors. The uncertainty of 10% used in DoubletCalc is more than sufficient to cover the uncertainty range. Also, the planned doublet lies no more than a few hundred meters from the NLW-GT-01 and LIR-45 wells. The actual uncertainty should be in the range of 1%.

# 7 Aquifer Characteristics

## 7.1 Stratigraphic correlation and lateral variety of the reservoirs

In Figure 7-1, a correlation panel is given for the wells in the area which drill into the Delft Sandstone Member and the Alblasserdam sands closest to the target location. The character of the Delft Sandstone Member is quite varying in terms of thickness and sand distribution. The perforation intervals of NLW-GT-01 are also shown in Figure 7-1. The lower perforation interval covers a section which is likely to be a sand of the Alblasserdam Member. The petrophysical analysis (see section 7.3) shows that sands in this part are less permeable. As such, it is expected that the production in NLW-GT-01 is dominantly originating from the upper perforation interval. Please note that no flow meter measurements are available.

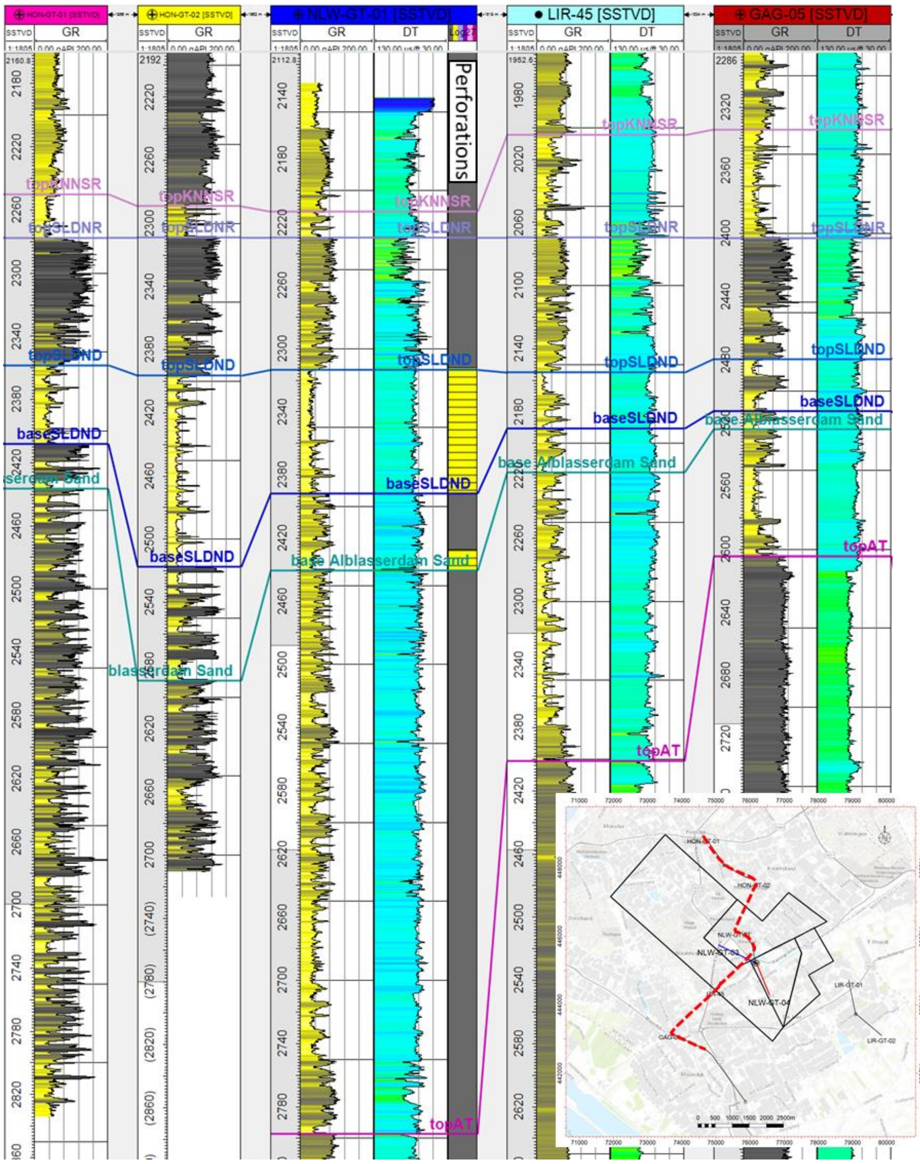


**Figure 7-1: Regional correlation panel showing the gamma ray logs (non-normalised) flattened with respect to the top Rodenrijs Member (the inlay map shows the location of the wells used, connected by the red, dashed line).**

### 7.1.1 Delft Sandstone and Alblasserdam

The Delft Sandstone is thought to be deposited in a floodplain by a river system flowing from southeast to northwest. The Delft Sandstone consists of fine- to coarse-grained sand. The thickness of the Delft Sandstone is influenced by the syn-rift deposition of the sediments (see Figure 7-2). The depositional model described by Den Hartog Jager

(1996) is found to correspond well with the observations made in the seismic and in the wells (see Figure 7-2 and Figure 7-3).

The well logs show an upper section with the clean, often blockey sands of the Delft Sandstone Member overlain by the shales of the Rodenrijs Claystone Member and a lower section with the alternating sands and shales of the Alblasserdam Member (see Figure 7-1). In the seismic, an angular unconformity is observed near the depth of the base of the Delft well top which is picked as the Near base Delft (see Figure 6-1, Figure 9-2 and Figure 9-3). The half-graben in Figure 7-2 is representative of the half graben in which the planned wells are situated. The planned wells are located on the southwestern part of the half-graben where the overall sequence is relatively thin. This thinning however, mostly affects the Alblasserdam Member. This can also be observed in the well correlation panel presented in Figure 7-1 (NLW-GT-01 to LIR-45).

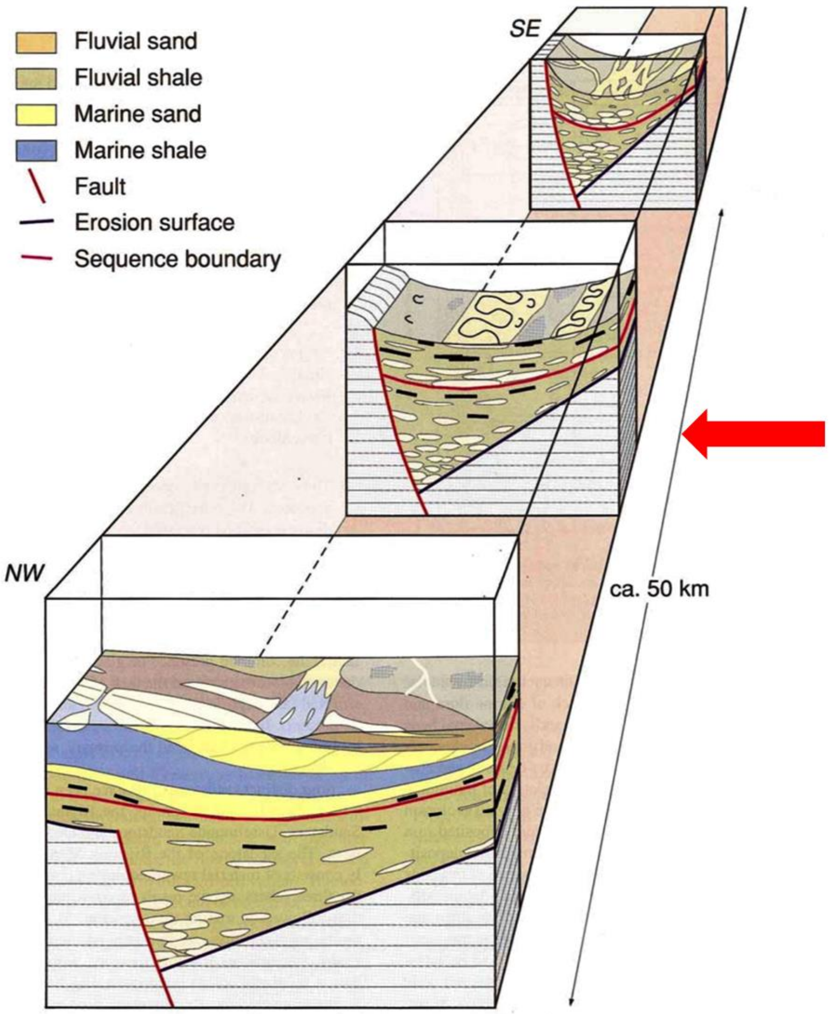


**Figure 7-2: Model for the deposition of the Delfland Subgroup in the West Netherlands Basin (from den Hartog Jager, 1996). The red arrow highlights the part of the mode which is appropriate for the current application. In this image the subgroup is divided into two parts; an upper and a lower part divided by a sequence boundary (red line). In the geological model presented here, this sequence boundary is the boundary between the Rodenrijs Mbr. plus Delft Sst Mbr. (top) and the Alblasserdam Mbr. (base).**

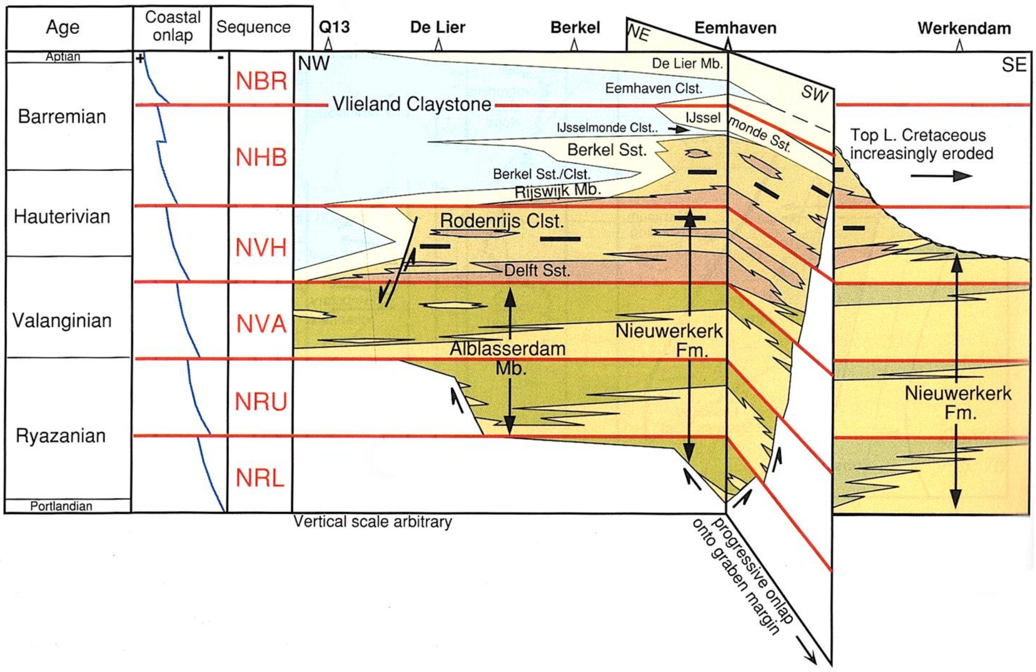


**Figure 7-3: Sequence stratigraphic scheme for the Lower Cretaceous of the West Netherlands Basin based on seismic and biostratigraphic data (from den Hartog Jager, 1996). Of particular importance to the current application are the Neocomian/Valangian (NVA) and the Neocomian/valanginian – Hautervivian (NVH) sequences.**

## 7.2 Gross thickness of the aquifer

The seismic interpretations of the near Top Rodenrijs and near Base Delft Sandstone Member show general thickening of the sequence towards the Northeast within the fault block (part of a larger half-graben). This can be explained by the influence of fault movement (specifically along the major faults which bound the syncline to the Northeast), in relation to the accommodation versus sediment supply during deposition. During deposition in the Early Cretaceous, the Late Kimmerian extension was still taking place.

As the logs in well NLW-GT-01 and LIR-45 show, this thickening affects both the Delft Sandstone and the Alblasserdam Member (Figure 7-1). However, the effect is more pronounced for the Alblasserdam Member. A similar observation can be made towards the West, where this part of the half-graben ends (see the map in Figure 6-2). As a consequence, the thickness of the reservoir is expected to gradually decrease from NLW-GT-01 towards LIR-45 with the planned wells in between. The thickness map is seismically restrained is assumed to be quite reliable. As such, an **8 m** uncertainty on an average reservoir thickness of **66 m** is found to be adequate.

### 7.2.1 Net to gross (N/G)

For the N/G calculation of the Delft Sandstone, the NLW-GT-01 and LIR-45 wells are considered most representative as these are closest to the new doublet. The petrophysical evaluation summarised in Table 7-1, shows that the N/G reduces from 0.94 in NLW-GT-01 to 0.84 in LIR-45 and may show the same trend as the thickness. For the DoubletCalc calculations, a **median N/G of 0.92** is assumed. The **minimum** has been set to **0.87** and the **maximum** to **0.96.**

## 7.3 Petrophysical evaluation

Reservoir parameters are mainly based on nearby geothermal well NLW-GT-01, which was petrophysically evaluated and tested. Nearby well LIR-45 was drilled in the same fault block as the planned doublet and NLW-GT-01 and was therefore also petrophysically evaluated. Other wells are further away from the planned doublet and not located in the same fault block and were therefore excluded from the petrophysical interpretation (see Figure 5-1).

### 7.3.1 Core data consolidation

Regional routine core analysis (RCA) data were collected to build the porosity-permeability relationships reported in section 7.3.2.

RCA Helium porosities were reportedly measured under near-atmospheric stress conditions and thus require correction for overburden stress, e.g. by the method of Hakvoort [1]. The average correction factor is 0.96. The RCA data relate to the total porosity system as sample preparation involved conventional (hot) oven drying. Juhasz-type stressed-brine correction was applied to the air permeability data [2] before application of the Phi-K transform (discussed in section 7.3.2).

The cored target sections have not seen XRD analyses that could give calibration points for clay content. Electrical parameters from regional knowledge indicate a cementation factor m at around 2.0 and tortuosity pre-factor of 1.0 (default). Saturation exponents were assumed at n=m=2.0.

### 7.3.2 Phi-K transform

Horizontal permeability (kh) was modelled via Phi-K transform of RCA poro-perm data as described in the literature [3]. The database was compiled from screening of public RCA data (www.nlog.nl) that was filtered for core analyses from the target interval in the West Netherlands Basin.

All data were corrected as described in section 7.3.1 prior to processing. The Phi-K transform was executed for the 10th, 50th (median) and 90th percentile (X10, X50 and X90, resp.) for the RCA data cloud from the target interval (SLDN), according to best practices described in the literature [3] and consistent with SDE+ specifications. These regressions were used to calculate the scale-independent Swanson mean [4]. The median regression was used to calculate the base case permeability curve for the Alblasserdam Member. The Delft Sandstone Member in this part of the West Netherlands Basin has proven to exhibit significantly higher permeabilities than expected from petrophysics (e.g. well test Honselersdijk, De Lier). In order to better approximate these higher well test permeabilities, the Swanson Mean regression is preferred as the base case permeability model for the Delft Sandstone Member in this part of the West Netherlands Basin.

Regressions for the Nieuwerkerk Formation (SLDN) are shown in Figure 7-4. Note that all regional SLDN core data are assumed representative for both the Delft Sandstone Member (SLDND) and the Alblasserdam Member (SLDNA) due to inconsistencies in the SLDND picks in the public database (www.nlog.nl) that cannot be resolved within the scope of this study. Deployment of the permeability model is documented in section 7.3.7.

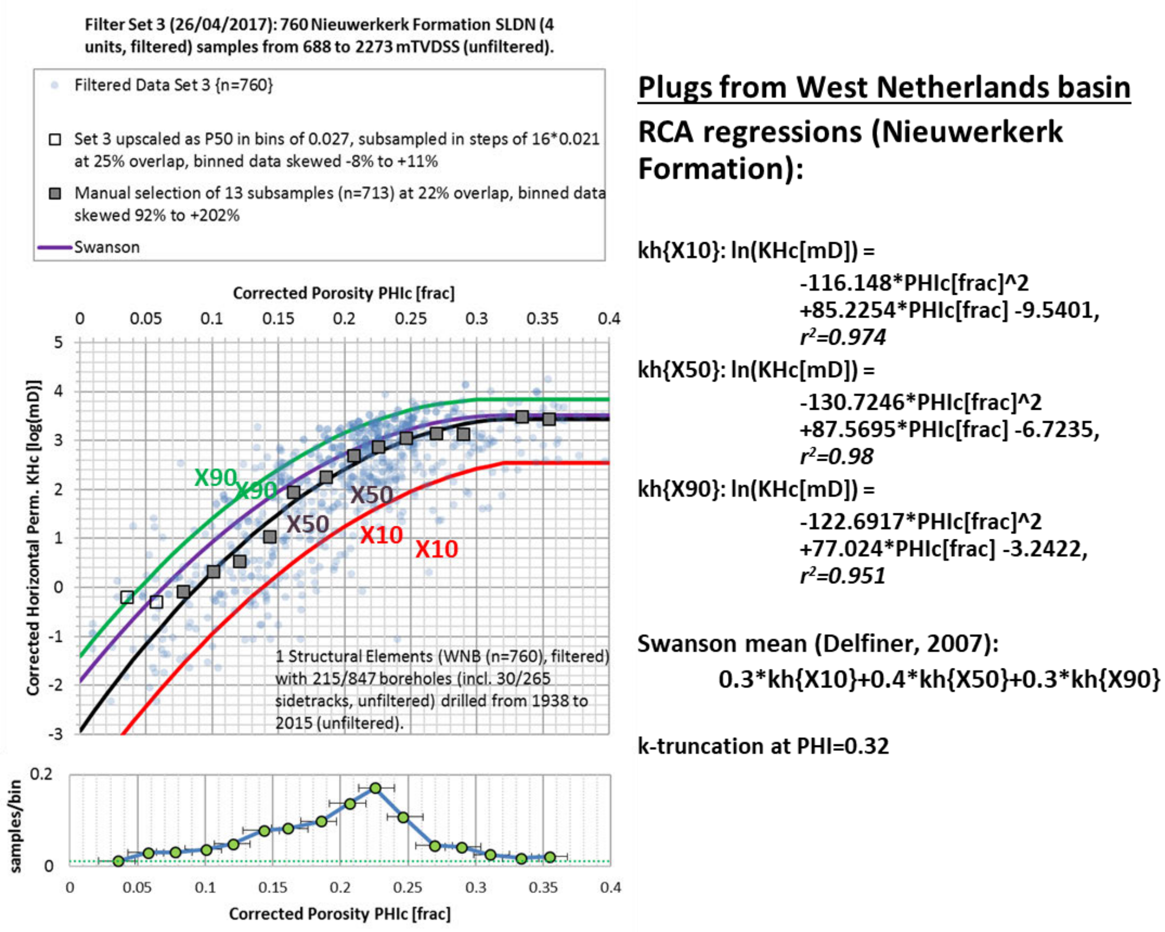


**Figure 7-4: Composite display of the Phi-K transform for the cored West Netherlands Basin Nieuwerkerk Formation Sandstone (SLDN) sections. The bottom histogram shows the bin size (displayed as horizontal error bars) and the normalized number of samples per bin. See text for brief description of methodology.**

### 7.3.3 Log curve consolidation

Digital logs of the well NLW-GT-01 and LIR-45 were loaded and processed in Interactive Petrophysics (IP). Quality control involved curve selection based on comparison of signals from different vintages (wireline, repeat runs etc.).

Wireline neutron signals were thus corrected for mud weight, mudcake, borehole salinity (WBM wells only) and formation temperature using the vendor's correction charts where considered necessary. All bulk density logs were already pre-corrected for hole size. The caliper is engaged in all processed sections and porosity logs (density, neutron, also sonic) are not notably affected by borehole washout effects.

All processed well logs were measured in water-based mud systems. In well NLW-GT-01 resistivity logs were not run. Mud and invasion corrections for electric logs were not conducted. The use of uncorrected resistivity curves is not critical for the purposes of this study

### 7.3.4 Conventional log processing workflow

Following standard processing procedure, clay volume is modelled prior to deployment of the integrated porosity (PHI) and water saturation (SW) module of the processing software (IP). VCL is used to estimate clay bound water (CBW) in order to model effective porosity (PHIE) from the total porosity signal (PHIT) that is picked up by the porosity logs (bulk density, neutron and sonic curves). PHIT and SW are solved simultaneously because the saturation determines the bulk fluid signal (e.g. brine density) whereas SW is coupled to porosity.

### 7.3.5 **Shale and clay volume**

Clay content is first modelled in the shale domain (VSH) before it is cast into the clay mineral domain (VCL). This procedure has the advantage that shale end-member at VSH=100% can be picked from the well log signals whereas VCL=100% is always located outside the data range (since rocks entirely composed of clay minerals do not exist in nature). The following relationship represents the default estimate for the clay mineral content of a 'standard shale':

VCL = VSH * 0.7 [vol.frac]

In other words, shales are approximated to contain an average of about 70% clay minerals. Calibration of VSH was performed iteratively using the Gamma Ray method (VSH_GR) and the neutron-density method (VSH_ND). End-members for the VSH_GR linear model were picked in histograms for each individual well in order to compensate for vintage-related differences between the Gamma Ray logs.

Calibration of the neutron-density cross-plot (for VSH_ND) was done by iterative matching of VSH_GR versus VSH_ND. Overestimation of clay content is avoided by determination of the minimum VSH curve for further petrophysical processing: VSH = min{VSH_ND, VSH_GR}.

### 7.3.6 **Porosity and water saturation**

Total porosity curves (PHIT) were calculated using the density method, neutron-density method and sonic method. Model parameters are adopted from the VSH parameters on a well-by-well basis (7.3.5). The different methods result in similar porosity logs. The neutron-density derived porosity logs were selected for further calculations. In the Alblasserdam Member of well LIR-45, neutron and density logs were not run successfully; porosity is therefore calculated from the sonic log. Effective porosity (PHIE) is modelled by stripping the clay-bound water (CBW) off the PHIT curve. CBW is a function of the VCL curve, wet clay densities as picked in the neutron-density cross-plot for each well, and the average dry clay density of 2.78 $g/cm^3$ for Illite-prone clay mineralogy.

The SCAL-based electrical parameters discussed in section 7.3.1 plug into the Archie water saturation equation (only well LIR-45, NLW-GT-01 does not have the required log suite). Deployment of the Archie-type saturation model is important for the purposes of this study as the final porosity curve is impacted by the formation water salinity that plugs into the simultaneous analytical solution for porosity and water saturation. Formation water salinity was obtained by the Pickett calibration method. The equivalent fluid density in conjunction with the matrix density (shale+quartz) is utilized by the interpretation software to solve for total and effective porosity curves (PHIT and PHIE, resp.).

### 7.3.7 **Permeability modelling**

Horizontal permeability (kh) curves were modelled via application of the Phi-K transforms (section 7.3.2) to the effective porosity curves (PHIE). Low (X10), mid (X50 for the Alblasserdam Member and Swanson Mean for the Delft Sandstone Member) and high case (X90) permeabilities were calculated. As described in section 5.2.2, all model-derived permeabilities are truncated near the maximum measured core porosity.

### 7.3.8 **Reservoir definition**

Reservoir zones are defined as such if they have a minimum (horizontal) permeability of 1 mD and Vshale of <50%. In the reservoir, arithmetic averaging of the kh-curves was used to obtain regular horizontal permeability values for each zone of interest. Reservoir properties for the evaluated wells are shown in Table 7-1.

Table 7-1: Aquifer characteristics based on log evaluation.

| Well | Zone Name | Top<br>m TVDSS | Bottom<br>m TVDSS | Gross<br>m TVDSS | Net<br>m TVDSS | N/G<br>Dec | Av Phi<br>% | Av Perm P90<br>mD | Av Perm P50<br>mD | Av Perm P10<br>mD |
|---|---|---|---|---|---|---|---|---|---|---|
| LIR-45 | SLDND | 2154.9 | 2190.4 | 26.4 | 22.1 | 0.84 | 0.19 | 21.7 | 573.6 | 1486.1 |
| NLW-GT-01 | SLDND | 2313.2 | 2391.7 | 74.5 | 70.1 | 0.94 | 0.19 | 20.9 | 534.4 | 1381.3 |

## 7.4 Well test evaluation

### 7.4.1 NLW-GT-01

A well test was performed of the Delft Sandstone Member in well NLW-GT-01 (Analysis of Well Test NLW-GT-01, 2018). During the 30 hours test (with 9 hours of water production) of well Naaldwijk GT-01, starting 28 Feb. 2018, the water production rates varied between 215 and 428 $m^3$/hr with a cumulative production of 3350 $m^3$.

Evaluation of the test indicates an average reservoir permeability of about 700 mD if all layers of the 83 m thick cumulative perforation intervals contribute. It is likely however, that the lower perforation interval contributes relatively little which means the average permeability may actually be higher.

The permeability derived from the well test is higher than the permeability derived from the petrophysical analysis (section 7.3.8). Please note that the permeability from the well test is regarded as more reliable.

### 7.4.2 Honselaarsdijk

A well test was performed for HON-GT-02 and evaluated by PanTerra in 2012 (described in *advies aanvraag Garantieregeling AARD03002 Geothermie De Lier* found on www.rvo.nl). The evaluation concluded that the permeability of the Delft Sandstone Member is 1190 mD. The reservoir at HON-GT-02 is situated approximately 2 to 4 km from the target of NLW-GT-03 and -04.

### 7.4.3 De Lier

An analysis for the well tests for LIR-GT-01 and GT-02 is also published (*Analysis of Welltest LIR-GT-01* and *Analysis of Welltest LIR-GT-02* from August 2014 by Panterra, G1107 on www.rvo.nl). These tests show that the average reservoir permeability of the Delft Sandstone Member is 1000 mD and 1300 mD for well -01 and -2 respectively assuming that the whole net sand contributes to flow. An interference test showed that the permeability between the wells is as high as 2000 mD. The reservoir at LIR-GT-01 and -02 is situated approximately 2.5 to 5 km from the target of NLW-GT-03 and -04.

## 7.5 Evaluation production data

Production data were not evaluated.

## 7.6 Permeability estimates from the public domain

A petrophysical evaluation of the Delft Sandstone was performed by TNO. Porosity and permeability averages of 20 wells were calculated. Figure 7-5 shows the range of calculated porosities and permeabilities. The results are also found in more detail on NLOG and summarised in Table 7-2 (for the wells nearest the concession). The well closest to the NLW-GT doublet is LIR-45. Compared to the PanTerra LIR-45 well tops, the Delft Sandstone as picked by TNO is relatively thin, but clean and has an average permeability of 747 mD.

Important to note is that most of the results from the petrophysical analysis give permeabilities which are lower than those from the well tests described above. These well tests give the most reliable measure of average permeability for the whole producing reservoir.

In an effort to visualise the permeability measurements from all public sources a bit more comprehensively, the data has been gridded (see Figure 7-6). In addition, the well test result from NLW-GT-01 has been included. Fault lines have not been included, but there appears the be a permeability trend where permeability reduced towards the Southwest and towards the West.

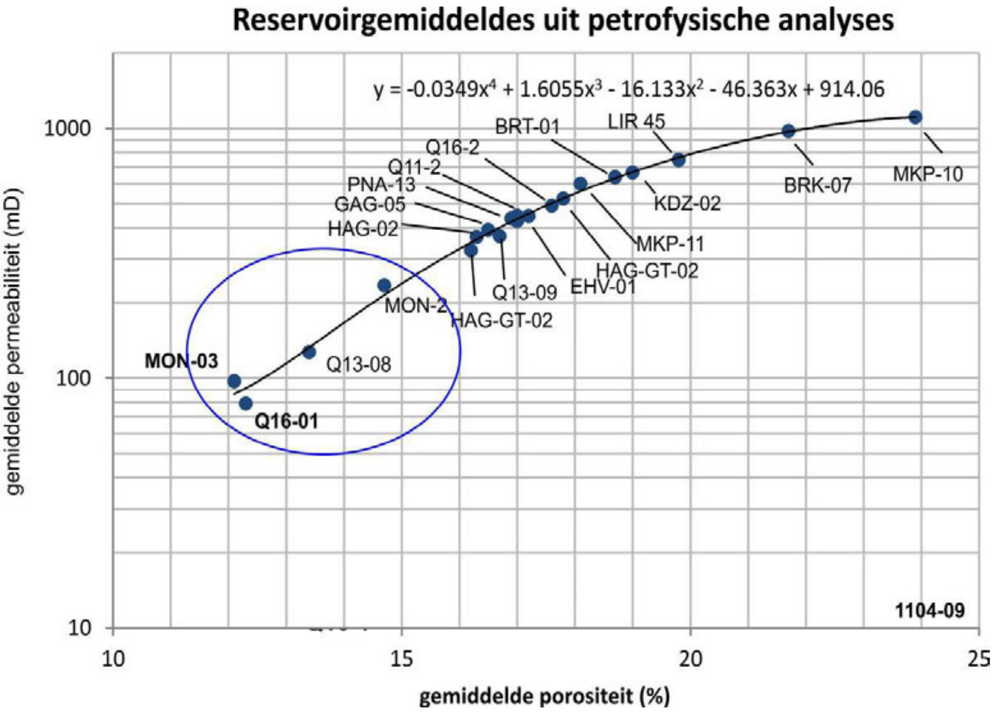


**Figure 7-5: Mean porosity vs. mean permeability (per well) of the Delft sandstone, resulting from the petrophysical analysis performed by TNO in 2013.**

**Table 7-2: Summary of detailed petrophysical results from TNO (2013) as found on NLOG for the wells nearest the concession.**

| Well | Stratigraphy | Top MD (m) | Base MD (m) | Porosity (%) | Permeability (mD) | Nett-Gross (%) |
|---|---|---|---|---|---|---|
| **GAG-05** | SLDND | 2817.00 | 2978.00 | 15.7 | 367 | 52.0 |
| **HON-GT-01** | SLDND | 2553.00 | 2620.00 | 17.0 | 446 | 77.0 |
| **LIR-45** | SLDND | 2163.00 | 2183.00 | 19.8 | 747 | 83.0 |

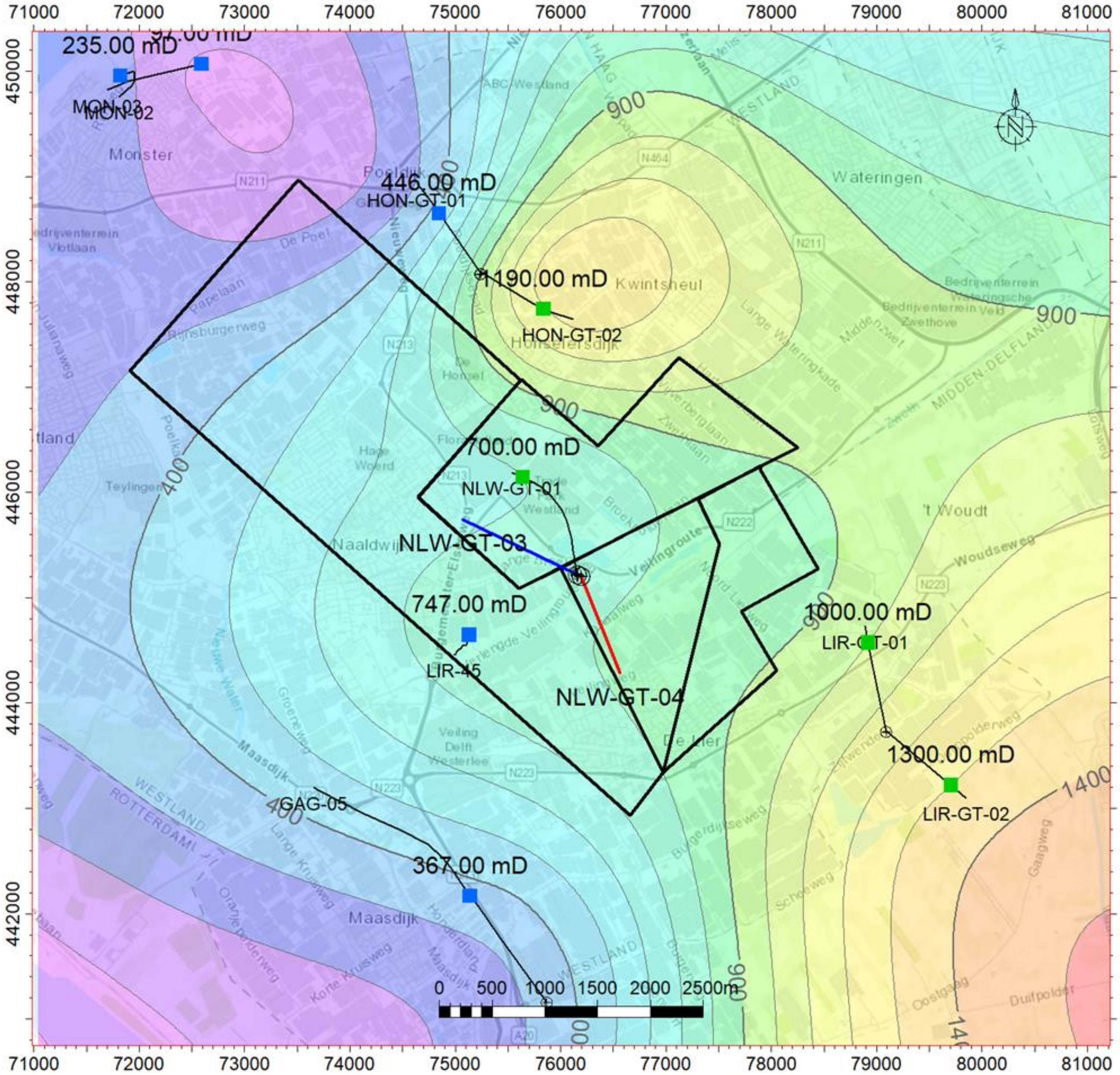


**Figure 7-6: Contour map of publicly available the average permeabilities calculated for the Delft Sandstone Member in the area around the planned doublet (red and blue) together with the result from the NLW-GT-01 well test. The data points are marked by squares which are colour coded according to source; well test in light green, and petrophysical analyses in blue.**

## 7.7 Reservoir properties at the target location

The nearest well test, which is considered to give the most reliable measure of average permeability for NLW-GT-03 and -04, is performed in the NLW-GT-01 well. The petrophysical results performed for this study, give lower values than those from that well test and those presented by TNO. This is partly due to the difference in well tops.

For the DoubletCalc calculations the P10, P50 and P90 permeability estimates are based on the numbers and considerations presented in the above sections. Given the trend observed in the map of Figure 7-6, the permeability is assumed to be lower than that found in the well test of NLW-GT-01. The permeability range determined for the new doublet is: **450 (minimum) – 650 (median) – 1,000 mD (maximum).**

## 7.8 Anisotropy

Anisotropy of the reservoir can be expressed as the ratio between horizontal and vertical permeability; Kh/Kv. This ratio is usually relatively high when the reservoir is layered and low when the reservoir is homogeneous (in horizontal and vertical sense). Kh/Kv can be expressed as the ratio between the arithmetic and harmonic permeability. The arithmetic average is considered to be representative for horizontal permeability and the harmonic average for vertical permeability. A value of **5** is used for DoubletCalc calculations.

## 7.9 Results and uncertainty discussion

The resulting reservoir parameters with uncertainty ranges are summarized in Table 7-3.

**Table 7-3: Min, median and max estimates for the Delft Sandstone.**

| | NLW-GT-03 & -04 | | |
|---|---|---|---|
| **Parameter** | **Min** | **Median** | **Max** |
| Gross thickness (m) | 58 | 66 | 64 |
| N/G (dec) | 0.87 | 0.92 | 0.96 |
| Average permeability (mD) | 450 | 650 | 1,000 |
| Salinity (ppm) | 120,000 | 140,000 | 160,000 |
| Kh/Kv | - | 5 | - |
| Temperature gradient (°C/100m) | - | 3.3 | - |

# 8 Evaluation of water temperature and salinity

## 8.1 Temperature

Based on temperature maps of the subsurface of the Netherland (Figure 8-1) the subsurface temperature below Naaldwijk is approximately 70-72°C at 2,000 m depth. This corresponds to a temperature gradient of approximately 3.4 °C/100m-3.6 °C/100m, assuming a surface temperature of 10°C.

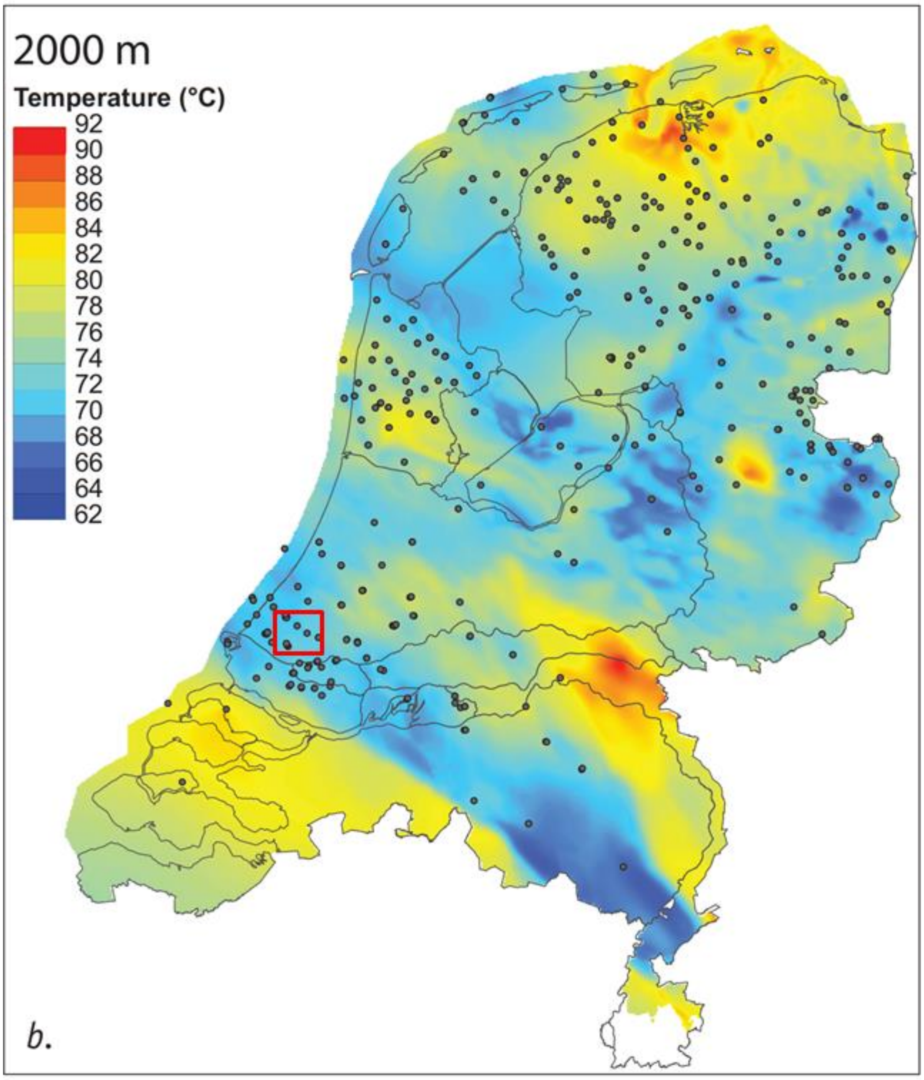


**Figure 8-1: Subsurface temperature maps of the Netherlands at a depth of 2000m (Bonté et al., 2012). These map is generated from thermal-tectonic forward modelling, calibrated with BHT measurement in wells (corrected for thermal perturbation during drilling) and few DST measurements in wells. Used wells are indicated by black dots.**

The temperature of produced water of NLW-GT-01 is 87°C with a mid-reservoir depth of around 2,350 m for the Delft. This leads to a temperature gradient of 3.3°C/100m which is somewhat lower than the average geothermal gradient of the of the local geothermal gradient in the study area (Figure 8-1). Here we assume the contribution of the lower Alblasserdam sands to the well test is negligible. Due to the vicinity of NLW-GT-01 the geothermal gradient from the well test is used as input for DoubletCalc:

$T = 10 + 0.033*h$

in which T = temperature in °C and h = depth in meters

## 8.2 Salinity

Based on the well test of NLW-GT-01, the formation water has a salinity of approximately 140,000 ppm NaCl equivalent, which is roughly in line with other geothermal doublets in Westland. A formation water samlple has been analysed but does not directly measure the NaCl equivalent (see appendix 10.9) The salinity estimate from the petrophysical evaluation of well LIR-45 supports a salinity of approximately 120,000 ppm NaCl equivalent. The salinity range for DoubletCalc calculations is listed in Table 8-1.

**Table 8-1: Estimated salinities of the formation water.**

| | Min | Median | Max |
|---|---|---|---|
| Salinity Nieuwerkerk Fm. (ppm NaCl equivalent) | 120,000 | 140,000 | 160,000 |

## 8.3 Aquifer pressure

The aquifer pressure is hydrostatic. The pressure influence of the pre-existing doublet (NLW-GT-01 and -02) on the planned doublet (NLW-GT-03 and -04) is described in section 9.1.

# 9 Doublet performances

## 9.1 Doublet configurations in the subsurface

The planned doublet will consist of wells NLW-GT-03 and NLW-GT-04 with NLW-GT-03 as the injector and NLW-GT-4 as the producer. Together with the existing NLW-GT-01 and the, at the time of writing, currently drilled NLW-GT-02, this configuration leads to a "sweep" or "tramline" configuration. Both the injection wells are located in the northwest while both the producers are situated in the southeast. Figure 9-1 shows the trajectory of the first doublet and the planned wells on the top reservoir depth map. The advantage of this configuration is that the subsurface targets can be located in the thicker area of the Delft sandstone and an acceptable breakthrough time of the cold front is preserved. The disadvantage is the increase of the reservoir pressure at the injecting side and pressure decrease at the producing side of the reservoir.

The difference between the initial reservoir pressure and the reservoir pressures at the target locations of the planned wells when first doublet is producing is quantified by using an analytical model (see Appendix 10.5). The analytical model does not include any faults or spatial information. The model calculates a pressure difference of around 1.8 bar when the first doublet produces 500 m3/hr and around 1.3 bar for 250 m3/hr. Therefore, the initial reservoir pressure is raised 2 bar for the injector and lowered 2 bar for the producer in DoubletCalc.

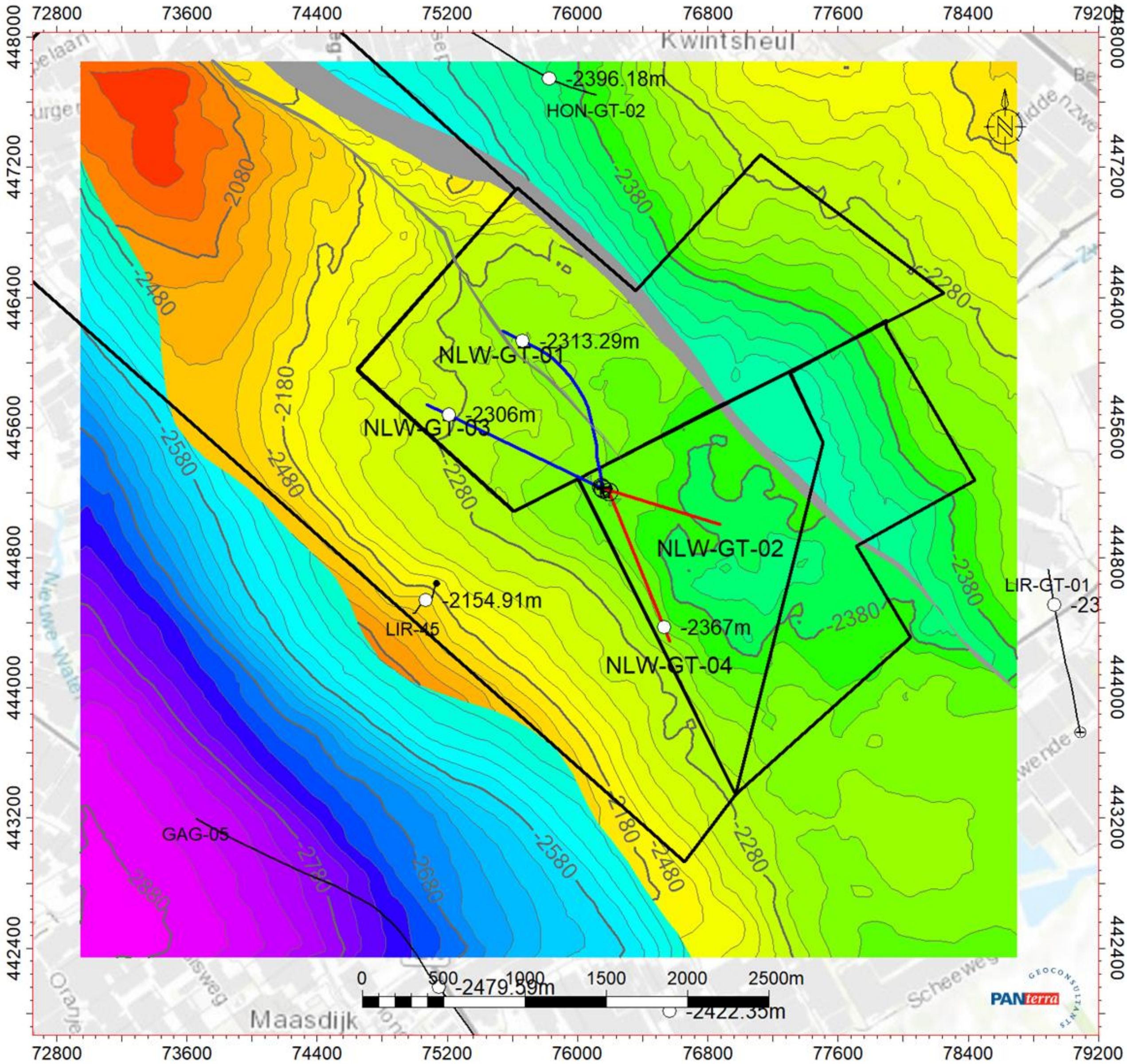


**Figure 9-1: Top reservoir map with the NLW-GT wells, the intersections of the (planned) wells with top reservoir are indicated by white the circles. The contour interval is 20 m and the contour level indications of -2480 at the trust to the southwest belong to the footwall of the trust. The random seismic lines of Figure 9-2 and Figure 9-3 are indicated with the purple dashed lines.**

The subsurface mid reservoir distance between the wells is approximately 1,800m. The doublet is situated parallel to the main fault direction in order to minimalize the chance of the presence of faults in between the two wells that may hinder pressure communication. A small fault at reservoir level is present between NLW-GT-01 and NLW-GT-03 that may hinder pressure communication between the injectors.

The wells are projected on the seismic in (see Figure 9-2 and Figure 9-3). The closest large fault to one of the planned wells is approximately 1,000 m away. Minor faults may also be present near the wells, but they cannot be distinguished on seismic. Because these faults are so small it is not expected that they form a significant barrier for flow or cause geomechanical problems.

The RD coordinates of the surface location, reservoir top and base and Total Depth (TD) are listed in Table 6-4 and Table 6-5.

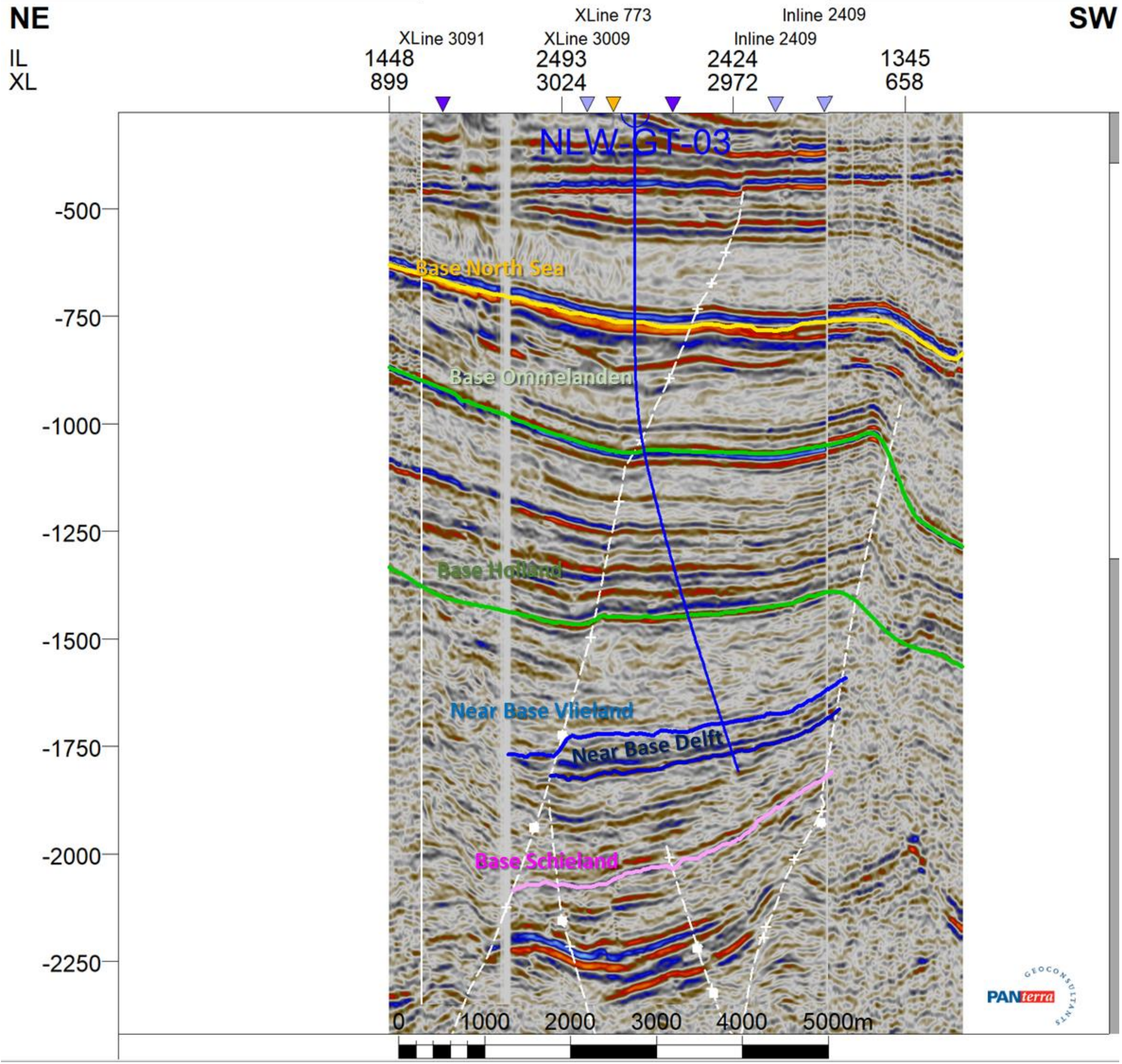


**Figure 9-2: NLW-GT-03 projected on the seismic, the location of the line is indicated in Figure 9-4.**

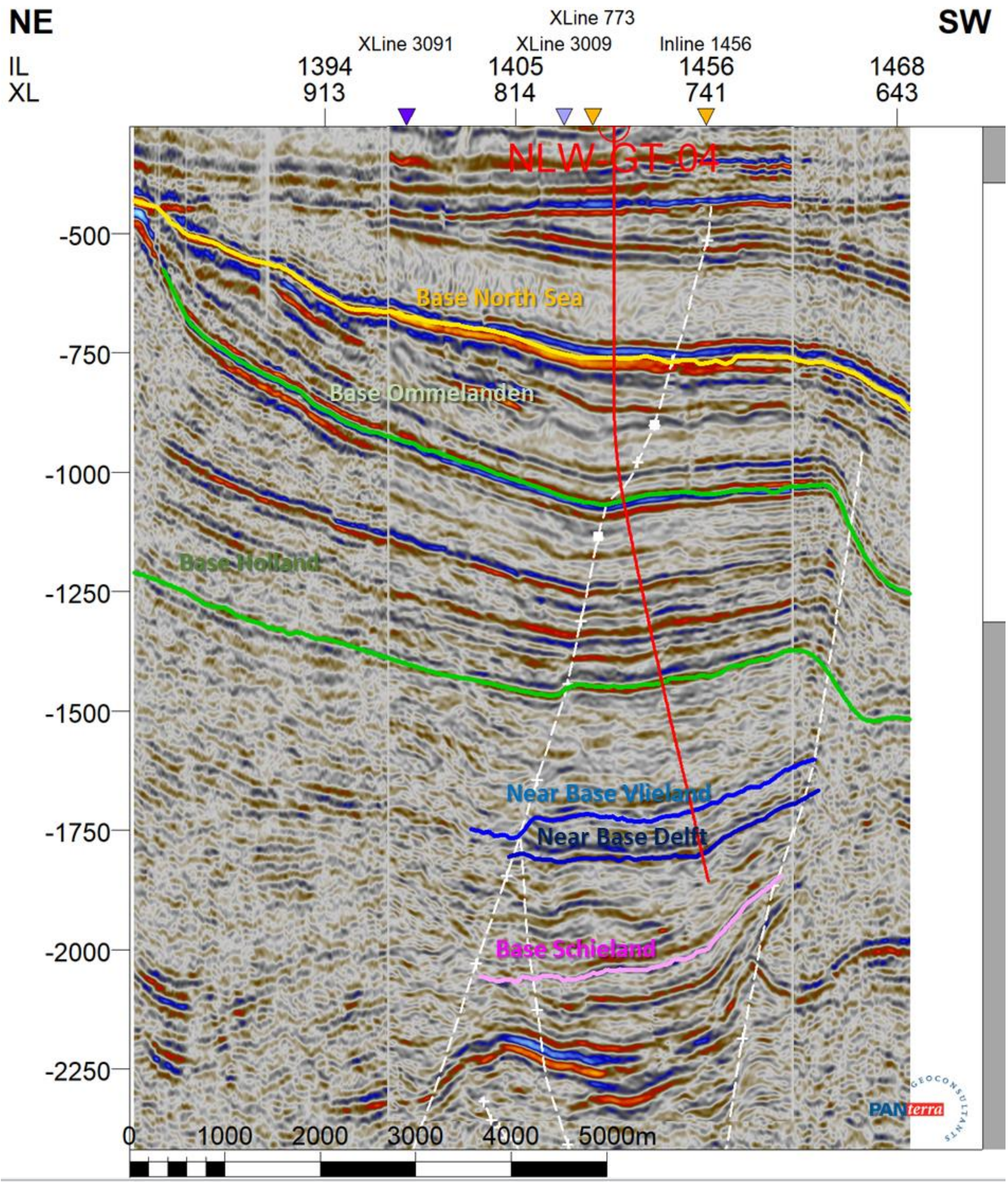


**Figure 9-3: NLW-GT-04 projected on the seismic, the location of the line is indicated in Figure 9-4.**

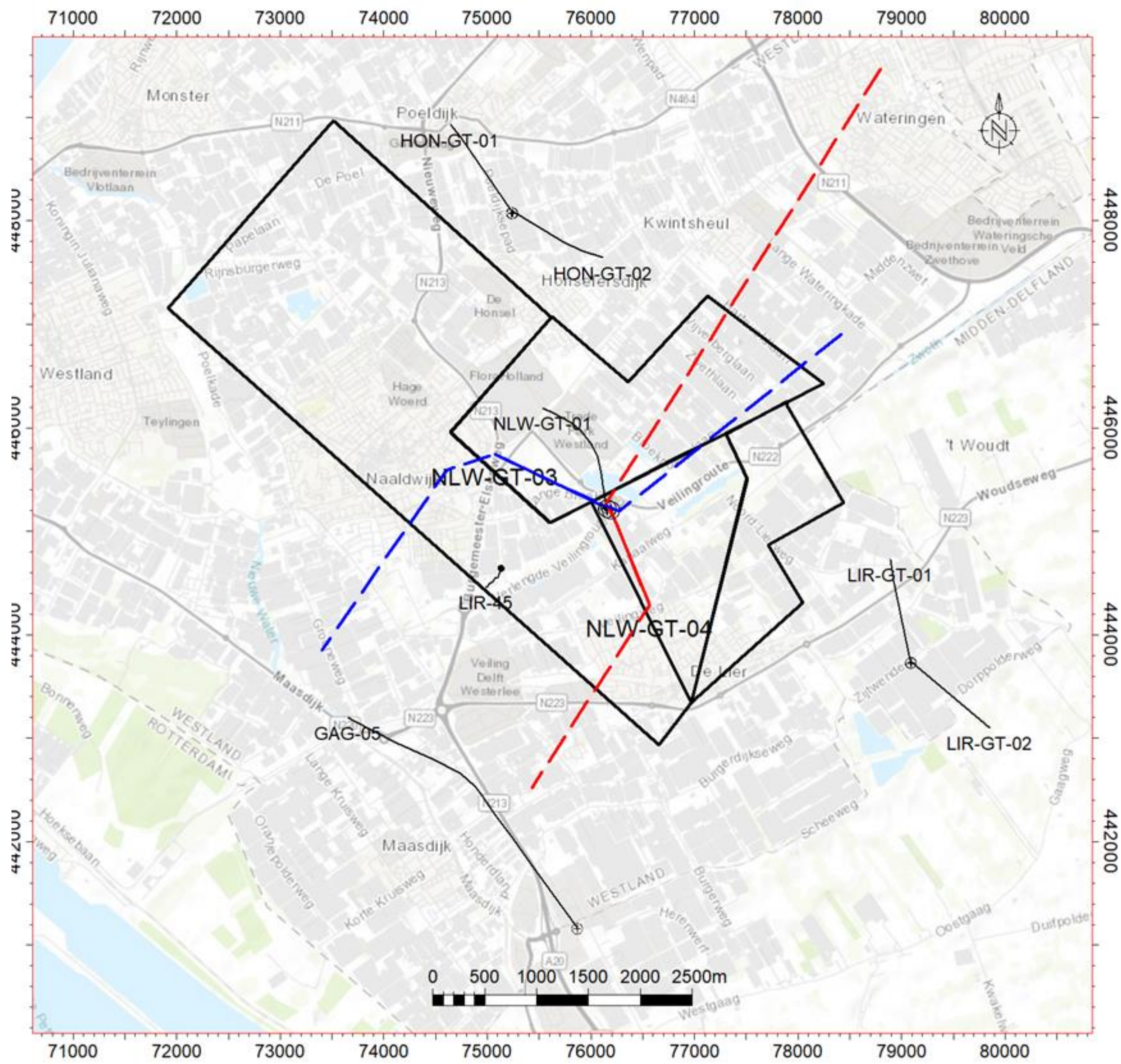


**Figure 9-4: Locations of the seismic sections displayed in Figure 9-2 (blue dashed line) and Figure 9-3 (red dashed line).**

## 9.2 Well architecture

Conceptual casing schemes for wells NLW-GT-03 and NLW-GT-04 are shown in Figure 9-5 and Figure 9-6 (the report by WEP regarding the basic well design is added to the SDE+ request). The Electronic Submersible Pump (ESP) is located at a depth of 800 m TVD in the producer. The open hole diameter is 9.5 inch in the reservoir, which is completed with wire wrapped screens. The inclination of the producer and injector in the reservoir is corrected for the dip of the top reservoir and are 21.3° for NLW-GT-03 and 6.75° for NLW-GT-04. The well trajectories are listed in Appendix 10.6.

Wellhead and Xmastree
**NLW-GT-03**

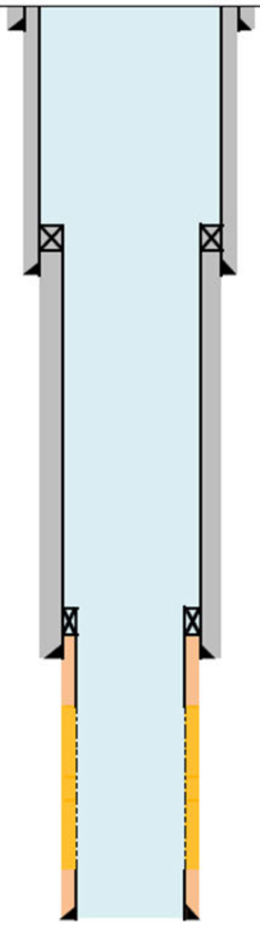

All depths from NAP

| Nr. | Item Description | Depth m tvd | Depth m ah | Hole ID in | Pipe OD in | Collar OD in (nom) | Pipe ID in | Pipe ID in (drift) |
|---|---|---|---|---|---|---|---|---|
| 1 | 24" 0,5" WT Conductor | 140 | 140 | - | 24,000 | welded | 23,000 | 23,000 |
| | 13 3/8" x 9 5/8" liner hanger | | 1100 | Top of liner (100 m liner lap) | | | | |
| 2 | 13 3/8" 72# L80 casing | 1180 | 1200 | 17,50 | 13,375 | 14,236 | 12,347 | 12,250 |
| | | 1184 | 1205 | section TD | | | | |
| | 9 5/8" x 7" Liner Hanger + Packer | | 2610 | Top of liner (50 m liner lap) | | | | |
| 3 | 9 5/8" 47# L80 Liner | 2274 | 2660 | 12,250 | 9,625 | 10,396 | 8,681 | 8,525 |
| | | 2278 | 2665 | section TD | | | | |
| | | 2306 | 2703 | Top Delft Sandstone | | | | |
| | | 2366 | 2784 | Base Delft Sandstone / Top Alblasserdam | | | | |
| 4 | 7 5/8" 26,4# L80 liner* with WWS | 2416 | 2850 | 9 1/2" | 7,625 | 8,141 | 6,969 | 6,844 |
| | *special clearance* | 2420 | 2855 | TD | | | | |
| Not in scale | | | | | | | | |

**Figure 9-5: Conceptual casing scheme of well NLW-GT-03.**

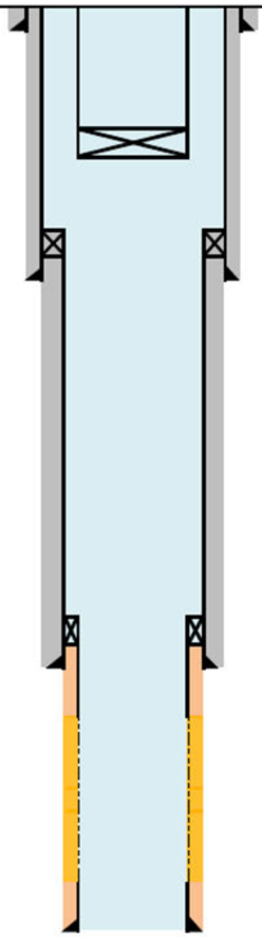


| Nr. | Item Description<br>All depths from NAP | Depth<br>m<br>tvd | Depth<br>m<br>ah | Hole ID<br>in | Pipe OD<br>in | Collar OD<br>in<br>(nom) | Pipe ID<br>in | Pipe ID<br>in<br>(drift) |
|---|---|---|---|---|---|---|---|---|
| 1 | 24" 0,5" WT Conductor | 140 | 140 | - | 24,000 | welded | 23,000 | 23,000 |
| | ESP on 8 5/8" 32# L80 tubing | 800 | 800 | | 8,625 | 9,650 | 7,921 | 7,796 |
| | 13 3/8" x 9 5/8" liner hanger | | 1098 | Top of liner (100 m liner lap) | | | | |
| 2 | 13 3/8" 72# L80 casing | 1178 | 1198 | 17,50 | 13,375 | 14,236 | 12,347 | 12,250 |
| | | 1182 | 1203 | section TD | | | | |
| | 9 5/8" x 7" Liner Hanger + Packer | | 2545 | Top of liner (50 m liner lap) | | | | |
| 3 | 9 5/8" 47# L80 Liner | 2339 | 2595 | 12,250 | 9,625 | 10,396 | 8,681 | 8,525 |
| | | 2343 | 2600 | section TD | | | | |
| | | 2367 | 2629 | Top Delft Sandstone | | | | |
| | | 2404 | 2673 | Base Delft Sandstone / Top Alblasserdam | | | | |
| 4 | 7 5/8" 26,4# L80 liner* with WWS | 2476 | 2760 | 9 1/2" | 7,625 | 8,141 | 6,969 | 6,844 |
| | *special clearance | 2479 | 2765 | TD | | | | |

*Not in scale

**Figure 9-6: Conceptual casing scheme of well NLW-GT-04.**

## 9.3 Operational settings

The injection temperature will be 31°C, the same injection temperature as at which the first doublet will be operated. The maximum Tubing Head Pressure (THP) and maximum pressure difference at the injector are calculated based on "Protocol bepaling maximale injectiedrukken bij aardwarmtewinning – versie 2" SodM and TNO-AGE, 2013) and the associated Geomech excel sheet version 2 (available on www. NLOG.nl). A hydraulic gradient of 0.106 bar/meter results in a maximum THP of 67.0 bar, the maximum pressure difference at the injector is 130.0 bar.

The total pressure difference (injection+ESP pressure) input in DoubletCalc is 110 bar, which results in a pressure difference at the injector of 57.7 bar in the P50 case, below the maximum pressure difference of 67.0 bar.

# 10 References

Bakker, T, 2011, Onvermijdelijk meegekomen gas en olie bij geothermal projecten. Unpublished presentation for Platform Geothermie.

Dalfsen, W. van, Gessel, S.F. van, Doornenbal, J.C. (2007): Velmod-2. Joint Industry Project, no. 034.62155. TNO report 2007-U-R1272C, TNO Utrecht, 97p.

De Jager, M.A., M.A. Doyle, P.J. Graham & J.E. Mabillard, 1996, Hydrocarbon habitat of the West Netherlands basin. In: Rondeel, H.E., Batjes, D.A.J. & Nieuwenhuijs, W.H. (eds): Geology of gas and oil under the Netherlands. Kluwer Academic Publishers (Dordrecht): 191-210.

Den Hartog Jager, D.G., 1996, Fluviomarine sequences in the Lower Cretaceous of the West Netherlands basin: correlation and seismic expression. In: Rondeel, H.E., Batjes, D.A.J. &

Donselaar, M., E., Groenenberg, R.,M., Gilding, D., T., 2015. Reservoir Geology and Geothermal Potential of the Delft Sandstone Member in the West Netherlands Basin. Proceedings World Geothermal Congress 2015, Melbourne, Australia, 19-25 April 2015.

Nieuwenhuijs, W.H. (eds): Geology of gas and oil under the Netherlands. Kluwer Academic Publishers (Dordrecht): 229-241.

PanTerra, 2014, Analysis of Welltest LIR-GT-01, Report G1107, August 2014.

PanTerra, 2014, Analysis of Welltest LIR-GT-02, Report G1107B, August 2014.

PanTerra , 2018, Analysis of Well Test NLW-GT-01, Report G1340_3, March 2018.

Racero-Baena, A. & Drake, S.J., 1996, Structural style and reservoir development in the West Netherlands oil province. In: Rondeel, H.E., Batjes, D.A.J. & Nieuwenhuijs, W.H. (eds): Geology of gas and oil under the Netherlands. Kluwer Academic Publishers (Dordrecht): 211-228.

TNO-AGE, 2013, advies aanvraag Garantieregeling AARD03002 Geothermie De Lier (date 3 July, 2013, referentie AGE 13-10.023)

TNO-AGE, 2015, Bezwaar op TNO-AGE advies Aard04003 (date 16 July, 2015, referentie AGE 15-10.046)

# Appendices

## 10.1 Details used data

### TNO Petrophysics

| Put | Stratigrafie | Top (m) | Basis (m) | Diepte Dimensie | Percentiel | Porositeit (%) | Permeabiliteit (mD) | Netto-Bruto (%) | Gebruikt voor | Referentie nr. |
|---|---|---|---|---|---|---|---|---|---|---|
| **BRK-07** | SLDND | 1921.00 | 1936.00 | MD | P50 | 21.7 | 974 | 94.0 | Y | 1129 |
| **BRT-01** | SLDND | 2082.00 | 2146.00 | MD | P50 | 18.7 | 637 | 64.0 | Y | 1129 |
| **EHV-01** | SLDND | 2043.00 | 2063.00 | MD | P50 | 17.2 | 445 | 68.0 | Y | 1129 |
| **GAG-05** | SLDND | 2817.00 | 2978.00 | MD | P50 | 15.7 | 367 | 52.0 | Y | 1129 |
| **HAG-02** | SLDND | 1730.00 | 1770.00 | MD | P50 | 16.5 | 391 | 79.0 | Y | 1129 |
| **HAG-GT-01** | SLDND | 2546.00 | 2702.00 | MD | P50 | 17.8 | 523 | 69.0 | Y | 1129 |
| **HAG-GT-02** | SLDND | 2150.00 | 2330.00 | MD | P50 | 16.2 | 324 | 83.0 | Y | 1129 |
| **HON-GT-01** | SLDND | 2553.00 | 2620.00 | MD | P50 | 17.0 | 446 | 77.0 | Y | 1129 |
| **KDZ-02** | SLDND | 1891.00 | 1936.00 | MD | P50 | 19.0 | 666 | 79.0 | Y | 1129 |
| **LIR-45** | SLDND | 2163.00 | 2183.00 | MD | P50 | 19.8 | 747 | 83.0 | Y | 1129 |
| **MKP-10** | SLDND | 647.00 | 720.00 | MD | P50 | 23.9 | 1110 | 76.0 | Y | 1129 |
| **MKP-11** | SLDND | 860.00 | 910.00 | MD | P50 | 18.1 | 599 | 63.0 | Y | 1129 |
| **MON-02** | SLDND | 2224.00 | 2256.00 | MD | P50 | 14.7 | 235 | 86.0 | Y | 1129 |
| **MON-03** | SLDND | 2317.00 | 2347.00 | MD | P50 | 12.1 | 97.0 | 27.0 | Y | 1129 |
| **PNA-13** | SLDND | 1864.00 | 1939.00 | MD | P50 | 17.2 | 435 | 69.0 | Y | 1129 |
| **Q11-02** | SLDND | 1028.00 | 1168.00 | MD | P50 | 17.0 | 425 | 58.0 | Y | 1129 |
| **Q13-01** | SLDND | 1904.60 | 1974.00 | MD | P50 | 13.4 | | 72.0 | Y | 328 |
| **Q13-02** | SLDND | 1950.70 | 2163.80 | MD | P50 | 14.8 | | 50.4 | Y | 328 |
| **Q13-02** | SLDND | 1951.00 | 2164.00 | MD | P50 | 14.8 | | 50.4 | Y | 314 |
| **Q13-04** | SLDND | 1535.20 | 1668.40 | MD | P50 | 16.0 | | 72.7 | N | 328 |
| **Q13-07-S2** | SLDND | 2018.00 | 2130.00 | TVD NAP | P50 | 13.8 | 19.6 | 55.8 | Y | 160 |
| **Q13-08** | SLDND | 1891.34 | 1908.79 | MD | P50 | 13.4 | 127 | 58.0 | Y | 1129 |
| **Q13-08** | SLDND | 1905.00 | 1907.00 | MD | P50 | 18.4 | | 100.0 | Y | 314 |
| **Q13-09** | SLDND | 1872.99 | 1984.13 | MD | P50 | 17.5 | | 60.5 | N | 328 |
| **Q13-09** | SLDND | 1873.00 | 1909.00 | MD | P50 | 16.9 | | 76.1 | N | 314 |
| **Q13-09** | SLDND | 1913.45 | 2028.00 | MD | P50 | 16.7 | 370 | 60.0 | Y | 1129 |
| **Q16-01** | SLDND | 1993.90 | 2077.00 | TVD NAP | P50 | 11.2 | | 48.5 | N | 160 |
| **Q16-01** | SLDND | 1994.00 | 2077.00 | MD | P50 | 12.3 | 79.0 | 38.0 | Y | 1129 |
| **Q16-02** | SLDND | 2089.00 | 2131.00 | TVD NAP | P50 | 17.7 | | 90.0 | Y | 160 |
| **Q16-02** | SLDND | 2089.00 | 2183.00 | MD | P50 | 17.6 | 490 | 62.0 | Y | 1129 |

### PanTerra Petrophysics

| Well | Zone Name | Top | Bottom | Gross | Net | N/G | Av Phi | Av Perm P90 | Av Perm P50 | Av Perm P1 |
|---|---|---|---|---|---|---|---|---|---|---|
| | | m TVDSS | m TVDSS | m TVDSS | m TVDSS | TVDSS | % | mD | mD | mD |
| LIR-45 | SLDND | 2154.93 | 2190.44 | 26.36 | 22.05 | 0.84 | 0.19 | 21.7 | 573.6 | 1486.1 |
| NLW-GT-01 | SLDND | 2313.26 | 2391.74 | 74.53 | 70.13 | 0.94 | 0.19 | 20.9 | 534.4 | 1381.3 |
| LIR-45 | SLDNA_upper | 2273.83 | 2378.07 | 104.26 | 73.52 | 0.705 | 0.168 | 9.249 | 137.707 | 773.14 |
| NLW-GT-01 | SLDNA_upper | 2646.94 | 2748.93 | 101.89 | 65.5 | 0.643 | 0.143 | 2.423 | 39.552 | 278.76 |
| LIR-45 | SLDNA_lower | 2378.07 | 2400.95 | 22.97 | 1.44 | 0.063 | 0.139 | 2.448 | 39.901 | 278.905 |
| NLW-GT-01 | SLDNA_Lower | 2748.93 | 2797.24 | 48.29 | $$2.90 | 0.06 | 0.111 | 1.529 | 24.802 | 172.917 |

## 10.2 Well tests

# Resultaten van de put test

| **Gegevens voor test interpretatie** | Waarde | Dimensie |
|---|---|---|
| Naam van de put | NLW-GT-01 | |
| Top aquifer | 2604 | m (langs boorgat) |
| “ | 2312 | en m (TVD) |
| Basis aquifer | 2752 | m (langs boorgat) |
| “ | 2440 | en m (TVD) |
| Netto dikte Aquifer | 83.4 | m (TVD) |
| Netto/bruto aquifer | 89 | % |

| | | |
|---|---|---|
| Gemiddelde porositeit aquifer | 18.7 | % |
| Zoutgehalte formatiewater van sample | 120 | kg/m3 |
| Verwachte max. temperatuur geproduceerde water[1] | 87 | ºC |
| | | |
| Casing 20" | 1158 | m tv |
| Casing 13 3/8" | 2168 | m tv |
| Casing 9 5/8" | 3773 | m tv |
| Diameter boorgat bij aquifer | 9 5/8 | Inch |
| Top productie-interval/filter (6 5/8 x 7") | 2604 | m (langs boorgat) |
| " | 2312 | m (TVD) |
| Basis productie-interval/filter (6 5/8 x 7") | 2752 | m (langs boorgat) |
| " | 2440.4 | m (TVD) |
| Weerstand over screens[2] | 0 | bar |
| | | |
| Locatie pomp | 752 | m (ah) |
| Locatie meetsonde voor druk | 752 | m (tv) |
| Locatie diepe wireline gauge | 2600 | m (langs boorgat) |
| " | 2317 | m tv |
| | | |
| | | |
| **Meetreeksen Puttest**[4] | Eind ESP druk, bar | Eind Debiet, m3/uur |
| **Flow 1** | 64.4 | 215 |
| **Flow 2** | 61.1 | 327 |
| **Flow 3** | 57.1 | 428 |
| **Flow 4** | 64.7 | 226 |
| **Flow 5** | 56.4 | 427 |
| **BU** | 70.65 | 0 |
| | | |
| **Uitkomsten test interpretatie en analyses** | | |
| Skin | -0.25 to 1.43 | |
| H | 83.5 | m |
| K | 700 | mD |
| KH | 58.1 | D*m |
| PI (transient 30 hrs) | 24.1 | $m^3$/hr/bar |
| Two flow-barriers/baffles at approximately | 270 and 670 | m from well |
| | | |
| **Deviatie** | | |

| | | | |
|---|---|---|---|
| Diepte langs boorgat | Diepte m tv | East | North |
| 0 | 0 | 76147,00 | 445237,00 |
| 2604 | 2312 | | |
| Mid reservoir ~2670 | 2376 | | |
| 2752 | 2440 | | |

1 Deze temperatuur wordt als gemiddelde aquifer temperatuur beschouwd
2 Geen meting van weerstand over filter

## 10.3 Production data

Not used

## 10.4 Maps

### 10.4.1 Time maps

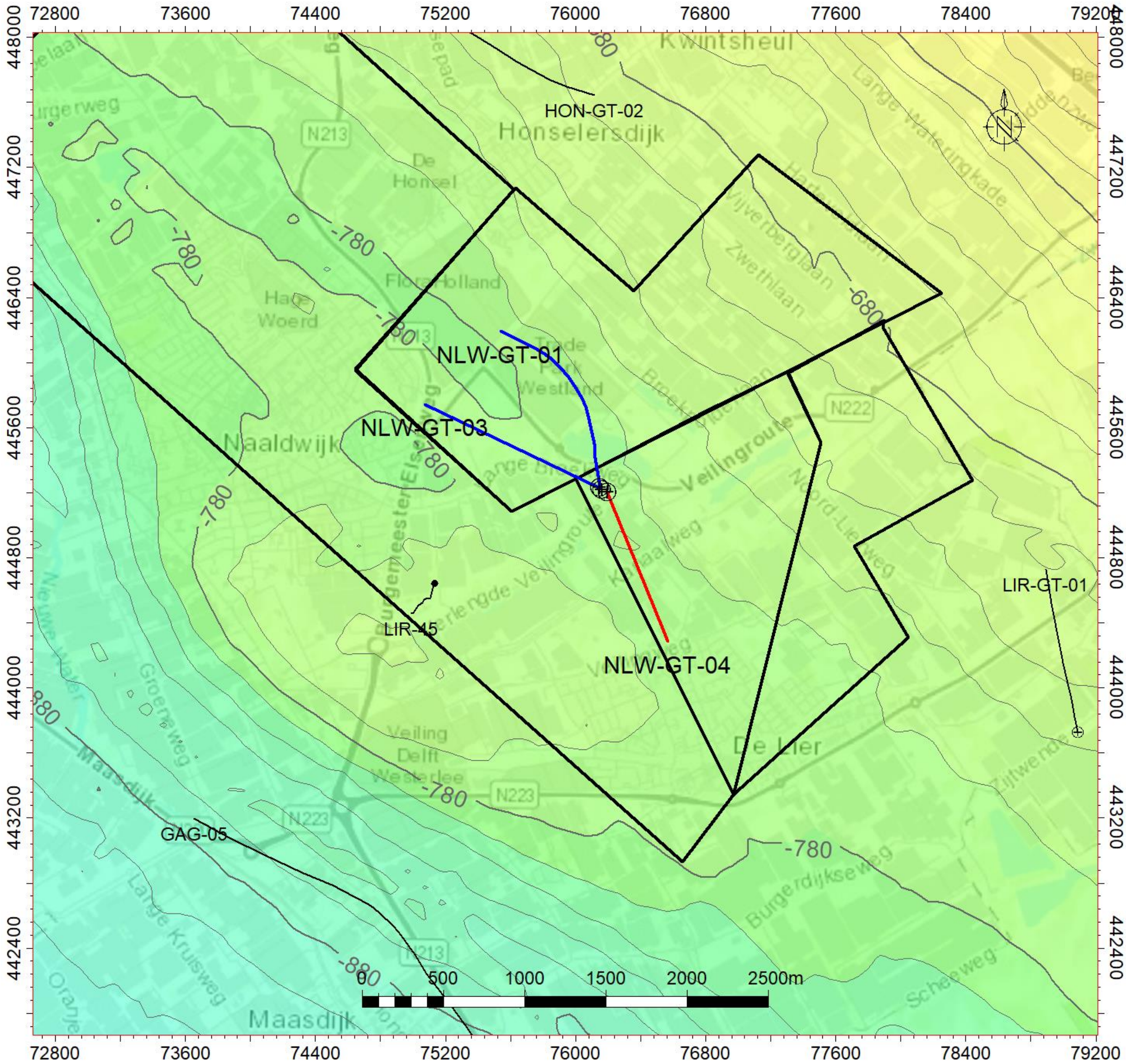


**Figure 10-1: Time map of the base of the North Sea Supergroup.**

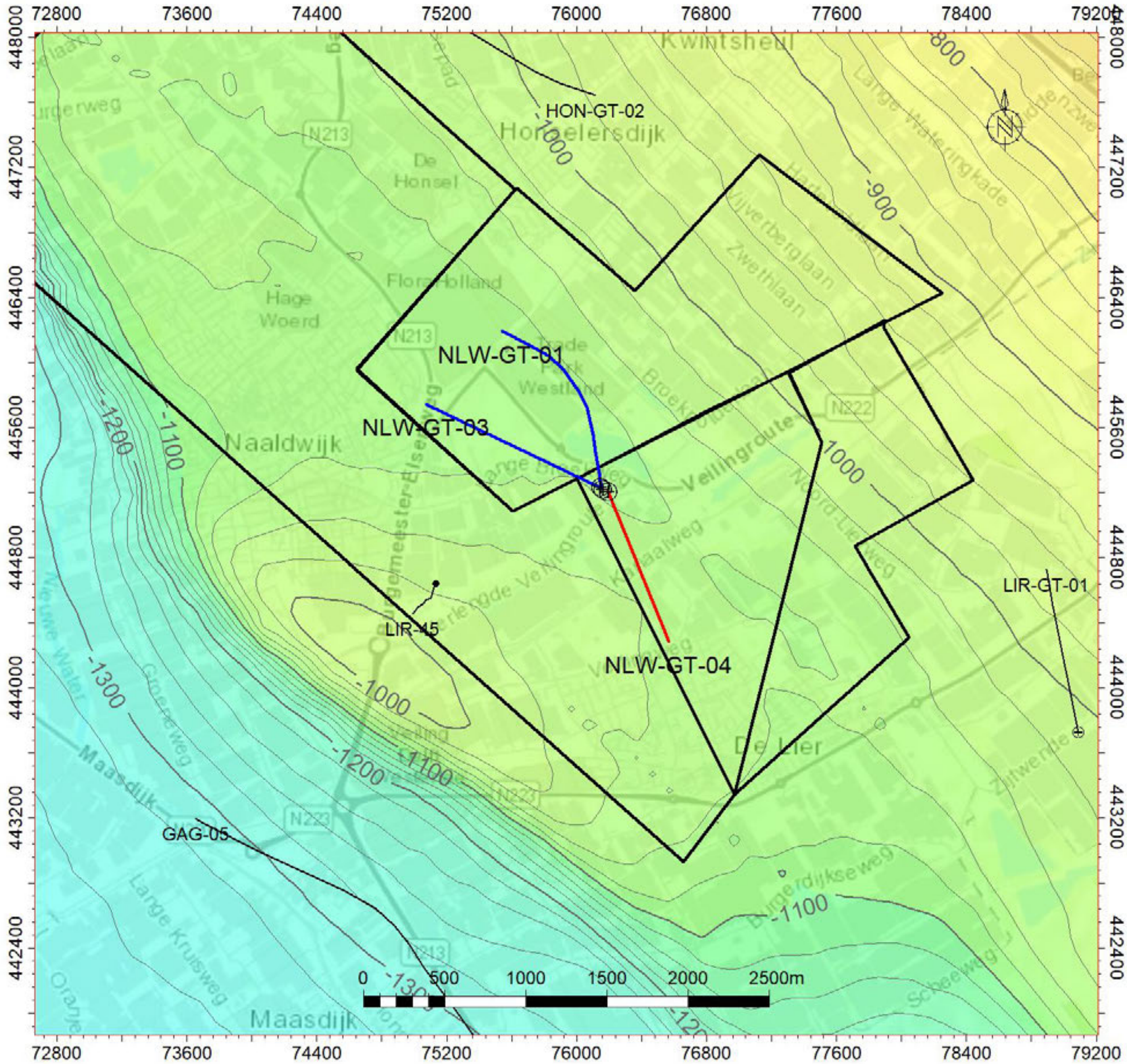


**Figure 10-2: Time map of the base of the Chalk Group.**

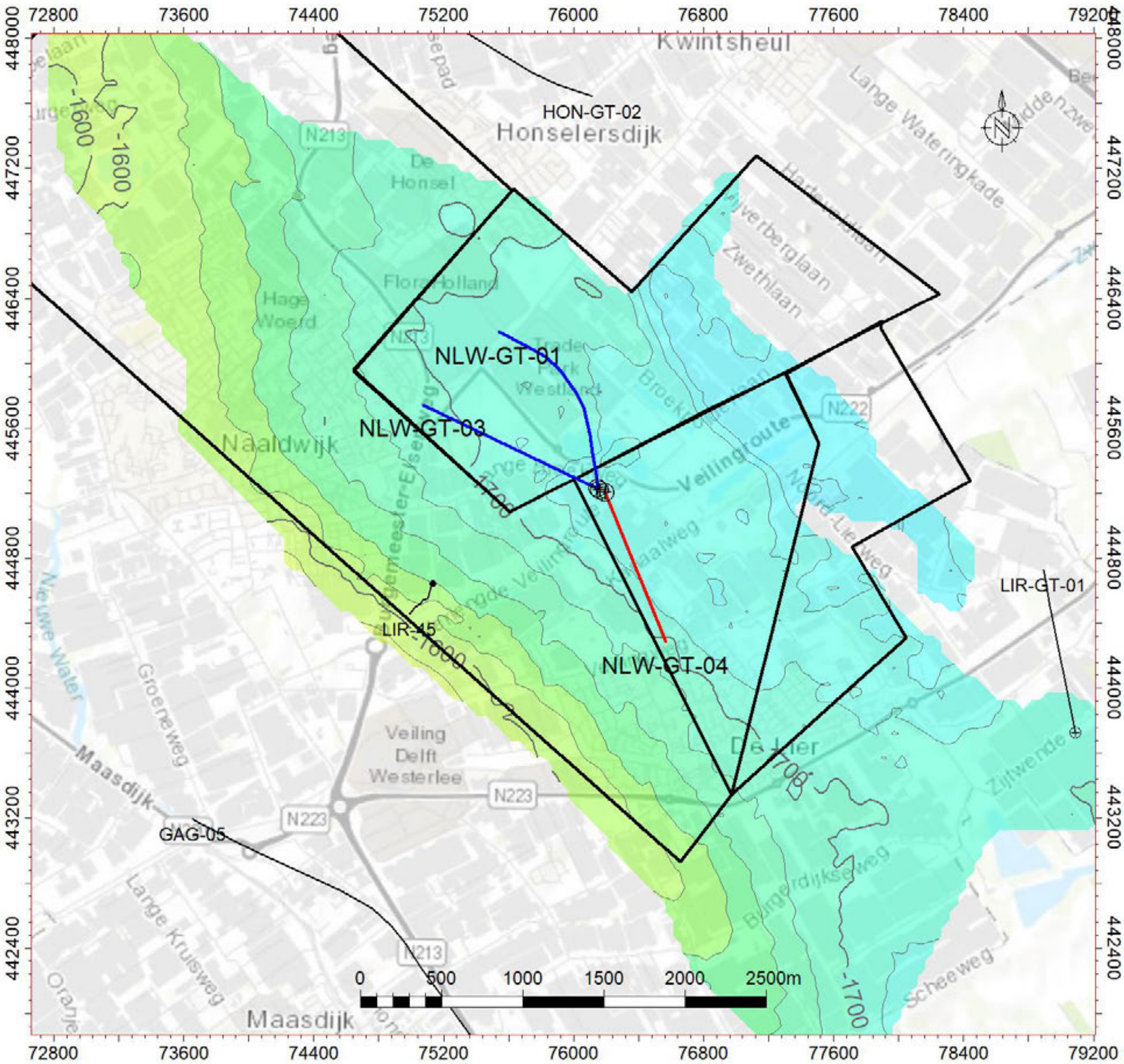


**Figure 10-3: Time map of the Near base of the Vlieland Formation.**

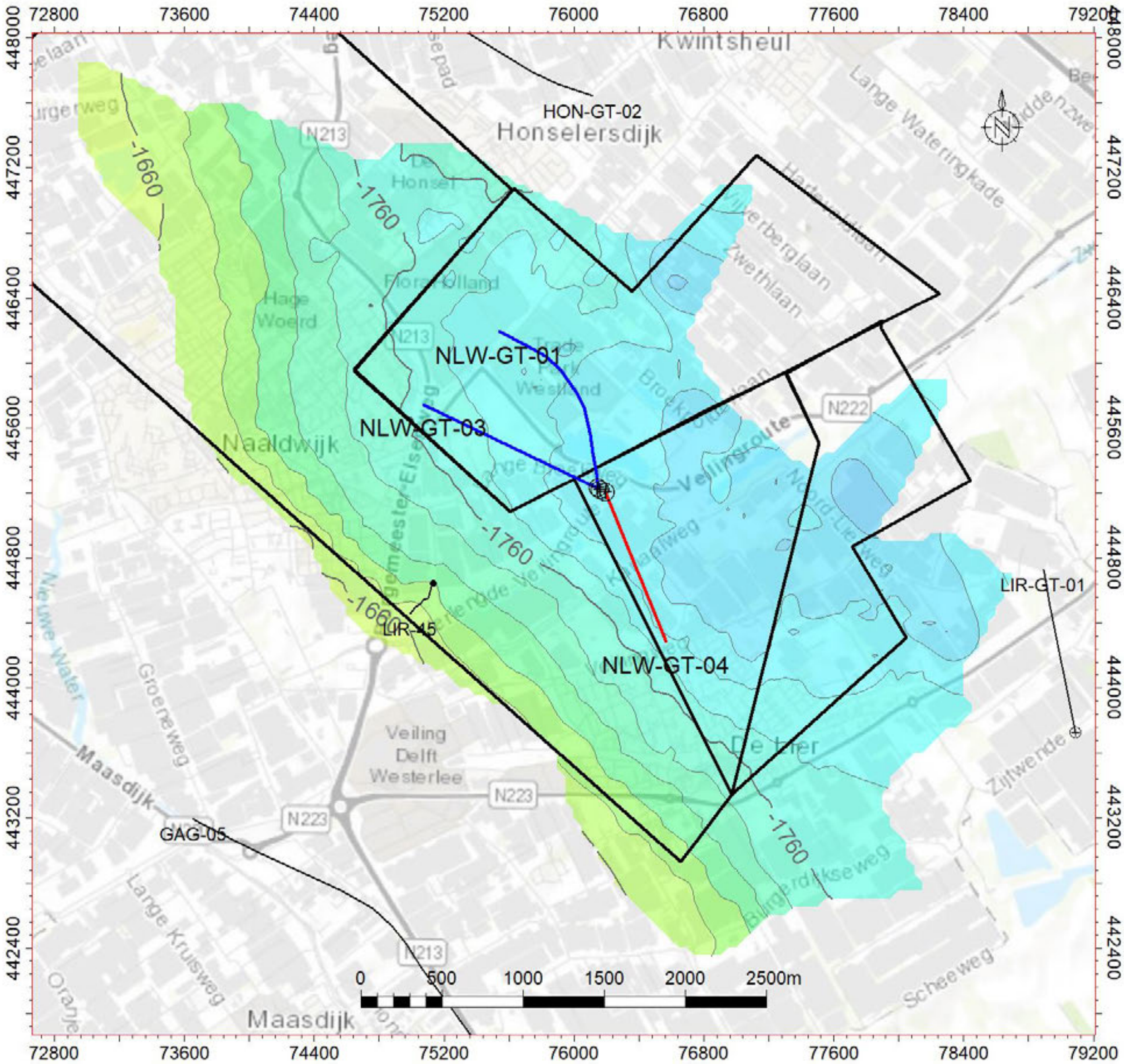


**Figure 10-4: Time map of the top of the Near base Delft Sst Mbr.**

### 10.4.2 Depth maps

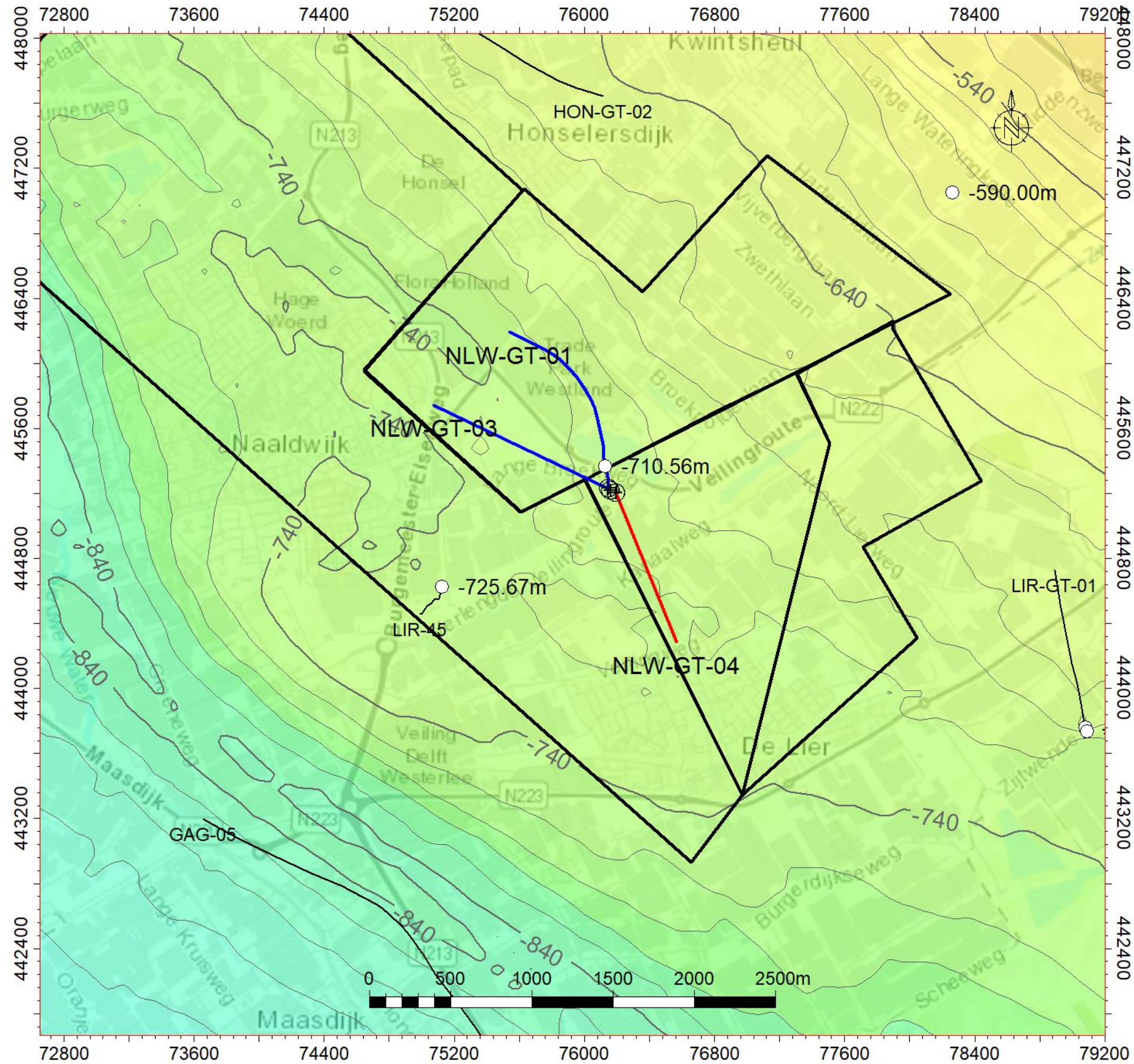


Figure 10-5: Depth map of the base of the North Sea Supergroup.

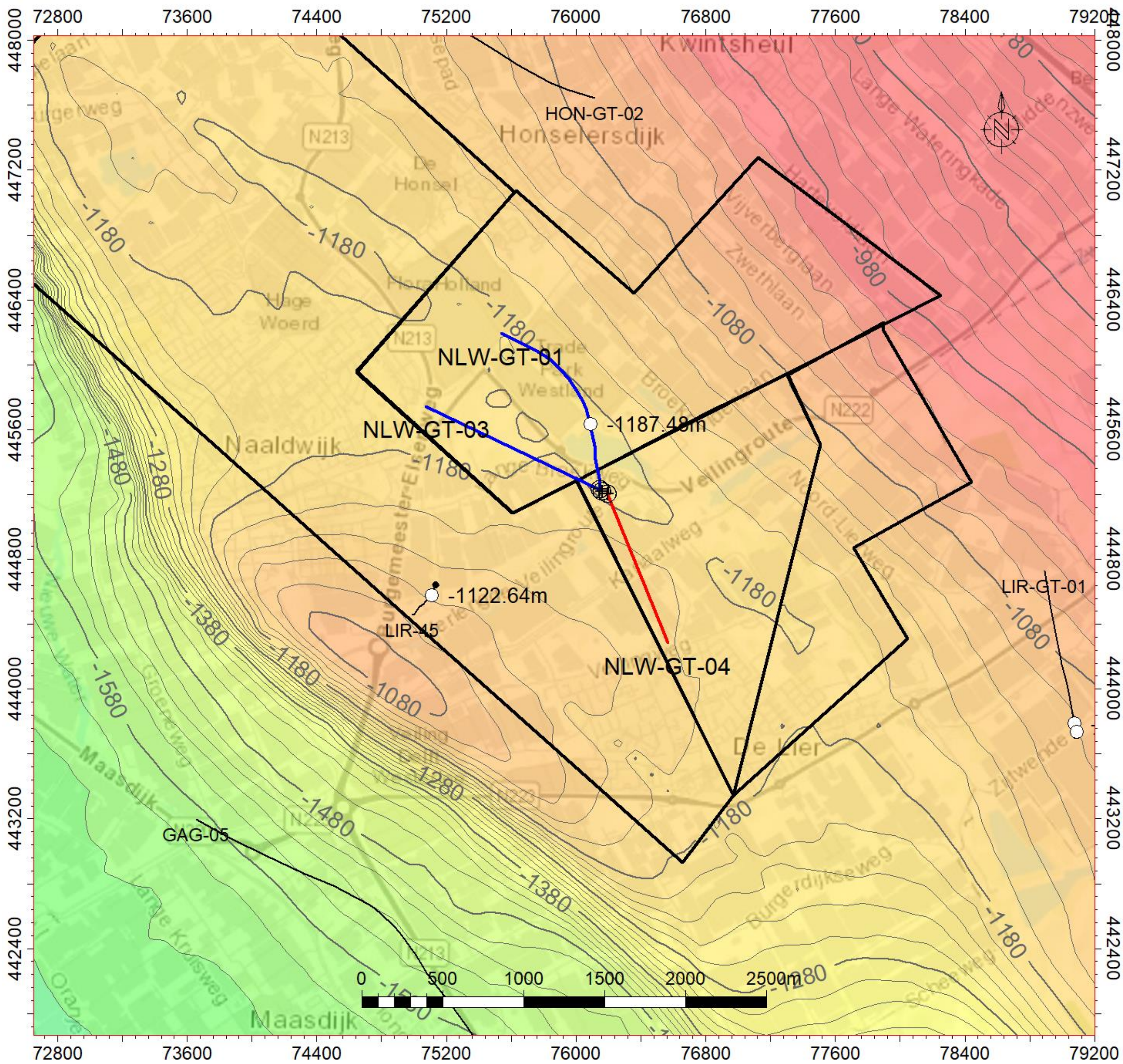


Figure 10-6: Depth map of the base of the Ommelanden

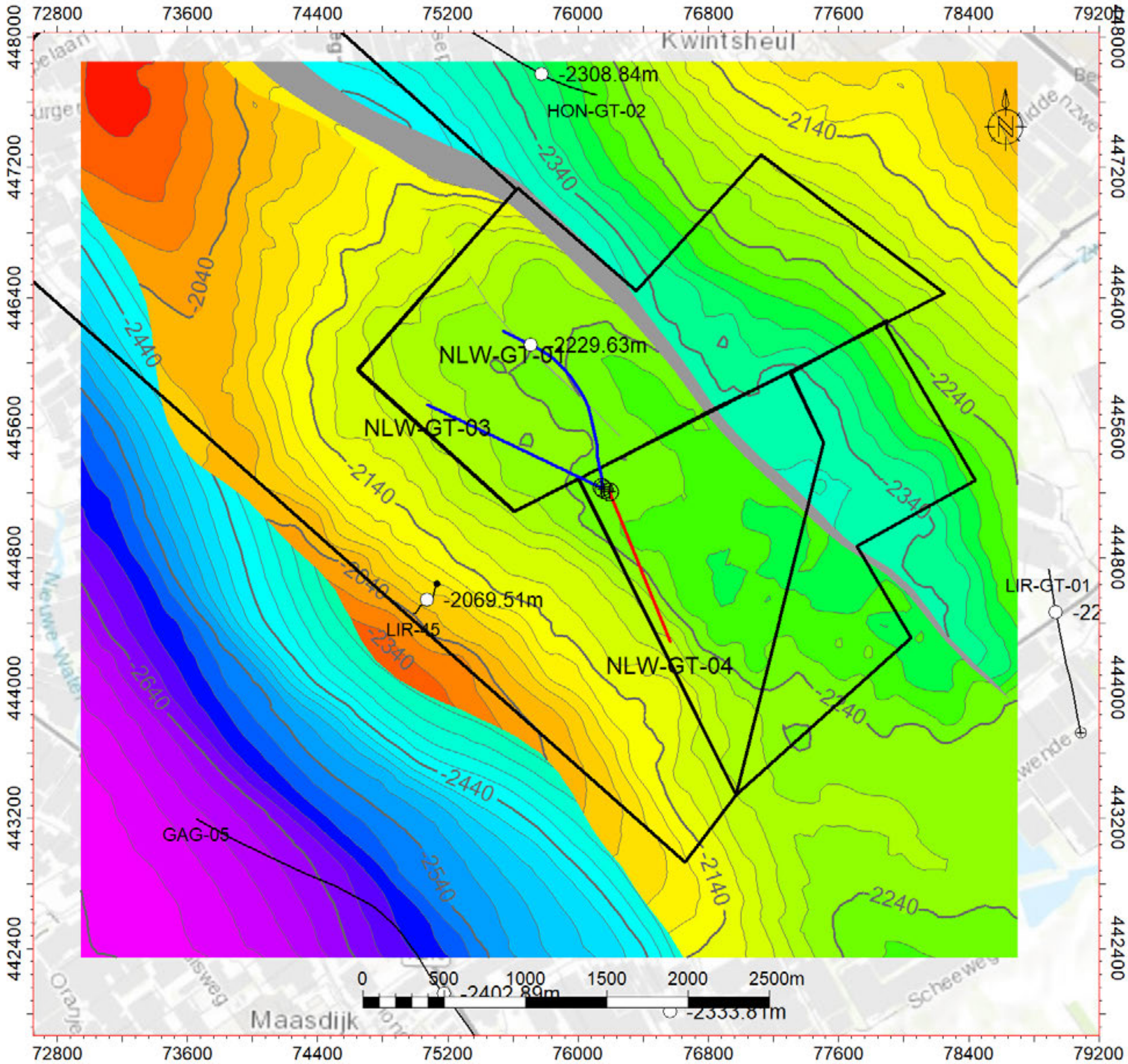


**Figure 10-7: Depth map of the base of the Vlieland Formation.**

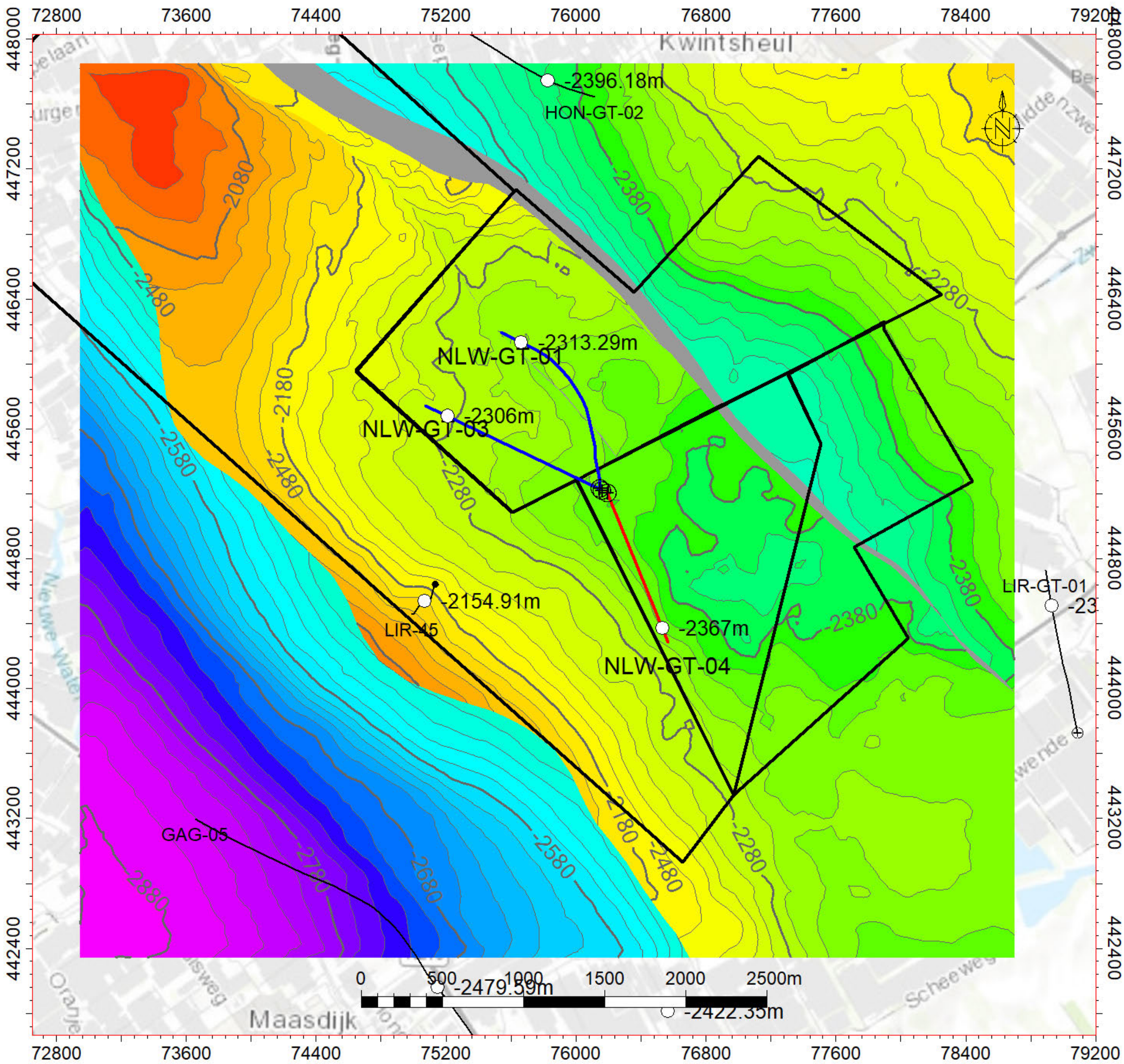


**Figure 10-8: Depth map of the top of the Delft Sst Mbr.**

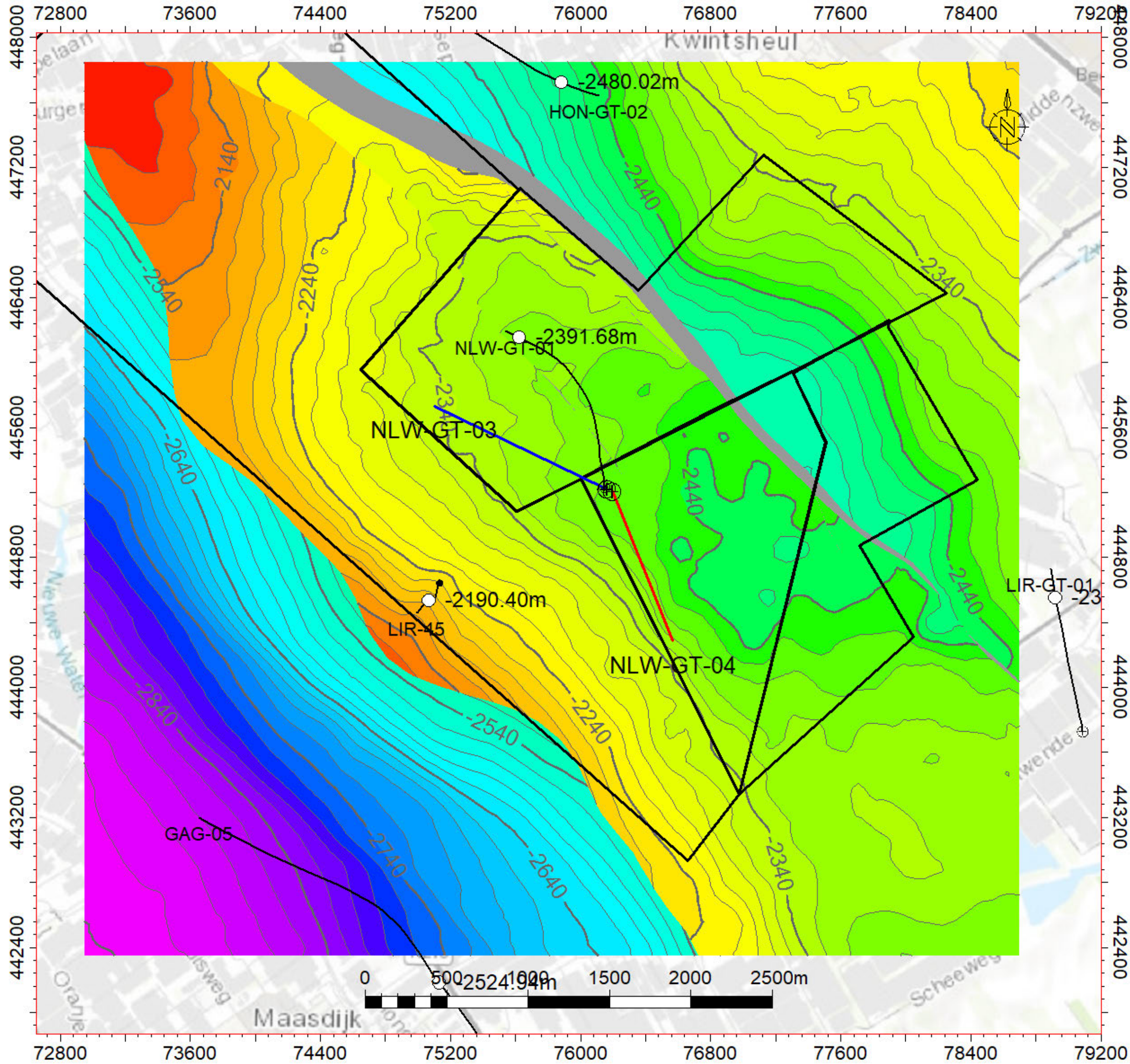


**Figure 10-9: Depth map of the base of the Delft Sst Mbr.**

## 10.5 Pressure influence from the first doublet on planned doublet

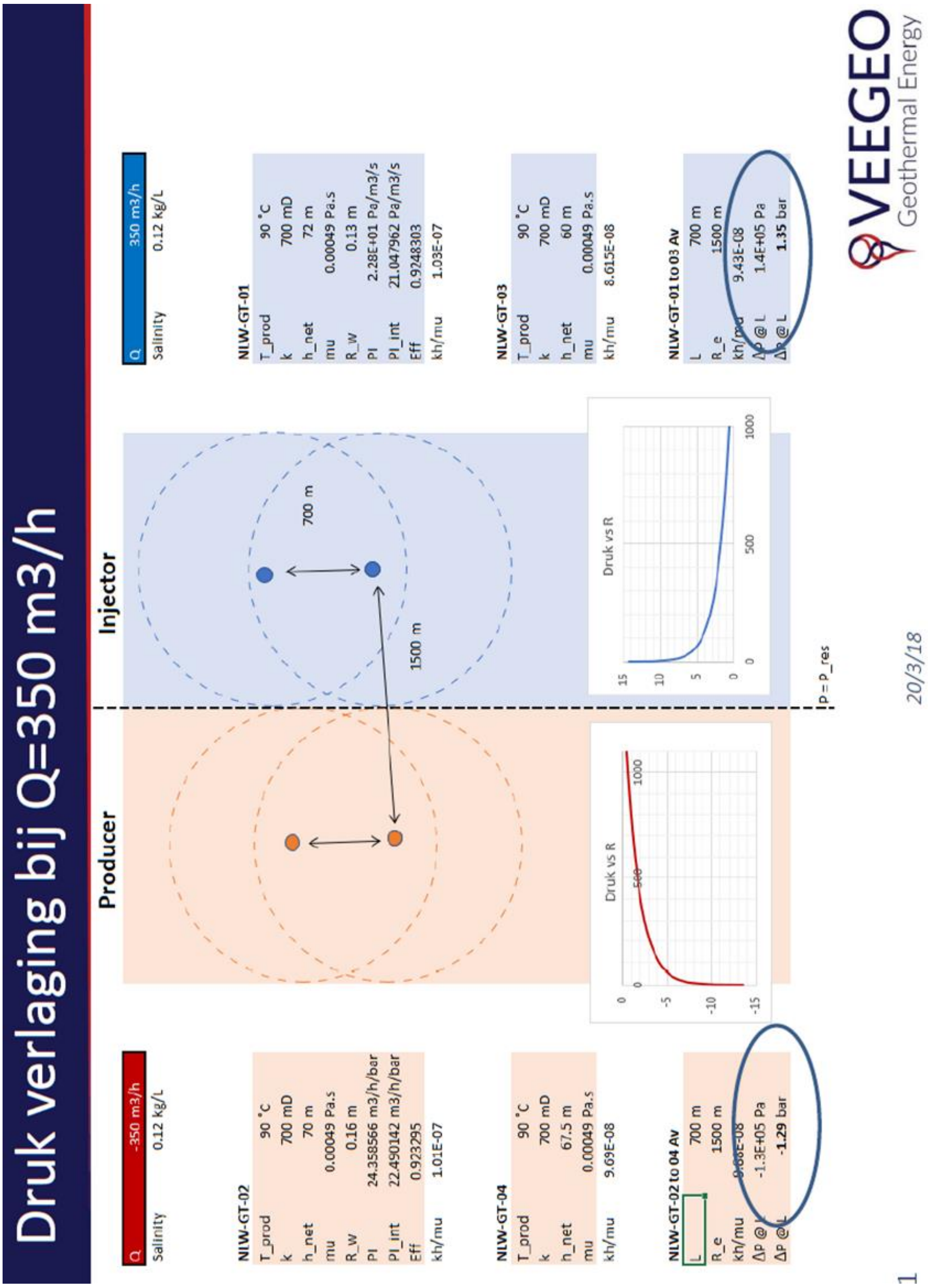

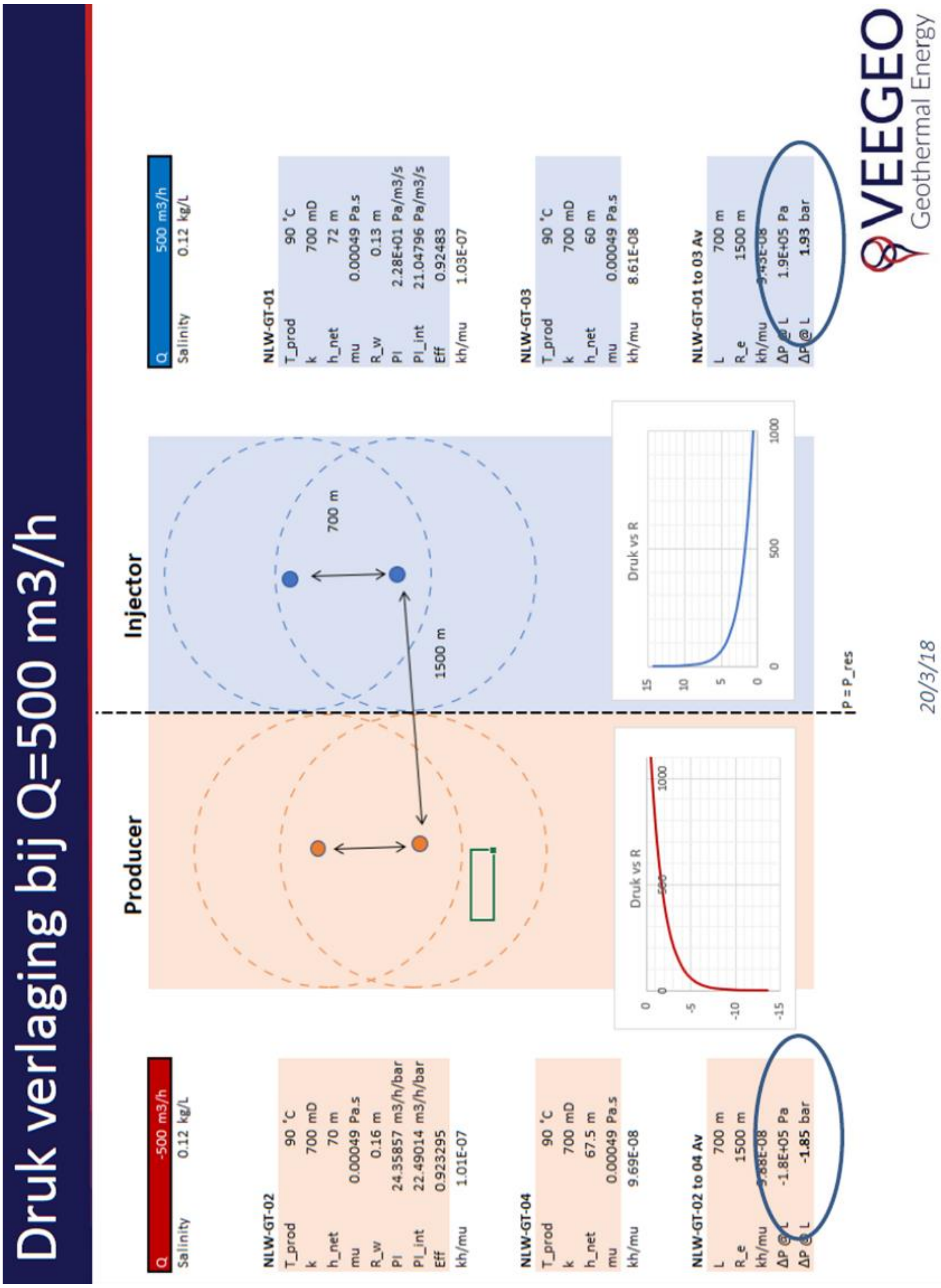


## 10.6 Deviation data planned wells

### 10.6.1 NLW-GT-03

| x (RD) | y (RD) | z (m) | md (m) | inc | dec |
|---|---|---|---|---|---|
| 76159 | 445224 | 0 | 0 | 0 | 295.6 |
| 76159 | 445224 | -800 | 800 | 0 | 295.6 |
| 76158.9843 | 445224.008 | -804.99996 | 805 | 0.4 | 295.6 |
| 76158.937 | 445224.03 | -809.99968 | 810 | 0.8 | 295.6 |
| 76158.8584 | 445224.068 | -814.9989 | 815 | 1.2 | 295.6 |
| 76158.7482 | 445224.121 | -819.9974 | 820 | 1.6 | 295.6 |
| 76158.6066 | 445224.189 | -824.99492 | 825 | 2 | 295.6 |
| 76158.4335 | 445224.271 | -829.99123 | 830 | 2.4 | 295.6 |
| 76158.2289 | 445224.369 | -834.98607 | 835 | 2.8 | 295.6 |

| | | | | | |
|---|---|---|---|---|---|
| 76157.993 | 445224.482 | -839.97921 | 840 | 3.2 | 295.6 |
| 76157.7255 | 445224.611 | -844.9704 | 845 | 3.6 | 295.6 |
| 76157.4267 | 445224.754 | -849.95939 | 850 | 4 | 295.6 |
| 76157.0965 | 445224.912 | -854.94596 | 855 | 4.4 | 295.6 |
| 76156.7349 | 445225.085 | -859.92984 | 860 | 4.8 | 295.6 |
| 76156.3419 | 445225.274 | -864.9108 | 865 | 5.2 | 295.6 |
| 76155.9176 | 445225.477 | -869.8886 | 870 | 5.6 | 295.6 |
| 76155.4619 | 445225.695 | -874.863 | 875 | 6 | 295.6 |
| 76154.975 | 445225.928 | -879.83374 | 880 | 6.4 | 295.6 |
| 76154.4567 | 445226.177 | -884.8006 | 885 | 6.8 | 295.6 |
| 76153.9072 | 445226.44 | -889.76332 | 890 | 7.2 | 295.6 |
| 76153.3265 | 445226.718 | -894.72166 | 895 | 7.6 | 295.6 |
| 76152.7146 | 445227.011 | -899.67539 | 900 | 8 | 295.6 |
| 76152.0715 | 445227.32 | -904.62426 | 905 | 8.4 | 295.6 |
| 76151.3972 | 445227.643 | -909.56803 | 910 | 8.8 | 295.6 |
| 76150.6919 | 445227.981 | -914.50647 | 915 | 9.2 | 295.6 |
| 76149.9555 | 445228.333 | -919.43932 | 920 | 9.6 | 295.6 |
| 76149.188 | 445228.701 | -924.36635 | 925 | 10 | 295.6 |
| 76148.3895 | 445229.084 | -929.28731 | 930 | 10.4 | 295.6 |
| 76147.5601 | 445229.481 | -934.20198 | 935 | 10.8 | 295.6 |
| 76146.6998 | 445229.893 | -939.11011 | 940 | 11.2 | 295.6 |
| 76145.8085 | 445230.32 | -944.01145 | 945 | 11.6 | 295.6 |
| 76144.8865 | 445230.762 | -948.90578 | 950 | 12 | 295.6 |
| 76143.9336 | 445231.219 | -953.79285 | 955 | 12.4 | 295.6 |
| 76142.9501 | 445231.69 | -958.67242 | 960 | 12.8 | 295.6 |
| 76141.9358 | 445232.176 | -963.54426 | 965 | 13.2 | 295.6 |
| 76140.8908 | 445232.676 | -968.40813 | 970 | 13.6 | 295.6 |
| 76139.8153 | 445233.192 | -973.26379 | 975 | 14 | 295.6 |
| 76138.7092 | 445233.722 | -978.11101 | 980 | 14.4 | 295.6 |
| 76137.5727 | 445234.266 | -982.94955 | 985 | 14.8 | 295.6 |
| 76136.4057 | 445234.825 | -987.77917 | 990 | 15.2 | 295.6 |
| 76135.2083 | 445235.399 | -992.59963 | 995 | 15.6 | 295.6 |
| 76133.9806 | 445235.987 | -997.41071 | 1000 | 16 | 295.6 |
| 76132.7227 | 445236.59 | -1002.2122 | 1005 | 16.4 | 295.6 |
| 76131.4345 | 445237.207 | -1007.0038 | 1010 | 16.8 | 295.6 |
| 76130.1162 | 445237.839 | -1011.7853 | 1015 | 17.2 | 295.6 |
| 76128.7679 | 445238.485 | -1016.5565 | 1020 | 17.6 | 295.6 |
| 76127.3895 | 445239.145 | -1021.3171 | 1025 | 18 | 295.6 |
| 76125.9812 | 445239.82 | -1026.067 | 1030 | 18.4 | 295.6 |
| 76124.5431 | 445240.509 | -1030.8058 | 1035 | 18.8 | 295.6 |
| 76123.0751 | 445241.212 | -1035.5334 | 1040 | 19.2 | 295.6 |
| 76121.5774 | 445241.93 | -1040.2495 | 1045 | 19.6 | 295.6 |
| 76120.0501 | 445242.662 | -1044.9539 | 1050 | 20 | 295.6 |
| 76118.4932 | 445243.408 | -1049.6463 | 1055 | 20.4 | 295.6 |
| 76116.9067 | 445244.168 | -1054.3266 | 1060 | 20.8 | 295.6 |
| 76115.2909 | 445244.942 | -1058.9945 | 1065 | 21.2 | 295.6 |
| 76113.6457 | 445245.73 | -1063.6498 | 1070 | 21.6 | 295.6 |
| 76111.9712 | 445246.532 | -1068.2922 | 1075 | 22 | 295.6 |
| 76110.2676 | 445247.349 | -1072.9216 | 1080 | 22.4 | 295.6 |
| 76108.5348 | 445248.179 | -1077.5376 | 1085 | 22.8 | 295.6 |
| 76106.773 | 445249.023 | -1082.1401 | 1090 | 23.2 | 295.6 |
| 76104.9823 | 445249.881 | -1086.7289 | 1095 | 23.6 | 295.6 |
| 76103.1628 | 445250.753 | -1091.3037 | 1100 | 24 | 295.6 |
| 76101.3145 | 445251.638 | -1095.8643 | 1105 | 24.4 | 295.6 |
| 76099.4375 | 445252.538 | -1100.4104 | 1110 | 24.8 | 295.6 |
| 76097.5319 | 445253.451 | -1104.942 | 1115 | 25.2 | 295.6 |
| 76095.5979 | 445254.377 | -1109.4586 | 1120 | 25.6 | 295.6 |
| 76093.6355 | 445255.317 | -1113.9602 | 1125 | 26 | 295.6 |
| 76091.6448 | 445256.271 | -1118.4465 | 1130 | 26.4 | 295.6 |
| 76089.6259 | 445257.239 | -1122.9173 | 1135 | 26.8 | 295.6 |
| 76087.5789 | 445258.219 | -1127.3723 | 1140 | 27.2 | 295.6 |
| 76085.5039 | 445259.213 | -1131.8113 | 1145 | 27.6 | 295.6 |
| 76083.401 | 445260.221 | -1136.2342 | 1150 | 28 | 295.6 |
| 76081.2703 | 445261.242 | -1140.6407 | 1155 | 28.4 | 295.6 |
| 76079.1119 | 445262.276 | -1145.0307 | 1160 | 28.8 | 295.6 |
| 76076.9259 | 445263.323 | -1149.4037 | 1165 | 29.2 | 295.6 |
| 76074.7125 | 445264.384 | -1153.7598 | 1170 | 29.6 | 295.6 |
| 76072.4717 | 445265.457 | -1158.0986 | 1175 | 30 | 295.6 |
| 76070.2036 | 445266.544 | -1162.42 | 1180 | 30.4 | 295.6 |
| 76067.9083 | 445267.644 | -1166.7237 | 1185 | 30.8 | 295.6 |
| 76065.5861 | 445268.756 | -1171.0095 | 1190 | 31.2 | 295.6 |
| 76063.2369 | 445269.882 | -1175.2773 | 1195 | 31.6 | 295.6 |
| 76060.8609 | 445271.02 | -1179.5267 | 1200 | 32 | 295.6 |
| 76058.4582 | 445272.172 | -1183.7577 | 1205 | 32.4 | 295.6 |
| 76056.0289 | 445273.335 | -1187.9699 | 1210 | 32.8 | 295.6 |
| 76053.5732 | 445274.512 | -1192.1633 | 1215 | 33.2 | 295.6 |
| 76051.0911 | 445275.701 | -1196.3375 | 1220 | 33.6 | 295.6 |

| | | | | | |
|---|---|---|---|---|---|
| 76048.5828 | 445276.903 | -1200.4924 | 1225 | 34 | 295.6 |
| 76046.0484 | 445278.117 | -1204.6278 | 1230 | 34.4 | 295.6 |
| 76043.4881 | 445279.344 | -1208.7435 | 1235 | 34.8 | 295.6 |
| 76040.9019 | 445280.583 | -1212.8392 | 1240 | 35.2 | 295.6 |
| 76038.2899 | 445281.835 | -1216.9149 | 1245 | 35.6 | 295.6 |
| 76035.6524 | 445283.098 | -1220.9702 | 1250 | 36 | 295.6 |
| 76032.9894 | 445284.374 | -1225.005 | 1255 | 36.4 | 295.6 |
| 76030.3011 | 445285.662 | -1229.0191 | 1260 | 36.8 | 295.6 |
| 76027.5875 | 445286.962 | -1233.0122 | 1265 | 37.2 | 295.6 |
| 76024.8489 | 445288.274 | -1236.9843 | 1270 | 37.6 | 295.6 |
| 76022.0854 | 445289.598 | -1240.9351 | 1275 | 38 | 295.6 |
| 76019.297 | 445290.934 | -1244.8643 | 1280 | 38.4 | 295.6 |
| 76016.484 | 445292.282 | -1248.7719 | 1285 | 38.8 | 295.6 |
| 76013.6465 | 445293.642 | -1252.6576 | 1290 | 39.2 | 295.6 |
| 76010.7845 | 445295.013 | -1256.5213 | 1295 | 39.6 | 295.6 |
| 76007.8983 | 445296.396 | -1260.3627 | 1300 | 40 | 295.6 |
| 76004.988 | 445297.79 | -1264.1817 | 1305 | 40.4 | 295.6 |
| 76002.0537 | 445299.196 | -1267.978 | 1310 | 40.8 | 295.6 |
| 75999.0956 | 445300.613 | -1271.7516 | 1315 | 41.2 | 295.6 |
| 75996.1138 | 445302.042 | -1275.5021 | 1320 | 41.6 | 295.6 |
| 75993.1172 | 445303.478 | -1279.2382 | 1325 | 41.7 | 295.6 |
| 75990.1148 | 445304.916 | -1282.9685 | 1330 | 41.8 | 295.6 |
| 75984.1041 | 445307.796 | -1290.4233 | 1340 | 41.8 | 295.6 |
| 75978.0934 | 445310.676 | -1297.878 | 1350 | 41.8 | 295.6 |
| 75972.0827 | 445313.556 | -1305.3328 | 1360 | 41.8 | 295.6 |
| 75966.0721 | 445316.436 | -1312.7875 | 1370 | 41.8 | 295.6 |
| 75960.0614 | 445319.315 | -1320.2423 | 1380 | 41.8 | 295.6 |
| 75954.0507 | 445322.195 | -1327.6971 | 1390 | 41.8 | 295.6 |
| 75079.4944 | 445741.213 | -2412.3646 | 2845 | 41.8 | 295.6 |
| 75073.4837 | 445744.093 | -2419.8194 | 2855 | 41.8 | 295.6 |

### 10.6.2 **NLW-GT-04**

| x | y | z | md | inc | dec |
|---|---|---|---|---|---|
| 76193 | 445209 | 0 | 0 | 0 | 158 |
| 76193 | 445209 | -800 | 800 | 0 | 158 |
| 76193.01 | 445209 | -805 | 805 | 0.4 | 158 |
| 76193.03 | 445208.9 | -810 | 810 | 0.8 | 158 |
| 76193.06 | 445208.9 | -814.999 | 815 | 1.2 | 158 |
| 76193.1 | 445208.7 | -819.997 | 820 | 1.6 | 158 |
| 76193.16 | 445208.6 | -824.995 | 825 | 2 | 158 |
| 76193.24 | 445208.4 | -829.991 | 830 | 2.4 | 158 |
| 76193.32 | 445208.2 | -834.986 | 835 | 2.8 | 158 |
| 76193.42 | 445208 | -839.979 | 840 | 3.2 | 158 |
| 76193.53 | 445207.7 | -844.97 | 845 | 3.6 | 158 |
| 76193.65 | 445207.4 | -849.959 | 850 | 4 | 158 |
| 76193.79 | 445207 | -854.946 | 855 | 4.4 | 158 |
| 76193.94 | 445206.7 | -859.93 | 860 | 4.8 | 158 |
| 76194.1 | 445206.3 | -864.911 | 865 | 5.2 | 158 |
| 76194.28 | 445205.8 | -869.889 | 870 | 5.6 | 158 |
| 76194.47 | 445205.4 | -874.863 | 875 | 6 | 158 |
| 76194.67 | 445204.9 | -879.834 | 880 | 6.4 | 158 |
| 76194.89 | 445204.3 | -884.801 | 885 | 6.8 | 158 |
| 76195.12 | 445203.8 | -889.763 | 890 | 7.2 | 158 |
| 76195.36 | 445203.2 | -894.722 | 895 | 7.6 | 158 |
| 76195.61 | 445202.5 | -899.675 | 900 | 8 | 158 |
| 76195.88 | 445201.9 | -904.624 | 905 | 8.4 | 158 |
| 76196.16 | 445201.2 | -909.568 | 910 | 8.8 | 158 |
| 76196.45 | 445200.5 | -914.506 | 915 | 9.2 | 158 |
| 76196.76 | 445199.7 | -919.439 | 920 | 9.6 | 158 |
| 76197.08 | 445198.9 | -924.366 | 925 | 10 | 158 |
| 76197.41 | 445198.1 | -929.287 | 930 | 10.4 | 158 |
| 76197.75 | 445197.2 | -934.202 | 935 | 10.8 | 158 |
| 76198.11 | 445196.4 | -939.11 | 940 | 11.2 | 158 |
| 76198.48 | 445195.4 | -944.011 | 945 | 11.6 | 158 |
| 76198.86 | 445194.5 | -948.906 | 950 | 12 | 158 |
| 76199.26 | 445193.5 | -953.793 | 955 | 12.4 | 158 |
| 76199.67 | 445192.5 | -958.672 | 960 | 12.8 | 158 |
| 76200.09 | 445191.5 | -963.544 | 965 | 13.2 | 158 |
| 76200.52 | 445190.4 | -968.408 | 970 | 13.6 | 158 |
| 76200.97 | 445189.3 | -973.264 | 975 | 14 | 158 |
| 76201.43 | 445188.1 | -978.111 | 980 | 14.4 | 158 |
| 76201.9 | 445187 | -982.95 | 985 | 14.8 | 158 |
| 76202.39 | 445185.8 | -987.779 | 990 | 15.2 | 158 |
| 76202.88 | 445184.5 | -992.6 | 995 | 15.6 | 158 |
| 76203.39 | 445183.3 | -997.411 | 1000 | 16 | 158 |
| 76203.92 | 445182 | -1002.21 | 1005 | 16.4 | 158 |

| | | | | | |
|---|---|---|---|---|---|
| 76204.45 | 445180.7 | -1007 | 1010 | 16.8 | 158 |
| 76205 | 445179.3 | -1011.79 | 1015 | 17.2 | 158 |
| 76205.56 | 445177.9 | -1016.56 | 1020 | 17.6 | 158 |
| 76206.13 | 445176.5 | -1021.32 | 1025 | 18 | 158 |
| 76206.72 | 445175.1 | -1026.07 | 1030 | 18.4 | 158 |
| 76207.31 | 445173.6 | -1030.81 | 1035 | 18.8 | 158 |
| 76207.92 | 445172.1 | -1035.53 | 1040 | 19.2 | 158 |
| 76208.54 | 445170.5 | -1040.25 | 1045 | 19.6 | 158 |
| 76209.18 | 445169 | -1044.95 | 1050 | 20 | 158 |
| 76209.83 | 445167.4 | -1049.65 | 1055 | 20.4 | 158 |
| 76210.48 | 445165.7 | -1054.33 | 1060 | 20.8 | 158 |
| 76211.16 | 445164.1 | -1058.99 | 1065 | 21.2 | 158 |
| 76211.84 | 445162.4 | -1063.65 | 1070 | 21.6 | 158 |
| 76212.53 | 445160.6 | -1068.29 | 1075 | 22 | 158 |
| 76213.24 | 445158.9 | -1072.92 | 1080 | 22.4 | 158 |
| 76213.96 | 445157.1 | -1077.54 | 1085 | 22.8 | 158 |
| 76214.69 | 445155.3 | -1082.14 | 1090 | 23.2 | 158 |
| 76215.44 | 445153.5 | -1086.73 | 1095 | 23.6 | 158 |
| 76216.19 | 445151.6 | -1091.3 | 1100 | 24 | 158 |
| 76216.96 | 445149.7 | -1095.86 | 1105 | 24.4 | 158 |
| 76217.74 | 445147.8 | -1100.41 | 1110 | 24.8 | 158 |
| 76218.53 | 445145.8 | -1104.94 | 1115 | 25.2 | 158 |
| 76219.34 | 445143.8 | -1109.46 | 1120 | 25.6 | 158 |
| 76220.15 | 445141.8 | -1113.96 | 1125 | 26 | 158 |
| 76220.98 | 445139.8 | -1118.45 | 1130 | 26.4 | 158 |
| 76221.82 | 445137.7 | -1122.92 | 1135 | 26.8 | 158 |
| 76222.67 | 445135.6 | -1127.37 | 1140 | 27.2 | 158 |
| 76223.53 | 445133.4 | -1131.81 | 1145 | 27.6 | 158 |
| 76224.4 | 445131.3 | -1136.23 | 1150 | 28 | 158 |
| 76225.29 | 445129.1 | -1140.64 | 1155 | 28.4 | 158 |
| 76226.18 | 445126.9 | -1145.03 | 1160 | 28.8 | 158 |
| 76227.09 | 445124.6 | -1149.4 | 1165 | 29.2 | 158 |
| 76228.01 | 445122.3 | -1153.76 | 1170 | 29.6 | 158 |
| 76228.94 | 445120 | -1158.1 | 1175 | 30 | 158 |
| 76229.88 | 445117.7 | -1162.42 | 1180 | 30.4 | 158 |
| 76230.84 | 445115.3 | -1166.72 | 1185 | 30.8 | 158 |
| 76231.8 | 445113 | -1171.01 | 1190 | 31.2 | 158 |
| 76232.78 | 445110.5 | -1175.28 | 1195 | 31.6 | 158 |
| 76233.77 | 445108.1 | -1179.53 | 1200 | 32 | 158 |
| 76234.76 | 445105.6 | -1183.76 | 1205 | 32.4 | 158 |
| 76235.77 | 445103.1 | -1187.97 | 1210 | 32.8 | 158 |
| 76236.79 | 445100.6 | -1192.16 | 1215 | 33.2 | 158 |
| 76237.82 | 445098.1 | -1196.34 | 1220 | 33.6 | 158 |
| 76238.86 | 445095.5 | -1200.5 | 1225 | 33.7 | 158 |
| 76239.9 | 445092.9 | -1204.66 | 1230 | 33.8 | 158 |
| 76241.99 | 445087.8 | -1212.97 | 1240 | 33.8 | 158 |
| 76244.07 | 445082.6 | -1221.28 | 1250 | 33.8 | 158 |
| 76246.15 | 445077.4 | -1229.59 | 1260 | 33.8 | 158 |
| 76248.24 | 445072.3 | -1237.9 | 1270 | 33.8 | 158 |
| 76250.32 | 445067.1 | -1246.21 | 1280 | 33.8 | 158 |
| 76252.4 | 445062 | -1254.52 | 1290 | 33.8 | 158 |
| 76254.49 | 445056.8 | -1262.83 | 1300 | 33.8 | 158 |
| 76256.57 | 445051.7 | -1271.14 | 1310 | 33.8 | 158 |
| 76258.66 | 445046.5 | -1279.45 | 1320 | 33.8 | 158 |
| 76260.74 | 445041.3 | -1287.76 | 1330 | 33.8 | 158 |
| 76262.82 | 445036.2 | -1296.07 | 1340 | 33.8 | 158 |
| 76264.91 | 445031 | -1304.38 | 1350 | 33.8 | 158 |
| 76266.99 | 445025.9 | -1312.69 | 1360 | 33.8 | 158 |
| 76269.08 | 445020.7 | -1320.99 | 1370 | 33.8 | 158 |
| 76566.02 | 444285.7 | -2505.15 | 2795 | 33.8 | 158 |

## 10.7 Geomech pressure calculation sheet

| Invoer parameters | waarde | Default | eenheid |
|---|---|---|---|
| Diepte top aquifer in productieput | -2367 | x | m |
| Diepte top aquifer in injectieput | -2306 | x | m |
| Gemiddelde diepte top aquifer | -2337 | x | m |
| Diepte pomp | -800 | -500 | m |
| | | | |
| Aquiferdruk Productieput | 241 | x | bar |
| Aquiferdruk Injectieput | 238 | x | bar |
| Bottom hole pressure Productieput | 212 | x | bar |
| Bottom hole pressure Injectieput | 296 | x | bar |
| | | | |
| Drukverschil over put-aquifer interface in productieput | 28 | x | bar |
| Drukverschil over put-aquifer interface in injectieput | 58 | x | bar |
| | | | |
| hydrostatische gradient in injectieput | 0.106 | 0.106 | bar/m |
| lithostatische gradient | 0.225 | 0.225 | bar/m |
| minimale horizontale spanningsgradient (bar/m) | 0.16 | 0.16 | bar/m |
| | | | |
| Injectietemperatuur | 31 | x | °C |
| Aquifer temperatuur @ productieput | 89 | x | °C |
| Aquifer temperatuur @ injectieput | 89 | x | °C |
| Delta temperatuur @ injectieput | 58 | x | °C |
| Temperatuurgradient | 0.032 | 0.032 | °C/m |
| Gemiddelde oppervlaktetemperatuur | 10 | 10 | °C |
| | | | |
| Youngs modulus | 10000 | 10000 | Mpa |
| Poisson's ratio | 0.25 | 0.25 | frac |
| Arching coefficient | 0.4 | 0.4 | |
| Biot coefficient | 0.75 | 0.75 | |
| Linear thermal expansion coefficient ( °C-1) | 1.00E-05 | 1.00E-05 | $°C^{-1}$ |
| | | | |
| Cohesie | 0 | 0 | bar |
| Hoek van inwendige wrijving | 33 | 33 | ° |
| Invloed thermische stress | Ja | | |

| Uitvoer | Waarde | Validatie |
|---|---|---|
| Tubing Head Pressure toegestaan volgens SodM protocol | 67 | JA |
| Maximale verschildruk injectieput top reservoir | 73.3 | JA |
| Fracking | | NEE |
| Kans op breukreactivatie | | JA |

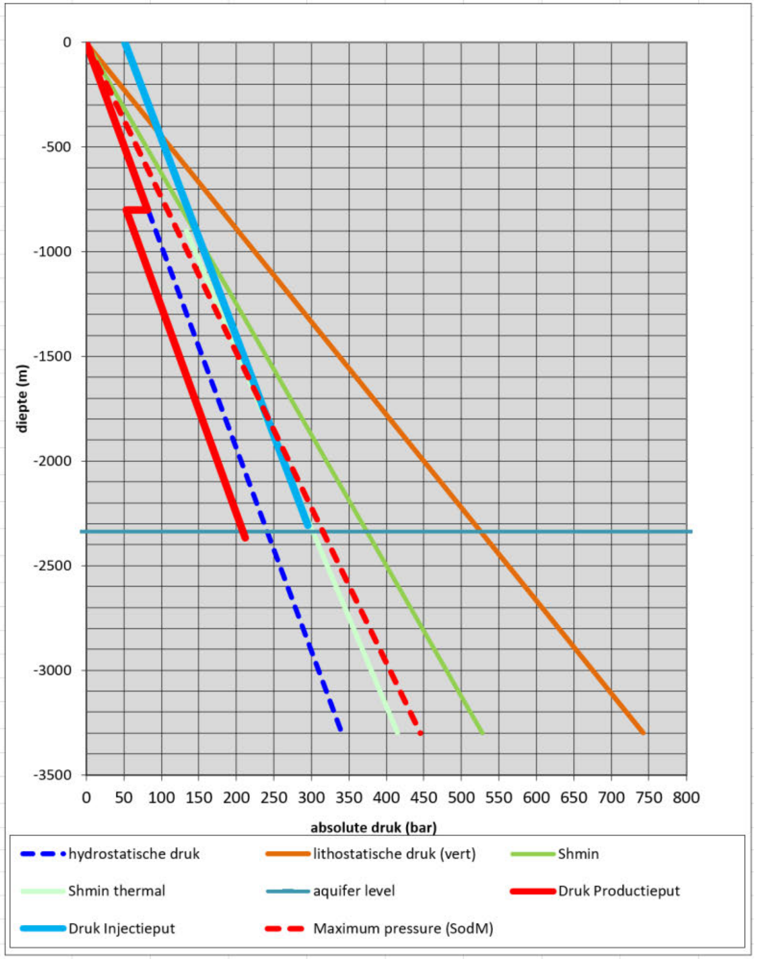

## 10.8 Velocity model residuals

| Base Tertiary_50.dat | Well | X-value | Y-value | Z-value | Horizon at | Diff after |
|---|---|---|---|---|---|---|
| | HON-GT-01 | 75244.2 | 448079.7 | -651.41 | -691.72 | 40.31 |
| | NLW-GT-01 | 76128.4 | 445365.5 | -710.56 | -739.84 | 29.28 |
| | GAG-05 | 75749.1 | 441323.6 | -886.07 | -885.36 | -0.72 |
| | LIR-45 | 75124.1 | 444624.2 | -725.67 | -721.96 | -3.71 |
| | LIR-GT-02 | 79091 | 443735 | -702.99 | -710.16 | 7.17 |
| | LIR-GT-01 | 79083.1 | 443758.4 | -683.66 | -709.09 | 25.43 |
| | | | | | | |
| Top Texel.dat | Well | X-value | Y-value | Z-value | Horizon at | Diff after |
| | HON-GT-01 | 75245.1 | 448078.6 | -1110.83 | -1112.74 | 1.91 |
| | NLW-GT-01 | 76088.4 | 445630.8 | -1187.48 | -1188.42 | 0.94 |
| | GAG-05 | 75485.6 | 441685.7 | -1585.26 | -1564.43 | -20.83 |
| | HON-GT-02 | 75244.5 | 448093.9 | -1112.38 | -1111.44 | -0.94 |
| | LIR-45 | 75112.2 | 444576.8 | -1122.64 | -1118.22 | -4.42 |
| | LIR-GT-02 | 79091 | 443735 | -1100.64 | -1104.16 | 3.51 |
| | LIR-GT-01 | 79076.4 | 443787 | -1101.63 | -1102.56 | 0.92 |
| | | | | | | |
| Top Schieland.dat_29May2017 | Well | X-value | Y-value | Z-value | Horizon at | Diff after |
| | HON-GT-01 | 74884.2 | 448601.7 | -2277.63 | -2273.69 | -3.93 |
| | NLW-GT-01 | 75708.8 | 446109.4 | -2229.63 | -2249.96 | 20.33 |
| | GAG-05 | 75175.3 | 442124.4 | -2402.89 | -2324.43 | -78.46 |
| | HON-GT-02 | 75778.5 | 447771.5 | -2308.84 | -2285.79 | -23.05 |
| | LIR-45 | 75072.3 | 444545.5 | -2069.51 | -2070.19 | 0.68 |
| | LIR-GT-02 | 79625.7 | 443286.3 | -2190.08 | -2160.34 | -29.74 |
| | LIR-GT-01 | 78936.2 | 444466.5 | -2256.13 | -2259.69 | 3.57 |
| | | | | | | |
| Top Altena_ajust_to_TopS_29May2017 | Well | X-value | Y-value | Z-value | Horizon at | Diff after |
| | NLW-GT-01 | 75538.8 | 446192 | -2803.53 | -2787.6 | -15.93 |
| | GAG-05 | 75103.5 | 442218.4 | -2604.42 | -2578.92 | -25.5 |
| | LIR-45 | 75045.5 | 444515.6 | -2401.01 | -2477.04 | 76.03 |

## 10.9 Water Analysis

ALcontrol Laboratories

Trias Westland B.V.

Blad 2 van 8

# Analyserapport

| | | | |
|---|---|---|---|
| Projectnaam | Geothermie monsters | Orderdatum | 01-03-2018 |
| Projectnummer | 2018-234-0404-05-FV | Startdatum | 01-03-2018 |
| Rapportnummer | 12730507 - 1 | Rapportagedatum | 09-03-2018 |

| Nummer | Monstersoort | Monsterspecificatie |
|---|---|---|
| 001 | Grondwater | Phase 5 2H NLW-GT-01 |
| 002 | Grondwater | Phase 5 3H NLW-GT-01 |

| Analyse | Eenheid | Q | 001 | 002 |
|---|---|---|---|---|
| pH | | Q | 6.2 | 6.2 |
| geleidingsvermogen (25°C)(EC) | µS/cm | Q | 111000 | 111000 |
| temperatuur t.b.v. pH | °C | | 19.4 | 19.4 |
| *METALEN* | | | | |
| filtreren metalen | - | | 1 [1)] | 1 [1)] |
| cadmium | µg/l | Q | <0.20 [1)] | <0.20 [1)] |
| kwik | µg/l | Q | <0.05 [1)] | <0.05 [1)] |
| lood | µg/l | Q | 42 [1)] | 33 [1)] |
| nikkel | µg/l | Q | 6.7 [1)] | 6.5 [1)] |
| zink | µg/l | Q | 180 [1)] | 180 [1)] |
| *ANORGANISCHE VERBINDINGEN* | | | | |
| Carbonaat | mg/l | Q | <10 | <10 |
| *VLUCHTIGE AROMATEN* | | | | |
| benzeen | µg/l | Q | 280 | 290 |
| tolueen | µg/l | Q | 40 | 44 |
| ethylbenzeen | µg/l | Q | 1.2 | 1.4 |
| o-xyleen | µg/l | Q | 3.3 | 3.2 |
| p- en m-xyleen | µg/l | Q | 3.8 | 3.6 |
| som BTEX | µg/l | | 330 | 340 |
| *MINERALE OLIE* | | | | |
| fractie C10-C12 | µg/l | | 65 | 75 |
| fractie C12-C22 | µg/l | | 130 | 120 |
| fractie C22-C30 | µg/l | | 85 | 70 |
| fractie C30-C40 | µg/l | | 65 | 50 |
| totaal olie C10 - C40 | µg/l | Q | 350 | 310 |
| *DIVERSE NATCHEMISCHE BEPALINGEN* | | | | |
| chloride | mg/l | Q | 86000 | 87000 |
| onopgel.best./zwev.stof | mg/l | Q | 64 | 410 |
| monstervolume tbv analyse | ml | | 500 | 500 |
| soortelijk gewicht | g/l | | 1091 | 1089 |
| Speciaal onderzoek | - | | zie bijlage | zie bijlage |